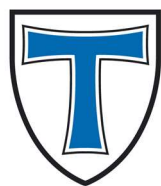


**JUSTUS-LIEBIG-**

---



**UNIVERSITÄT  
GIESSEN**

**Synthesis and Structure-Activity Relationship  
of 3-Chloropiperidines as Potential DNA  
Alkylating Agents**

**Kumulative Dissertation zur Erlangung des Grades  
„Doktor der Naturwissenschaften“ am Fachbereich  
Biologie und Chemie der Justus-Liebig-Universität Gießen**

**vorgelegt von**

**Tim Kramer, geb. Helbing**

Erstgutachter: Prof. Dr. Richard Göttlich

Zweitgutachter: Prof. Dr. Siegfried Schindler



## **Eidesstaatliche Erklärung**

„Ich erkläre: Ich habe die vorgelegte Dissertation selbstständig und ohne unerlaubte fremde Hilfe und nur mit den Hilfen angefertigt, die ich in der Dissertation angegeben habe. Alle Textstellen, die wörtlich oder sinngemäß aus veröffentlichten Schriften entnommen sind, und alle Angaben, die auf mündlichen Auskünften beruhen, sind als solche kenntlich gemacht. Ich stimme einer evtl. Überprüfung meiner Dissertation durch eine Antiplagiat-Software zu. Bei den von mir durchgeführten und in der Dissertation erwähnten Untersuchungen habe ich die Grundsätze guter wissenschaftlicher Praxis, wie sie in der „Satzung der Justus-Liebig-Universität Gießen zur Sicherung guter wissenschaftlicher Praxis“ niedergelegt sind, eingehalten.“

\_\_\_\_\_  
Datum

\_\_\_\_\_  
Unterschrift

*Do. Or do not. There is no try.*

*Yoda; Star Wars Episode V, The Empire strikes back.*

## Kurzzusammenfassung

Bereits seit ihrer Entdeckung während der Mitte des zwanzigsten Jahrhunderts finden Alkylanzien breite Anwendung in der Krebstherapie. Die Stickstofflose stellen eine Untergruppe dieser Medikamente dar und zeichnen sich durch ihre charakteristische 2-Chlorethylamin Einheit aus. Diese funktionelle Gruppe ermöglicht die Ausbildung eines extrem elektrophilen Aziridinium Ions, welches leicht von intrazellulären Nucleophilen, wie beispielsweise DNA Basen, angegriffen werden kann. Die hierbei entstehenden kovalenten Addukte können Depurinierungen und DNA-Strangbrüche zur Folge haben, wodurch es zu einer Inhibierung der Zellteilung und letztlich zur Apoptose der behandelten Tumorzellen kommen kann. Allerdings ist diese Reaktivität nicht nur auf Krebszellen beschränkt, was zu schwerwiegenden Nebenwirkungen und daher zu einer eingeschränkten therapeutischen Anwendbarkeit dieser Substanzen führt.

Während der letzten Jahrzehnte wurden verschiedene Stickstofflost-Derivate entwickelt, um diese Nebenwirkungen zu verringern und die Selektivität oder Zellaufnahme dieser Substanzklasse zu verbessern. Ein Beispiel hierfür stellt die Einführung von unterschiedlichen aromatischen Stickstoffsubstituenten, im Gegensatz zu den ursprünglichen aliphatischen Derivaten dar. Der elektronenziehende Effekt dieser aromatischen Einheiten reduziert dabei die Nucleophilie des Stickstoffatoms, was zu einer verlangsamten Bildung des Aziridinium Ions und damit zu einer verringerten Reaktivität führt. Ein weiterer Ansatz, um die Reaktivität solcher Substanzen zu verringern, wurde in unserer Arbeitsgruppe entwickelt. Hierzu wurde die 2-Chlorethylamin Einheit in ein heterocyclisches Piperidinsystem integriert, was aufgrund der erhöhten Ringspannung des entstehenden bicyclischen Systems zu einer verlangsamtten Bildung des Aziridinium Ions führt. Die so entwickelten 3-Chlorpiperidine zeigten in vorherigen Studien vielversprechende DNA Alkylierungsaktivitäten und werden daher im Zuge dieser Arbeit genauer analysiert.

Die Publikationen dieser Arbeit zeigen, dass die Reaktivität der untersuchten 3-Chlorpiperidine durch die Einführung verschiedener Substituenten sowohl am Stickstoffatom, als auch in der C5 Position des cyclischen Piperidinsystems beeinflusst werden kann. Weiterführende biologische Studien mono- und bifunktionaler 3-Chlorpiperidine zeigten außerdem eine außergewöhnliche Selektivität aromatischer Derivate für pankreatische Tumorzellen, welche später auf eine unzureichende zelluläre Antwort dieser spezifischen Zelllinie zurückgeführt werden konnte. Außerdem wurden aliphatische und aromatische 3-Chlorpiperidine durch NMR-kinetische Methoden untersucht und so die Einwirkung des C5 Ringsubstituenten entdeckt. Die An- oder Abwesenheit einer geminalen C5-Methylierung zeigte signifikanten Einfluss auf die Bildung des reaktiven bicyclischen Aziridinium Intermediats und damit auf den geschwindigkeitsbestimmenden Schritt des DNA Alkylierungsmechanismus. Außerdem konnte die bicyclische, bootartige Struktur des intermediären Aziridinium Ions durch Einkristall-Röntgenstrukturanalyse verifiziert und die verringerte Reaktivität unserer cyclischen Verbindungen im Vergleich zu aliphatischen Stickstofflosen bestätigt werden.

Weitere Untersuchungen der geminal C5 methylierten 3-Chlorpiperidine führten zu dem Schluss, dass die Erhöhung der Reaktionsgeschwindigkeit, verglichen mit dem entsprechenden unsubstituierten Derivat, durch einen klassischen, winkelabhängigen Thorpe-Ingold Effekt bedingt wird.

Dementsprechend führten sterisch anspruchsvolle Substituenten in der C5 Position zu kleineren Innenwinkeln und beschleunigten die Bildung des bicyclischen Aziridinium Ions. Im Gegensatz dazu, führte die Verwendung von gespannten Cycloalkan-Substituenten zu einer Erweiterung des Innenwinkels, was die Bildung des bicyclischen Systems verlangsamte. Neben der bereits etablierten Variation des Stickstoffsubstituenten konnte diese neu entdeckte Struktur-Aktivitätsbeziehung als weitere Möglichkeit zur Anpassung der Reaktivität von 3-Chlorpiperidinen eingesetzt werden.

## Abstract

Alkylating agents have been widely used in cancer treatment since their discovery during the mid-twentieth century. Nitrogen mustards represent a subclass of these medical agents and are characterized by their unique 2-chloroethylamine moiety. This functional group enables the intramolecular formation of a highly electrophilic aziridinium ion, which is readily attacked by cellular nucleophiles such as DNA bases. The resulting covalent adducts might cause depurination and DNA strand cleavage, leading to inhibition of DNA replication and eventually apoptosis of the treated cancer cells. However, this reactivity is not limited to malignant tissue, resulting in severe side effects and therefore limited therapeutic application of these drugs.

Over the last decades, several nitrogen mustard derivatives have been developed to reduce side effects and enhance their respective selectivity or cellular uptake. One example is the introduction of various aromatic nitrogen substituents instead of the early aliphatic derivatives. The electron-withdrawing effect of these aromatic moieties reduces the nucleophilicity of the nitrogen atom, consequently decreasing the rate of aziridinium ion formation and therefore lowering their reactivity. Another approach to reduce their reactivity was applied in our group by including the 2-chloroethylamine functional group into a heterocyclic piperidine system, leading to a reduced rate of aziridinium ion formation due to the increased ring strain of the emerging bicyclic system. The resulting 3-chloropiperidines showed promising DNA alkylating activities in previous studies and are therefore analyzed in more detail during this work.

The publications included in this work demonstrate, that the reactivity of the examined 3-chloropiperidine derivatives could be adjusted by introduction of different substituents on the nitrogen atom as well as the C5 position of the cyclic piperidine system. Further biological evaluation of mono- and bifunctional 3-chloropiperidines revealed a remarkable selectivity of aromatic nitrogen substituents for pancreatic cancer cells, which could be later attributed to an inappropriate cellular response of this specific cell line. In addition, we studied aliphatic and aromatic 3-chloropiperidines using NMR kinetic methods, revealing the importance of the C5 ring substituents. The presence or absence of the C5 geminal methylation had a significant effect towards the formation of the reactive bicyclic aziridinium intermediate, and therefore the rate-determining step of the DNA alkylation mechanism. The study also verified the bicyclic, boat-like structure of the intermediate aziridinium ions by single crystal X-ray analysis and confirmed the decreased reactivity of our cyclic compounds in comparison with aliphatic nitrogen mustards.

Further investigations of the C5 geminal methylated 3-chloropiperidines concluded that the acceleration of the reaction rate, compared to the corresponding unsubstituted derivatives, is a result of a classic, angle dependent Thorpe-Ingold effect. Accordingly, bulky substituents in C5 position lead to decreased internal angles and therefore accelerate the formation of the bicyclic aziridinium ion. In contrast, strained cycloalkyl substituents result in enlarged internal angles and retard the cyclization reaction. Beside the already established variation of the nitrogen substituent, this new structure-activity relationship demonstrated to be another useful tool to modulate the reactivity of 3-chloropiperidines.

## Preface

The present work is prepared as a cumulative dissertation and incorporates the scientific publications I was able to achieve during my doctoral studies in the organic chemistry working group of Prof. Dr. Richard Göttlich at the Justus-Liebig-University Gießen. In the first chapter the general theoretical background of my research topic is presented, while the second chapter deals with previous studies in this area and includes my contribution to the aforementioned findings. In addition, these chapters describe the relationship between the individual publications and the scientific problems they tackled. Some of these publications were prepared in cooperation with the pharmaceutical working group of Prof. Dr. Barbara Gatto from the University of Padova. The following chapter includes the original peer-reviewed publications, reprinted with permission of the respective copyright owners. The corresponding Supporting Information are publicly available on the publishers' website.

## Table of Contents

Eidesstaatliche Erklärung .....	I
Kurzzusammenfassung .....	III
Abstract .....	V
Preface .....	VI
1. Introduction .....	1
1.1. History of Alkylating Agents .....	1
1.2. Alkylation Mechanism of Nitrogen Mustards .....	3
1.3. Chemistry of Aziridinium Ions .....	4
1.4. Intramolecular Reactions and the Geminal Dialkyl Effect .....	5
2. 3-Chloropiperidines as DNA Alkylating Agents .....	7
2.1. Synthesis of 3-Chloropiperidines .....	7
2.2. 3-Chloropiperidines: Mechanism of Action .....	11
2.3. Structure-Activity Relationship .....	13
2.4. Summary and Perspective .....	17
3. References .....	19
4. Publications .....	23
4.1. Aromatic Linkers Unleash the Antiproliferative Potential of 3-Chloropiperidines Against Pancreatic Cancer Cells .....	23
4.2. Understanding the Alkylation Mechanism of 3-Chloropiperidines – NMR Kinetic Studies and Isolation of Bicyclic Aziridinium Ions .....	36
4.3. Separation of the Thorpe-Ingold and Reactive Rotamer Effect by Using the Formation of Bicyclic Aziridinium Ions .....	46
4.4. Further Co-Authored Publications .....	54
5. Acknowledgment .....	55

## 1. Introduction

Over the last 80 years alkylating agents, especially nitrogen mustards, have been extensively used in cancer therapy.<sup>[1,2]</sup> The application of these therapeutic agents afforded a new strategy for the treatment of cancer diseases, commonly known as chemotherapy. The term refers to the medication of malignant cells with special cytostatic agents, intending to inhibit their cell division. In contrast to local methods like surgery and radiation therapy, chemotherapy represents a systemic approach to cancer treatment, owing to the unselective nature of the applied chemotherapeutic agents. On the other hand, this lack of site specificity represents a major drawback of these drugs, leading to severe side effects due to harming of normal tissue, especially highly proliferating cells.<sup>[3,4]</sup> Furthermore, administration of high doses of anticancer drugs is usually required, resulting in the rapid development of resistance phenomena.<sup>[5]</sup> Nonetheless, chemotherapy remains an important aspect in today's cancer treatment. Emerging from the discovery of alkylating agents during the First and Second World War, a multitude of different nitrogen mustard analogues have been prepared and tested in clinical trials, designed to reduce their side effects and make use of several transport or activation mechanisms.<sup>[1,2]</sup> Successfully introduced anticancer agents, like Chlorambucil and Cyclophosphamide, are nowadays usually combined with other cytotoxic drugs, such as antimetabolites, cytoskeletal drugs and topoisomerase inhibitors.<sup>[6]</sup> This combination therapy, alongside radiation therapy, surgical operations and hyperthermia therapy represents a common strategy for the treatment of many cancer types.<sup>[7]</sup> Therefore, further research in this area is still required, possibly leading to drug candidates with reduced side effects and improved uptake profiles, which might surpass common resistance phenomena.

### 1.1. History of Alkylating Agents

The discovery of alkylating agents, and therefore the origin of modern chemotherapy, can be traced back to the use chemical warfare agents during the First and Second World War.<sup>[8]</sup> Beside the acute blistering effects, some victims of the chemical weapon "mustard gas" (*bis*(2-chloroethyl) sulphide; Figure 1) showed a significantly reduced number of white blood cells (leukopenia).<sup>[9]</sup> Accordingly, such sulphur mustards were clinically tested against leukemia, but could not be used therapeutically due to their strong acute toxicity. Instead, nitrogen-containing analogues of these compounds were developed as less toxic alternatives. In 1942 Goodman and Gilman started the first clinical trials of the nitrogen mustards *tris*(2-chloroethyl) amine and *bis*(2-chloroethyl) methylamine (Figure 1).<sup>[10,11]</sup> In the end, the bifunctional derivative, named Mechlorethamine, was found to be the more effective medical agent and is still used under the brand name Mustargen® for the treatment of Hodgkin's disease.<sup>[12]</sup> In this early stage of development, Gilman already correctly postulated the mode of action for these compounds as alkylation of cellular nucleophiles connected with cell proliferation (compare Chapter 1.2).<sup>[10]</sup>

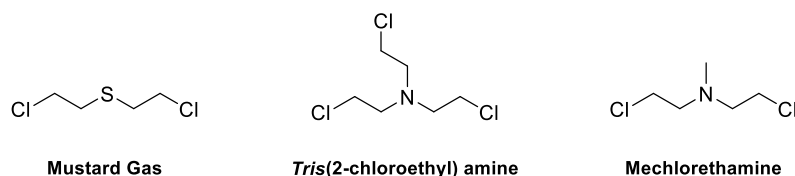


Figure 1: Chemical structures of the chemical warfare agent mustard gas and its nitrogen mustard analogues.

Aliphatic nitrogen mustards like mechlorethamine suffer from severe side effects, since they show a high tendency to form a highly reactive aziridinium ion (compare Scheme 2), that might react with other cell components, such as different proteins and enzymes. To overcome this problem, a series of analogues with aromatic substituents were synthesized, which should exhibit a lower electrophilicity. Indeed, kinetic studies of these compounds showed a reduced reactivity and accordingly a lower toxicity in animal studies.<sup>[13]</sup> By exchanging the substituents of the aromatic moiety, finally a sufficiently water soluble compound with desirable activity was obtained by Everett, Roberts and Ross, that was later entitled Chlorambucil (Figure 2).<sup>[14]</sup> A huge advantage of this compound was the possibility of oral administration in contrast to aliphatic alkylating agents, which had to be applied intravenously. Following this successful approach, efforts were made to synthesize aromatic nitrogen mustards inspired by nature, that should for instance be able to use amino acid transporters or act as antimetabolites in addition to their alkylating abilities.<sup>[15]</sup> Some successful candidates of these investigations were Melphalan or Sarcolysine and Bendamustine (Figure 2), which are still used in clinical applications.<sup>[16]</sup>

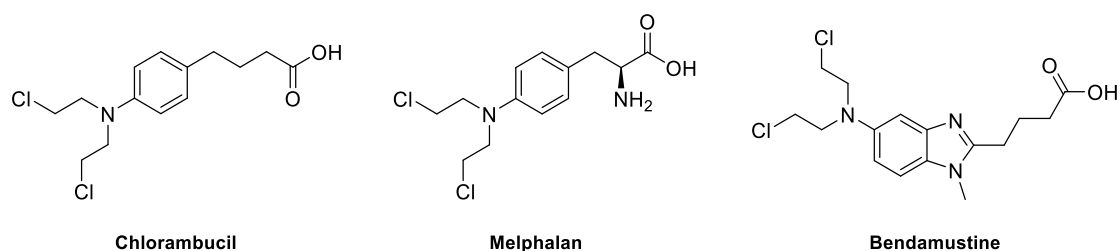
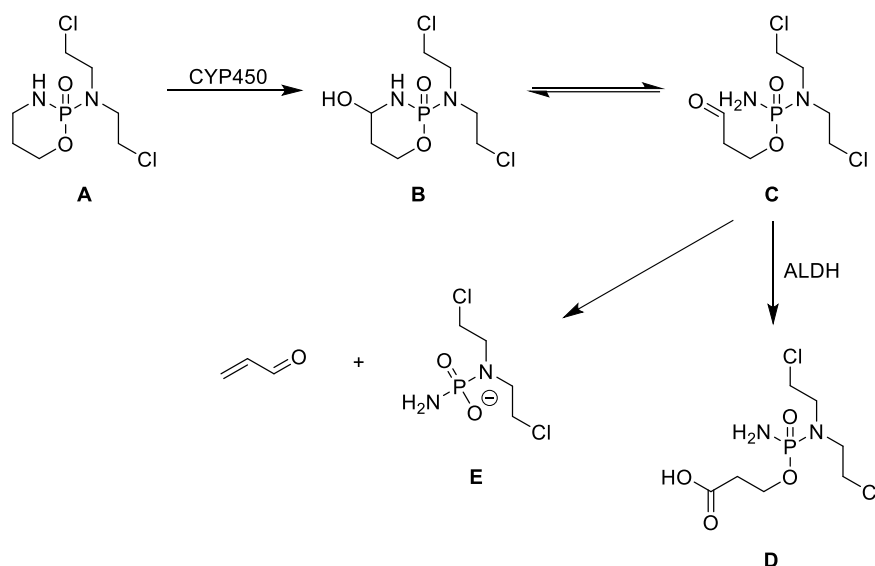


Figure 2: Chemical structures of the aromatic nitrogen mustards Chlorambucil, Melphalan and Bendamustine.

Another attempt to reduce the electrophilicity of nitrogen mustards was the introduction of a phosphoramidate bond to the nitrogen atom, which should be cleaved by cellular phosphoramidases.<sup>[17]</sup> But the initially synthesized phosphoramidate mustard **E** (Scheme 1) could not be used clinically, despite encouraging *in vitro* results.<sup>[18]</sup> Further research in this area provided the cyclic phosphorylated nitrogen mustard cyclophosphamide **A**, that showed significant therapeutic potential and excellent patient tolerance.<sup>[19]</sup> The compound itself serves as a prodrug, which is activated by oxidation of the enzyme cytochrome P450 (CYP450).<sup>[20]</sup> The resulting 4-hydroxycyclophosphamide **B** can isomerize to the open-chain form aldophosphamide **C**. This can either be further oxidized by the aldehyde dehydrogenase (ALDH) to the inactive carboxycyclophosphamide **D** or spontaneously eliminate acrolein, releasing the active metabolite phosphoramidate mustard **E** (Scheme 1).<sup>[18,21,22]</sup> Cyclophosphamide actually represents the most used alkylating agent in clinical application today due to this unique mechanism of activation, while the basic reactivity of its active metabolite is identical to earlier mentioned nitrogen mustards.<sup>[22]</sup>

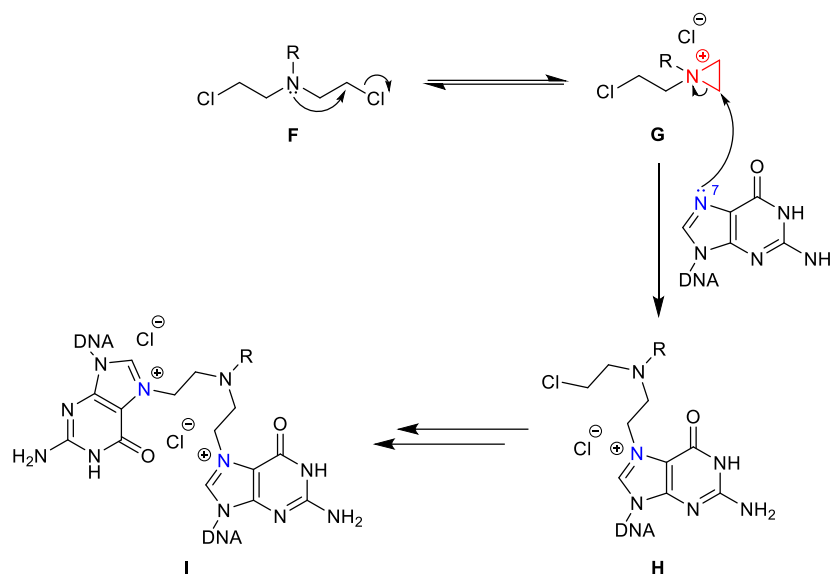


Scheme 1: Metabolic activation of the nitrogen mustard Cyclophosphamide **A**.

## 1.2. Alkylation Mechanism of Nitrogen Mustards

The cytotoxicity of nitrogen mustards arises from their ability to alkylate cellular components such as proteins or DNA, as already hypothesized shortly after their discovery in the mid-20<sup>th</sup> century.<sup>[10,23,24]</sup> Due to their ability of transferring an alkyl group to DNA under physiological conditions, these compounds are categorized as DNA alkylating agents.<sup>[6]</sup> However, this reaction is not limited to malignant cells and other highly proliferative cell types are also impaired, resulting in a vast amount of adverse side effects like bone marrow depression, hair loss and gastrointestinal distress.<sup>[4,6,7,25]</sup>

Generally, the alkylation mechanism of all nitrogen mustard derivatives **F** is a two-step process starting with an intramolecular S<sub>N</sub>2-like substitution of one chloride leaving group by nucleophilic attack of the nitrogen atom (Scheme 2).<sup>[26,27]</sup> The highly electrophilic aziridinium ion **G** is generated, which is quickly attacked by cellular nucleophiles such as DNA bases and the monoalkylation adduct **H** is formed.<sup>[28]</sup> This reaction preferentially occurs at the *N*7-position of the guanine nucleobase and can proceed again with the second reactive 2-chloroethyl moiety, resulting in a covalent bisalkylation adduct **I** (Scheme 2).<sup>[29]</sup> The second alkylation can either take place on the same or the complementary DNA strand, resulting in intrastrand or interstrand crosslinks respectively. Nitrogen mustards have been found to form interstrand crosslinks predominantly at 5'-GNC sequences.<sup>[30]</sup> The resulting DNA alkylation adducts inhibit cellular replication processes and are highly cytotoxic. They might also cause different follow-up reactions including depurination and DNA strand cleavage, which can ultimately lead to apoptosis (programmed cell death).<sup>[9,31]</sup>

Scheme 2: General alkylation mechanism of nitrogen mustards **F**.

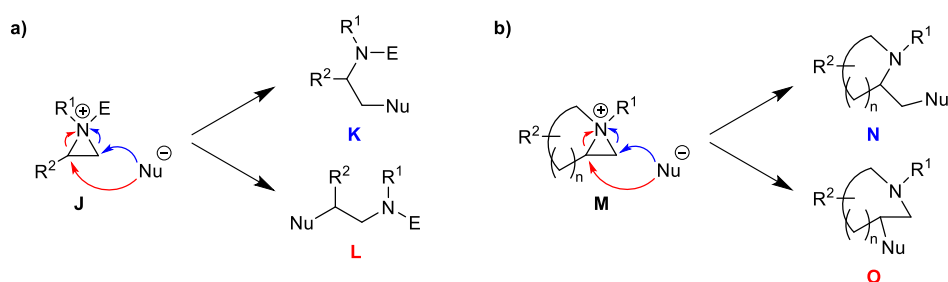
The reaction of nitrogen mustards with nucleophiles under non-acidic conditions always involves the formation of the highly reactive aziridinium ion **G** (Scheme 2), independent of aliphatic,<sup>[24]</sup> aromatic<sup>[27,32]</sup> or phosphoramidate<sup>[33]</sup> residues on the nitrogen atom and its formation has been verified as the rate-determining step of the DNA alkylation mechanism.<sup>[34]</sup> Several computational studies have been performed to get detailed insights into the reactivity of nitrogen mustards. They confirmed the assumed correlation between electrophilicity of the aziridinium intermediate and the activity of the corresponding alkylating agent, while also explaining the preference for *N*<sup>7</sup>-guanine alkylation by favorable thermodynamics.<sup>[35]</sup> Inspection of the activation energies for the formation of the second aziridinium ion, from the respective monoalkylation products, also enabled prediction of the tendency to cross-link DNA strands. Understanding the structure and reactivity of the corresponding aziridinium ions therefore seems to be crucial for the development of new mustard based alkylating agents.

### 1.3. Chemistry of Aziridinium Ions

Aziridinium ions are defined as the quaternary, cationic form of the three-membered aza-heterocycle aziridine. Activation of the strained aziridine ring by an electrophile, for instance provided by a simple protonation, will result in the formation of an aziridinium ion, which is very reactive towards nucleophilic attack.<sup>[36]</sup> The nucleophilic reaction induces C-N bond breaking and opens the small cyclic system, which provides a variety of synthetic applications in organic chemistry,<sup>[37,38]</sup> while also representing the fundamental reaction of nitrogen mustards. Furthermore, this enables access to biologically important, nitrogen-containing molecules such as different aza-sugars and alkaloids.<sup>[39]</sup> Depending on the attacking nucleophile,<sup>[40]</sup> the activating electrophile and the substituents of the aziridinium ion,<sup>[41]</sup> the reaction can proceed with specific regio- and stereoselectivity.<sup>[42]</sup>

For the ring opening of the aziridinium ion **J** two distinct pathways exist, the sterically less hindered attack at the unsubstituted carbon, resulting in product **K** or the attack of the nucleophile at the carbon atom bearing more substituents, which leads to product **L** (Scheme 3a). General predictions of the

preferred reaction products are problematic, because of various other factors influencing the exact product ratio, for instance solvent, temperature and the activating electrophile.<sup>[43,44]</sup> However, especially ring opening reactions with halide nucleophiles have been studied extensively and revealed that hard halides, such as fluoride or chloride, prefer the attack on the less substituted carbon atom (kinetic product **K**), while the attack of soft nucleophiles, for instance bromide or iodide, will preferably generate the thermodynamic product **L**.<sup>[44,45]</sup> In case of bromide and iodide, which are also good leaving groups, the aziridinium ion can be regenerated by nucleophilic attack of the nitrogen atom and equilibration results in almost exclusive appearance of the thermodynamic product **L**. For chloride, the equilibration is much slower, but can also proceed in the same way.



Scheme 3: Nucleophilic ring opening reaction pathways of mono- (a) and bicyclic aziridinium ions (b).

Achieving the thermodynamic product **O** is of particular interest, when bicyclic aziridinium ions **M** are involved in these ring opening reactions (Scheme 3b), since the nucleophilic attack on the sterically more hindered carbon atom leads to a ring expansion that provides access to enantiopure aza-heterocycles, such as piperidines or azepanes.<sup>[38,46–50]</sup> Again, this reaction is influenced by many factors, including the substitution pattern of the non-aziridinium heterocycle,<sup>[41,44,51]</sup> which leads to a mixture of the thermodynamic product **O** and the kinetic product **N**. Compared to the monocyclic aziridinium ions **J**, the preparation of bicyclic aziridinium ions **M** is more complicated due to the increased ring strain in the resulting bicyclic system. The second heterocycle is therefore usually generated *via* intramolecular reaction of the nucleophilic nitrogen atom and a leaving group attached to the heterocyclic precursor, similar to the aziridinium ion formation of nitrogen mustards (compare Scheme 2). Although, these intramolecular reactions are faster in comparison to their intermolecular counterparts, they can be further accelerated by the geminal dialkyl effect to facilitate the formation of the desired bicyclic system.

#### 1.4. Intramolecular Reactions and the Geminal Dialkyl Effect

The acceleration of an intramolecular reaction by introduction of a geminal substituent in the connective carbon chain is commonly known as the *gem*-dialkyl or *gem*-disubstituent effect.<sup>[52,53]</sup> This phenomenon has been used extensively in organic synthesis to promote challenging cyclization reactions, although a precise explanation is still lacking.<sup>[53–55]</sup> The earliest hypothesis about the origin of the observed rate enhancements was suggested by Thorpe and Ingold in 1915, thus entitled the “Thorpe-Ingold effect”.<sup>[56]</sup> They speculated, that the introduction of a *gem*-dialkyl substituent compresses the internal angle  $\theta$  due to increased steric repulsion of these groups compared to the corresponding unsubstituted homologue (Figure 3a). Consequently, the closer proximity of the reactive centers accelerates the intramolecular

reaction. Several experimental observations, including crystallographic data, later proved their assumption,<sup>[57]</sup> but computational investigations by Schleyer also revealed that the small angle changes of 2-3° cannot exclusively explain the observed rate enhancements.<sup>[58]</sup> An alternative theory was therefore established by Bruice and Pandit, who correlated the acceleration by *gem*-disubstitution with a favorable distribution of reactive *gauche* rotamers.<sup>[59]</sup> This concept was later termed the “reactive rotamer effect” and describes an increase in the population of conformers, in which the correct orientation of the reactive centers promotes the intramolecular reaction (Figure 3b).<sup>[60]</sup>

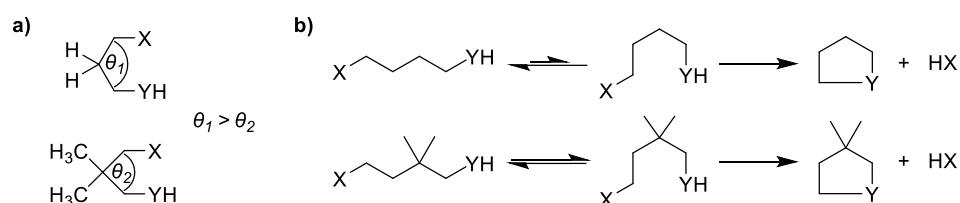
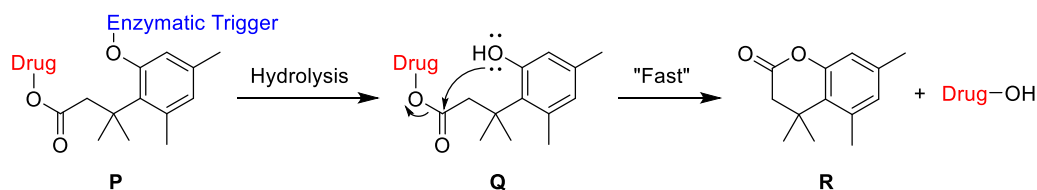


Figure 3: Angle contraction providing the “Thorpe-Ingold effect” (a) and illustration of the “reactive rotamer effect” (b).

Both popular theories have been questioned by several authors, while in the majority of cases both effects contribute to rate enhancements and are therefore combined in the term geminal dialkyl effect. Alternative explanations include the “facilitated transition”,<sup>[61]</sup> “stereopopulation control”,<sup>[62]</sup> and “relief of ground-state strain”<sup>[63]</sup> hypotheses as well as the consideration of a thermodynamic component for small<sup>[64]</sup> and medium sized rings.<sup>[65]</sup> Despite the absence of a concluding explanation for the acceleration of intramolecular reaction rates by the *gem*-dialkyl effect, a variety of cyclization reactions have been promoted by introduction of geminal substituents.<sup>[53–55]</sup>

*Gem*-methylation is also an important concept in drug design and has been used to increase the stability, lipophilicity or activity of several small molecule drugs and biologically active peptides.<sup>[66]</sup> Another interesting application is the design of a prodrug concept by combination of the geminal dialkyl effect with the “buttressing effect”,<sup>[67]</sup> resulting in strong conformational restrictions and thus extreme enhancements of reaction rates, known as the “trimethyl lock”.<sup>[68]</sup> The carboxylic acid function of a methylated hydrocoumarinic acid is therefore connected with the selected drug, while the phenol group is coupled with an “enzymatic trigger” (compare compound **P**, Scheme 4). This moiety consists of a functional group, which can be cleaved enzymatically, for instance by an esterase or phosphatase. After enzymatic hydrolysis of the prodrug **P**, the nucleophilic phenol of compound **Q** attacks the ester and releases the active drug *via* formation of the lactone **R**, accelerated by the “trimethyl lock” (Scheme 4). This approach has been successfully applied to several drugs<sup>[69]</sup> including the anticancer agents Taxol<sup>[70]</sup> and Daunorubicin,<sup>[71]</sup> demonstrating the importance of mechanistic concepts for drug development.



Scheme 4: Graphical illustration of the prodrug concept based on the “trimethyl lock”.

## 2. 3-Chloropiperidines as DNA Alkylating Agents

3-Chloropiperidines can be considered as cyclic analogues of classic nitrogen mustards. Just as their acyclic counterparts they have the ability to react with nucleophiles *via* a highly electrophilic aziridinium ion, accomplished by intramolecular substitution of the chloride leaving group.<sup>[72]</sup> The formation of this intermediate is more restricted due to the bicyclic character of the aziridinium ion and therefore reduces their reactivity, which has been confirmed by kinetic experiments in comparison with the half-mustard 2-chloroethyl diethylamine.<sup>[73]</sup> Inspired by the naturally occurring antibiotic 593A,<sup>[74]</sup> our working group developed a synthetic approach to nitrogen bridged *bis*-3-chloropiperidines as simplified and possibly less reactive analogues of this natural compound (Figure 4). Preliminary studies on double-stranded DNA confirmed the ability of these compounds to efficiently fragment the employed DNA plasmid,<sup>[75]</sup> while electrospray ionization mass spectrometry confirmed the anticipated *N*'-guanosine alkylation products.<sup>[76]</sup> Variation of the linker structure also proved to affect the alkylating abilities of the examined compounds and especially aromatic moieties seemed to reduce the activity of *bis*-3-chloropiperidines.<sup>[75,77,78]</sup> This interesting aspect was examined during studies on different cancer cell lines,<sup>[79,80]</sup> while further mechanistic<sup>[73]</sup> as well as structure-activity relationship studies<sup>[81,82]</sup> of these promising drug candidates were initiated. Therefore, the following chapters briefly present the results of these investigations and provide common strategies for the synthesis of these compounds.

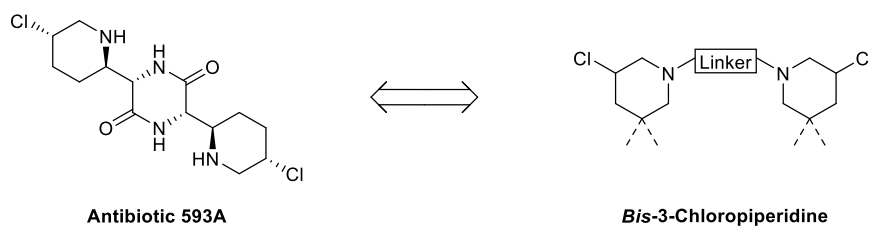
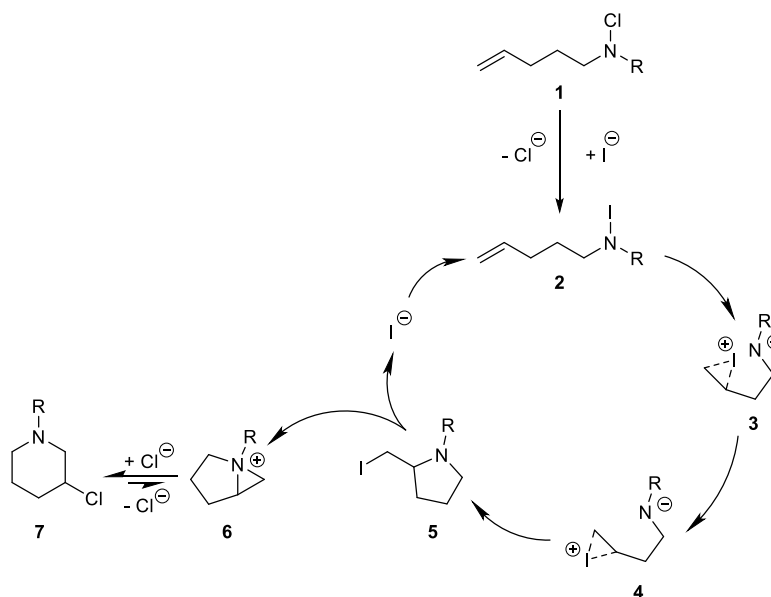


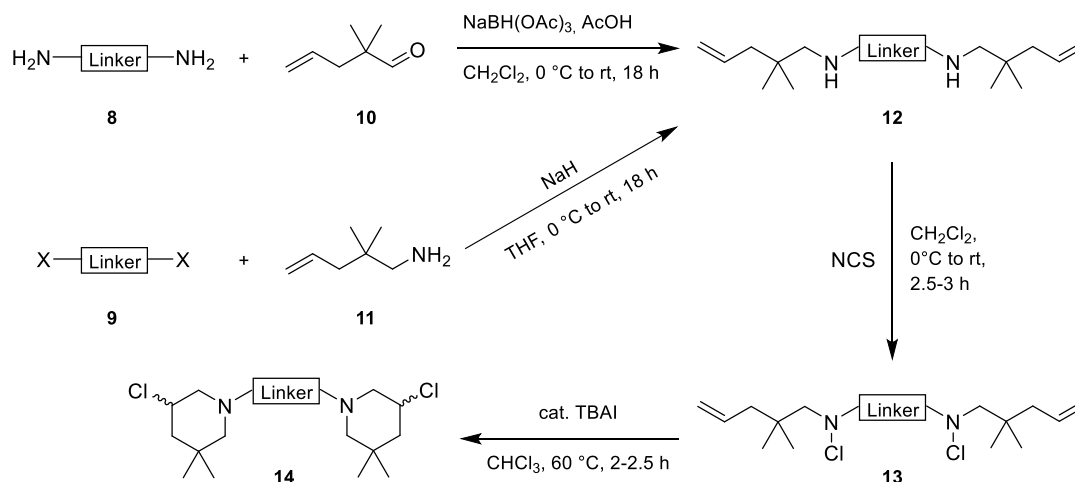
Figure 4: Chemical structures of the natural antibiotic 593A and *bis*-3-chloropiperidines as simplified analogues.

### 2.1. Synthesis of 3-Chloropiperidines

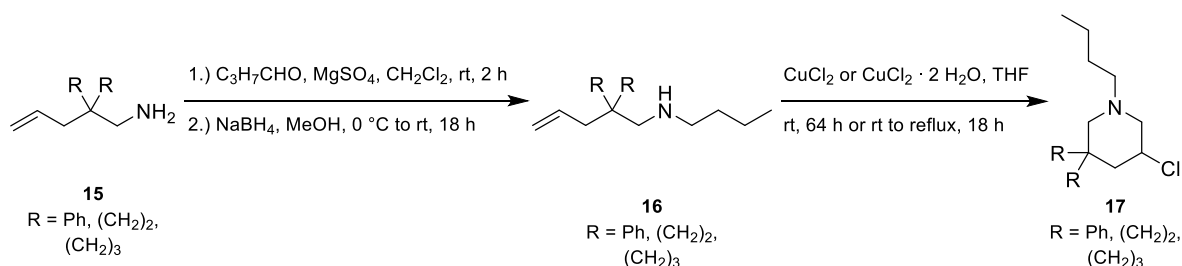
In general, there are two different concepts for the synthesis of 3-chloropiperidines. The formation of the piperidine moiety by cyclization of a linear precursor or modification of readily available heterocycles such as 3-hydroxypiperidine or proline derivatives. The first approach was used for the synthesis of most *bis*-3-chloropiperidine derivatives in our working group and is based on the iodide catalyzed cyclization of unsaturated *N*-chloroamines **1** (Scheme 5).<sup>[83]</sup> The proposed mechanism of this reaction involves a Finkelstein-type halogen exchange, using an iodide salt such as tetrabutylammonium iodide to generate the *N*-iodoamine **2**, which is very reactive and might add to the intramolecular double bond. The resulting iodonium ion **3** undergoes rotation around the single bond, generating compound **4**, which reacts with the intramolecular nitrogen atom in an  $S_N2$  ring opening reaction. The obtained 2-iodomethyl pyrrolidine **5** can then form the bicyclic aziridinium ion **6** and liberate iodide to close the catalytic cycle. Afterwards, the 3-chloropiperidine **7** is obtained *via* ring expansion initiated by nucleophilic attack of a chloride ion (compare Scheme 3b). Equilibration towards the thermodynamic piperidine product is promoted by elevated temperatures.

Scheme 5: Iodide catalyzed cyclization of unsaturated *N*-chloroamines **1** to 3-chloropiperidines **7**.

The reaction generally works for most unsaturated *N*-chloroamines, but employment of the accessible aldehyde precursor 2,2-dimethylpent-4-enal<sup>[84]</sup> **10** ensures rapid formation of the desired heterocycle by means of the geminal dialkyl effect (Scheme 6). The original strategy for the synthesis of *bis*-3-chloropiperidines was developed for the application of readily available diamine precursors **8** and involves a double reductive amination using sodium triacetoxyborohydride to yield the unsaturated diamine **12**.<sup>[75]</sup> However, utilization of 2,2-dimethylpent-4-enyl amine **11** allows modification of this procedure to grant access to a broad range of precursors (compare Chapter 4.1).<sup>[79]</sup> The starting material **9** with a suitable leaving group, for instance a halide or a sulfonate ester, can therefore react with the primary amine **11**, previously deprotonated by sodium hydride. The obtained unsaturated diamine **12** is then converted to the corresponding *bis-N*-chloroamine **13** in the presence of *N*-chlorosuccinimide. These compounds can be easily purified by column chromatography and are afterwards cyclized to the desired *bis*-3-chloro-5,5-dimethylpiperidines **14** using catalytic amounts of tetrabutylammonium iodide.

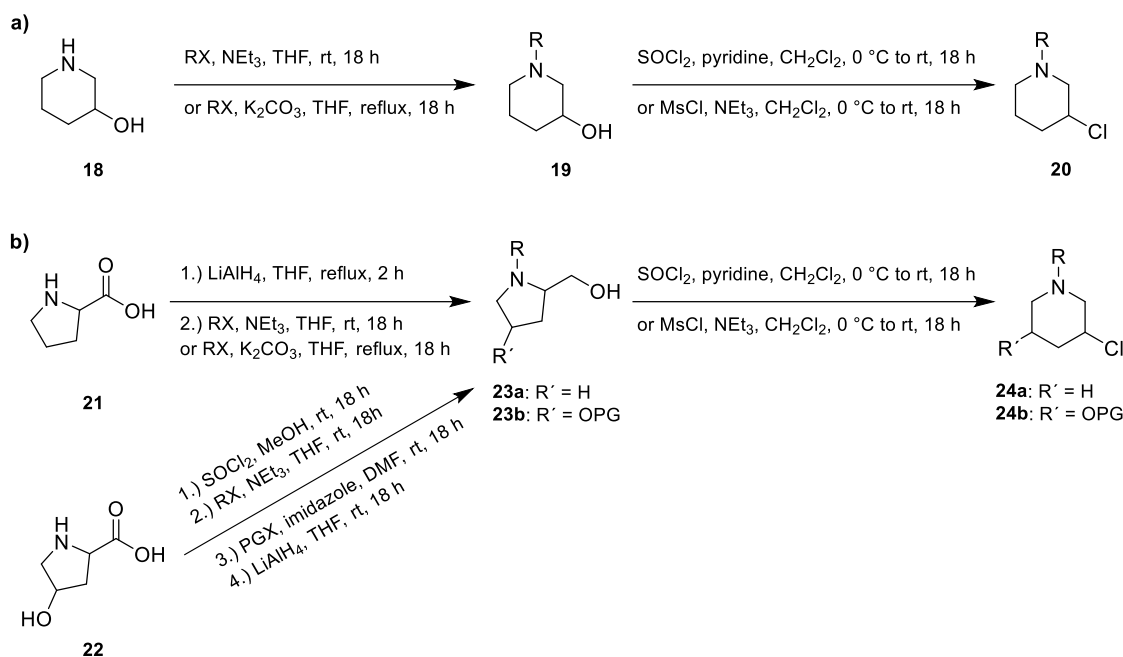
Scheme 6: General synthetic approach to *bis*-3-chloro-5,5-dimethylpiperidines **14** incorporating various linker structures.

This concept has been applied for a variety of different linker structures, such as linear and cyclic aliphatic compounds,<sup>[75]</sup> various lysine esters and amides<sup>[77,78,85]</sup> as well as substituted and unsubstituted aromatic systems.<sup>[75,79]</sup> Furthermore, several monofunctional 3-chloropiperidines<sup>[82,83]</sup> and the first *tris*-3-chloropiperidine<sup>[79]</sup> have been obtained by this strategy. Similar approaches to 3-chloropiperidines have been published, including cyclization of *N*-chloroamines using copper(I)<sup>[86]</sup>, Pd(0)<sup>[87]</sup> and samarium(II)<sup>[88]</sup> catalysts as well as one-pot chlorination/cyclization procedures *via* iodine,<sup>[89]</sup> Pd(II)acetate<sup>[90]</sup> and copper(II)chloride.<sup>[91]</sup> The method using copper(II)chloride proved to be relatively mild, since strong oxidizing agents such as *N*-chlorosuccinimide are omitted, and was therefore used in the synthesis of sensitive 5,5-disubstituted 3-chlorobutylpiperidines, designed for a special application, using the geminal disubstituent effect (see Chapter 2.3 and Chapter 4.3).<sup>[81]</sup> The primary amines **15**, obtained by allylation and subsequent reduction of readily available nitriles,<sup>[92]</sup> are converted to their secondary analogues **16** by a two-step reductive amination procedure (Scheme 7). First, the corresponding imine is generated using *n*-butanal and magnesium sulfate, followed by reduction with sodium borohydride. The one-pot chlorination/cyclization of these compounds with anhydrous copper(II)chloride or the respective dihydrate affords the desired 3-chloropiperidines **17** after prolonged stirring or heating to reflux (Scheme 7). All of these cyclization methods commonly provide isomeric mixtures with the exact ratio depending on the substituents of the acyclic precursor, due to the unselective addition of the nitrogen atom to the double bond.



Scheme 7: Synthesis of 5,5-disubstituted 3-chlorobutylpiperidines **17** using the one-pot copper(II)chloride procedure.

Another possibility to synthesize 3-chloropiperidines is the use of readily available aza-heterocycles like 3-hydroxypiperidine **18** or proline derivatives **21/22** (Scheme 8). The former approach is rather straightforward, starting with the functionalization of the free amine by simple nucleophilic substitution to yield amino alcohol **19**. Afterwards, the desired chloride group can be obtained either by direct reaction of the alcohol with a chlorination reagent, such as thionyl chloride, or conversion into a suitable leaving group and subsequent nucleophilic substitution to the 3-chloropiperidine **20**, for instance provided by methanesulfonyl chloride (Scheme 8a). This concept has been used by Searcey and coworkers to synthesize analogues of the anticancer drug Azinomycin, bearing one alkylating 3-chloropiperidine moiety<sup>[93]</sup> as a substitute for the unstable bicyclic aziridine, as well as anthraquinone based DNA intercalators, which incorporate two alkylating agents such as 3-chloropiperidines, 2-chloromethylpyrrolidines and 2-chloromethylpiperidines.<sup>[94]</sup>



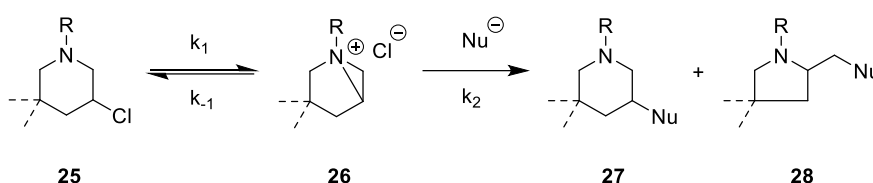
Scheme 8: General synthesis of 3-chloropiperidines **20/24** from 3-hydroxypiperidine (**a**) and proline derivatives (**b**).

While the aforementioned compounds were all synthesized racemic, the use of enantiopure 3-hydroxypiperidine could provide access to the corresponding optically active 3-chloropiperidines. However, less expensive naturally occurring alternatives exist in the amino acids proline **21** and 4-hydroxyproline **22** (Scheme 8b). In the first step, D- or L-proline **21** is reduced to the respective prolinol with lithium aluminum hydride and afterwards functionalized by nucleophilic substitution to yield amino alcohol **23a**, comparable to the 3-hydroxypiperidine strategy. In case of the 4-hydroxyproline precursors **22**, the carboxylic acid is usually converted into a methyl ester, followed by functionalization of the amine as well as protection of the alcohol group and subsequent reduction of the ester to obtain the substituted alcohol **23b**. The final chlorination reaction, using conditions similar to the 3-hydroxypiperidine approach, again makes use of the ring expansion *via* bicyclic aziridinium ion **6** (compare Scheme 3b), to obtain the thermodynamic 3-chloropiperidine products **24a** and **24b** respectively. The ring opening reaction proceeds stereoconvergent,<sup>[44,46,48,50]</sup> therefore the absolute configuration of the 3-chloropiperidines is determined by the corresponding amino acid precursor.

Using this synthetic strategy, the two enantiomers of monofunctional 3-chloropiperidines have been prepared,<sup>[73,82]</sup> showing significantly different activity against isolated DNA and various cancer cell lines.<sup>[82]</sup> Furthermore, this ring expansion approach has been used in one of the first synthesis of a 3-chloropiperidine<sup>[95]</sup> and is still an important strategy to obtain optically active 3-substituted piperidines, which represent essential building blocks in natural products with various biological activities.<sup>[46–49,96]</sup> The presented strategies were used in our working group to obtain all biologically and kinetically tested derivatives,<sup>[73,75–82,85]</sup> while literature provides many other synthetic approaches to obtain 3-substituted piperidine compounds.<sup>[97]</sup>

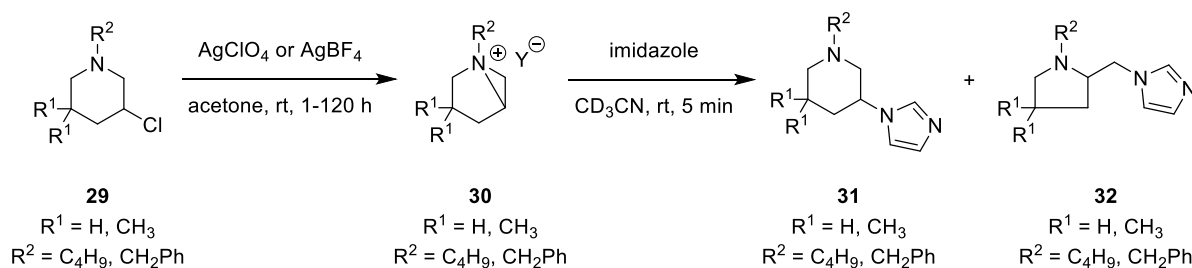
## 2.2. 3-Chloropiperidines: Mechanism of Action

The reaction of 3-chloropiperidines **25** with nucleophiles, such as DNA bases, is suggested to proceed *via* the bicyclic aziridinium ion **26** (Scheme 9), which has been established by NMR spectroscopy<sup>[72]</sup> and electrospray ionization mass spectrometry.<sup>[77]</sup> Once this highly electrophilic intermediate is generated by nucleophilic attack of the nitrogen atom at the C-3 carbon and liberation of the chloride leaving group, it should be rapidly consumed by alkylation reactions with nucleophilic centers of cellular targets, like the *N7*-position of the guanine nucleobase (compare Scheme 2). The ring opening of the bicyclic system affords a mixture of six-membered piperidine **27** and five-membered pyrrolidine **28** products, while the exact ratio of these compounds depends on the aforementioned factors for reactions of aziridinium ions with nucleophiles (compare Chapter 1.3).



Scheme 9: General mechanism for the reaction of 3-chloropiperidines **25** with nucleophiles.

Since the bicyclic aziridinium ion represents a key-intermediate in the alkylation mechanism of 3-chloropiperidines, we initiated detailed structural and kinetic studies of such compounds.<sup>[73]</sup> The structure of these highly reactive intermediates was found to be boat-like by computational analysis.<sup>[41]</sup> The crystal structure of a similar aziridinium ion, obtained by cationic tandem cyclization,<sup>[98]</sup> showed comparable results. Through halide abstraction, using silver salts with weakly coordinating anions, we were able to isolate the aziridinium ions **30** of different 3-chloropiperidines **29** (Scheme 10) and analyzed their reactivity in NMR kinetic studies. Furthermore, we succeeded in crystallization of two compounds, confirming the bicyclic, boat-like structure also in case of our intermediates. Examination of their respective kinetic behavior revealed remarkable reactivity differences for the formation as well as the nucleophilic reactions of C5 *gem*-methylated and unsubstituted aziridinium ions (see Chapter 4.2). We assumed, that the accelerated formation of the *gem*-methylated intermediates is a result of the geminal dialkyl effect (compare Chapter 1.4), which increases the rate of the intramolecular cyclization and addressed this interesting observation in a separate study (see Chapter 4.3).



Scheme 10: Reaction conditions for isolation and subsequent nucleophilic reaction of the bicyclic aziridinium ions **30**.

However, the reaction of all aziridinium ions with imidazole, as a model nucleophile for DNA, proceeded immediately at room temperature and preferably afforded the piperidine product **31** for the *gem*-methylated compounds, while the pyrrolidine **32** was favored for the unsubstituted aziridinium ions (Scheme 10). This preference is in accordance with studies on the ring opening reactions of other bicyclic aziridinium ions<sup>[46,48,51]</sup> and was similarly obtained by direct reaction of the corresponding 3-chloropiperidines with excess imidazole.<sup>[73]</sup>

With this observation we investigated the kinetics of this reaction quantitatively employing Equation 1. The bicyclic intermediate is very reactive and will be consumed almost immediately after its generation. Therefore, the concentration of the highly reactive aziridinium ion **26** essentially does not change during the reaction and the steady-state approximation ( $\frac{d[26]}{dt} = 0$ ) can be applied to Equation 1. Accordingly, the rate law can be rewritten as Equation 2 and with the additional assumption that the reaction with the nitrogen nucleophile (Nu) is much faster than the reaction back to the starting material ( $k_2 \gg k_{-1}$ ), the term can be simplified to Equation 3. Applying this to Equation 4, which represents the rate of formation of the ring opening products **27** and **28**, ultimately yields Equation 5, showing that the product formation is only dependent on the rate of aziridinium ion formation. Accordingly, the formation of the aziridinium ion ( $k_1$ ) is the rate-determining step of the reaction depicted in Scheme 9 and we can directly correlate the rate of product formation with the decrease in concentration of the 3-chloropiperidine ( $-\frac{d[25]}{dt}$ ).

$$\frac{d[26]}{dt} = k_1[25] - k_{-1}[26] - k_2[26][\text{Nu}] = 0 \quad (1)$$

$$[26] = \frac{k_1[25]}{k_{-1} + k_2[\text{Nu}]} \quad (2)$$

$$[26] \approx \frac{k_1[25]}{k_2[\text{Nu}]} \quad (3)$$

$$\frac{d[27/28]}{dt} = k_2[26][\text{Nu}] \quad (4)$$

$$\frac{d[27/28]}{dt} = \frac{k_2 k_1 [25] [\text{Nu}]}{k_2 [\text{Nu}]} = k_1 [25] = -\frac{d[25]}{dt} \quad (5)$$

Consequently, NMR kinetic studies in aqueous solution with 2'-desoxyguanosine, as a nucleophile which appropriately resembles DNA, were performed.<sup>[73]</sup> The decrease of the 3-chloropiperidine signals was monitored by <sup>1</sup>H-NMR spectroscopy, resulting in simple first order kinetics for the examined compounds. Comparison of the resulting rate constants showed similar results to our established DNA cleavage assay<sup>[75,77,78,82]</sup> and thus provides an effective method for the initial determination of the reactivity of 3-chloropiperidine derivatives (see Chapter 4.3). In general, we developed a new approach to verify the structure-activity relationship of our alkylating agents and further optimize their reactivity prior to complex biological studies.

### 2.3. Structure-Activity Relationship

In our previous studies on bridged *bis*-3-chloropiperidines (compare Figure 4) we established a method to classify the reactivity of these compounds by their ability to fragment circular double stranded DNA.<sup>[75,77,78]</sup> The alkylating agents were incubated with DNA plasmids for 3 hours at 37 °C in aqueous, buffered solution at different concentrations (usually 0.5 μM, 5 μM and 50 μM). Afterwards, a gel electrophoretic analysis<sup>[99]</sup> was performed to determine the alkylating activity of the respective compound, judged by the fluorescence intensity of the stained DNA bands (Figure 5a). The naturally occurring supercoiled form of the DNA plasmid (SC) is very dense and therefore moves quickly through the gel, this is for instance visible as an intense band of unreacted SC-plasmid at the bottom of the gel for the control lane (Figure 5a). If a DNA strand break is induced by reaction with the alkylating agent (compare Chapter 1.2), the supercoiled plasmid relaxes and an open circular DNA form (OC) is obtained (compare Figure 5a). The electrophoretic mobility of this species is reduced compared to the supercoiled form.<sup>[100]</sup> The increase in intensity of the corresponding OC band, as well as the decrease in intensity of the supercoiled form, can therefore be correlated with the alkylating activity of the examined *bis*-3-chloropiperidine. From the relative intensities of the bands of supercoiled as well as the open circular forms, determined at different compound concentrations, an effective concentration that causes conversion of half of the SC-DNA to the OC-DNA can be calculated (using the GeneTools™ software by PerkinElmer®) and expressed as an EC<sub>50</sub> value. These values provide easier comparison of the different alkylating activities compared to the visual inspection of the corresponding gel electrophoretic analyses and will therefore be discussed as results of these DNA cleavage assays in most cases.

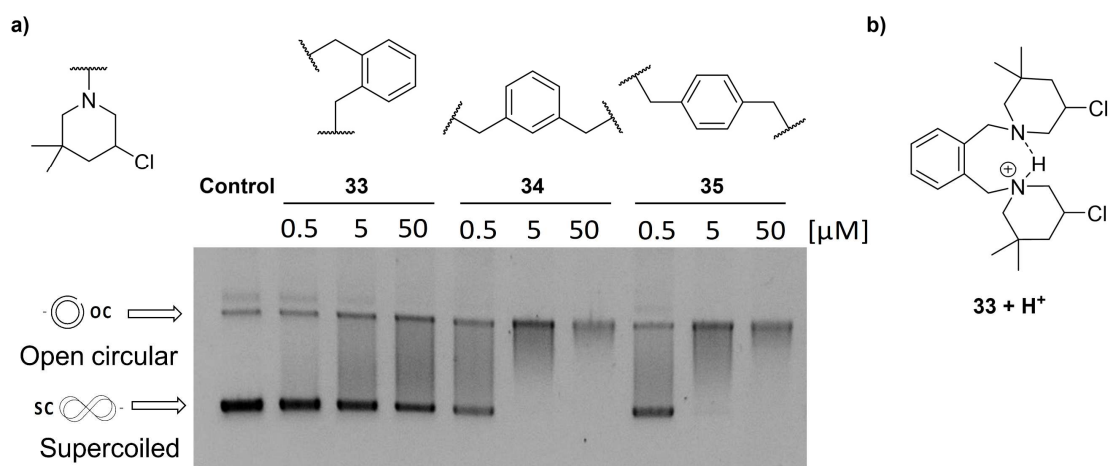


Figure 5: DNA cleavage assay of *bis*-3-chloropiperidines **33-35** (a, modified<sup>[79]</sup>) and hydrogen bonding in **33 + H<sup>+</sup>** (b).

As previously mentioned, the introduction of an aromatic linker<sup>[75]</sup> or the attachment of an aromatic moiety to the bridging lysine linker<sup>[77,78]</sup> seemed to reduce the alkylating activity of the respective *bis*-3-chloropiperidines compared to similar aliphatic linkers. Since the introduction of an aromatic nitrogen substituent was successfully used to reduce the reactivity of nitrogen mustards (compare Chapter 1.1), which are still clinically used anticancer drugs, we chose to particularly study aromatic *bis*-3-chloropiperidines. Several questions concerning the aromatic linker structure were addressed in this study (see also Chapter 4.1).<sup>[79]</sup> Since former analyses only examined a *para*-xylene linker **35**, the

effect of varying the relative position of the two 3-chloropiperidine units was investigated. Furthermore, the influence of different substituents on the aromatic linker as well as the introduction of an aromatic heterocycle and finally the impact of a third reactive 3-chloropiperidine unit was explored.

As a comparison, we added *bis*-3-chloropiperidines containing a flexible pentyl- and a more rigid cyclohexyl-linker to the study, which already showed similar activities in a previous study ( $EC_{50} \approx 1$ ).<sup>[75]</sup> DNA cleavage assays were performed as previously mentioned and Figure 5a illustrates the results for the variation of the substitution pattern. Clearly, the *ortho*-xylene compound **33** is less reactive compared to the *meta*- **34** and *para*-xylene linkers **35**. Even at the highest concentration (50  $\mu$ M) almost no reactivity can be detected ( $EC_{50} \approx 89$ ), while the other two compounds seem to be quite similar in terms of DNA cleavage activity ( $EC_{50} \approx 2$ ). The experiment was repeated using a longer incubation time of 18 h and showed, that *bis*-3-chloropiperidine **33** is still able to efficiently fragment the DNA plasmid. This delayed reactivity could be explained by the formation of an intramolecular hydrogen bond between the two piperidine moieties (see Figure 5b), one being protonated under physiological conditions as shown for compound **33** +  $H^+$ . This would in turn reduce the nucleophilicity and thus the reactivity of this compound, while the increased distance of the *meta* and *para* analogues prevents such interactions. Furthermore, the increased steric hindrance, due to the *ortho* orientation in *bis*-3-chloropiperidine **33**, could prevent an efficient attack of the nucleophilic centers of the DNA plasmid, an effect that has been previously observed after introduction of bulky lysine esters.<sup>[77]</sup>

The effects of additional substituents on the aromatic linker as well as for the introduction of an aromatic heterocycle were more subtle and are therefore evaluated from the respective  $EC_{50}$  values.<sup>[79]</sup> Although, there is no direct conjugation between the aromatic linker and the nucleophilic nitrogen of the 3-chloropiperidines, the inductive effects provided by the different substituents seem to affect the activity of the examined compounds (Figure 6). Similar effects have been observed for nucleophilic reactions of substituted benzyl amines,<sup>[101]</sup> which appears to be a suitable comparison for our system since a nucleophilic attack of the benzylic piperidine nitrogen is necessary to generate the reactive aziridinium intermediate (compare Chapter 1.2). The methoxy **36** as well as the methyl ester **38** substituents provide negative inductive effects, just as the pyridine linker **37**, and therefore reduce the reactivity of the respective *bis*-3-chloropiperidines compared to the unsubstituted homologue **34** (Figure 6). The effect is small but still detectable, while the introduction of a third 3-chloropiperidine moiety in compound **39** unintuitively reduces the reactivity by one order of magnitude. As already discussed for the *ortho*-xylene linker **33**, steric hindrance, in this case caused by the third 3-chloropiperidine unit, might inhibit the nucleophilic attack of the guanine nucleobases and therefore hamper the reactivity of compound **39**.

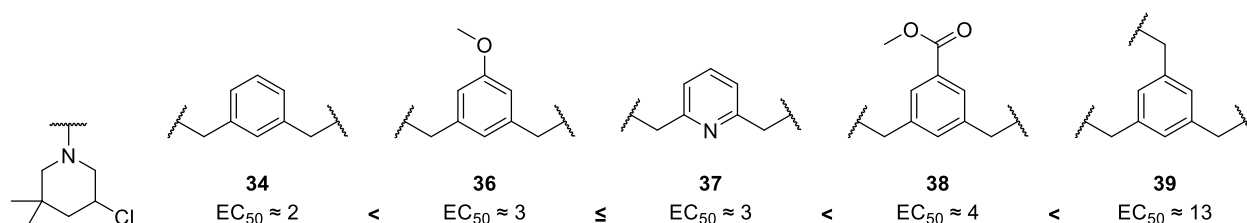


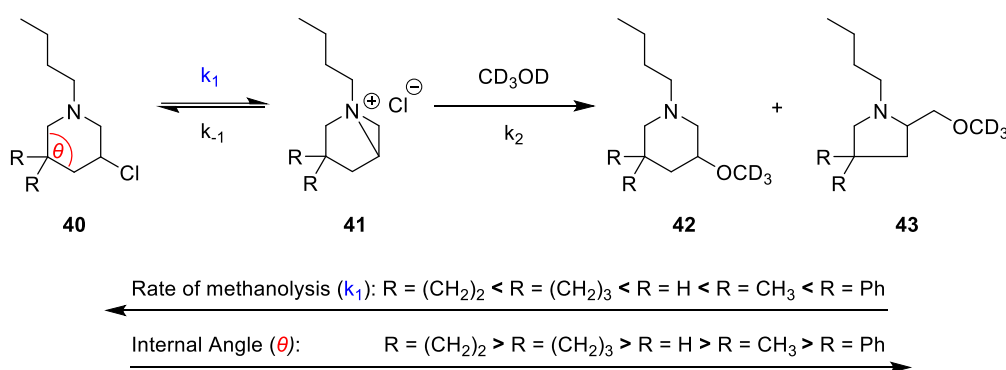
Figure 6:  $EC_{50}$  values of substituted aromatic *bis*-3-chloropiperidines **34**, **36**-**38** and *tris*-3-chloropiperidine **39**

Since the aliphatic, thus electron-donating, pentyl- and cyclohexyl linkers were more reactive ( $EC_{50} \approx 1$ ) compared to all aromatic compounds, the DNA cleavage activity of bridged *bis*-3-chloropiperidines seems to correlate with the nucleophilicity, and therefore the electron density, of the nucleophilic piperidine nitrogen atom as well as with the steric hindrance provided by the substitution pattern. This result supports our investigation about the reaction mechanism of 3-chloropiperidines, considering the formation of the bicyclic aziridinium ion **26** (compare Scheme 9) by intramolecular nucleophilic substitution as the rate-determining step of the alkylation reaction (compare Chapter 2.2). A reduced reactivity of the respective alkylating agent might result in a favorable side effect profile, as successfully demonstrated by the development of aromatic nitrogen mustards, such as Chlorambucil (compare Chapter 1.1). Encouraged by these results, cytotoxicity studies on different cancer cell lines, namely colorectal and pancreatic adenocarcinoma as well as ovarian carcinoma, were initiated with this set of aromatic *bis*-3-chloropiperidines.<sup>[79]</sup> The investigation demonstrated the potential of our compounds as anticancer drugs, while most of them showed an increased cytotoxicity in comparison to Chlorambucil. Especially interesting results were obtained against pancreatic cancer cells, as all aromatic *bis*-3-chloropiperidines were about 200 times more cytotoxic compared to Chlorambucil against this specific cell line (see Chapter 4.1). This effect was exclusively attributed to the aromatic linker structures and was reflected by introduction of different aromatic esters to lysine-bridged *bis*-3-chloropiperidines<sup>[85]</sup> as well as for monofunctional 3-chloropiperidines.<sup>[82]</sup> Further examination of this phenomenon could exclude a selective transport mechanism for the aromatic compounds, while the cytotoxic effects towards cancer cells could be associated with damage to the cellular DNA,<sup>[79]</sup> which does not significantly vary among the tested cell lines. Ultimately, the increased cytotoxicity against pancreatic cancer cells could be explained by an insufficient cellular response to the DNA damage induced by aromatic 3-chloropiperidines, which was not observed for other cancer cell lines.<sup>[80]</sup>

The previously mentioned studies confirm an effect towards the reactivity of 3-chloropiperidines caused by the electronic nature, structure and substitution pattern of the linker, while showing neglectable effects of the linker length and rigidity. Furthermore, the nitrogen substituent as well as the influence of stereochemistry (compare Chapter 2.1) seem to be especially important in studies on cancer cell lines, as there are additional effects in cellular environment, such as uptake and metabolism of the alkylating agents. Nonetheless, our primary cellular study on monofunctional 3-chloropiperidines revealed an unexpected effect of the 5,5-dimethylation of the central piperidine ring.<sup>[82]</sup> This structural feature was originally introduced due to the accessible synthesis of the 2,2-dimethylpent-4-enal precursor and will also accelerate the iodide catalyzed cyclization to the desired 3-chloropiperine moiety (compare Chapter 2.1) *via* the geminal dialkyl effect (compare Chapter 1.4). The absence of this *gem*-methylation substantially reduced the alkylating activity of the corresponding 3-chloropiperidine, which was also shown in NMR kinetic experiments (see also Chapter 4.2).<sup>[73]</sup> Taken together with our studies about the reaction mechanism of these compounds (compare Chapter 2.2), these results indicate the participation of the geminal dialkyl effect in the formation of the reactive bicyclic aziridinium ion **26** (compare Scheme 9). Since this intramolecular reaction is the rate-determining step for the reaction of 3-chloropiperidines with nucleophiles (compare Equation 5), the 5,5-dimethylation will accelerate the cyclization and therefore enhance the reactivity of the *gem*-methylated compound in comparison with the unsubstituted homologue. The effect of this rate enhancement by geminal ring methylation even

exceeded the impact of different nitrogen substituents in DNA cleavage assays as well as in kinetic studies of monofunctional 3-chloropiperidines<sup>[79]</sup> and was therefore further evaluated in another kinetic study (see Chapter 4.3).

The intramolecular reaction of the nucleophilic nitrogen atom and the chloride leaving group in 3-chloropiperidines takes place in a six-membered heterocycle, which fixes the orientation of the reactive centers towards each other. Participation of conformational effects, such as the reactive-rotamer effect (compare Chapter 1.4), can therefore be excluded and the observed rate acceleration should exclusively result from the compression of the internal angle  $\theta$  (compare Figure 3a and Scheme 11). This conclusion was employed in a kinetic study to separate the angle dependent Thorpe-Ingold effect from the reactive-rotamer effect (see Chapter 4.3) and revealed another interesting structure-activity relationship of 5,5-disubstituted 3-chloropiperidines (Scheme 11). The rate of methanolysis of the 3-chlorobutylpiperidine **40** was monitored by <sup>1</sup>H-NMR, similar to the aforementioned NMR kinetics in aqueous solution (see Chapter 2.2 and Chapter 4.2). This reaction rate ( $k_1$ ) can be correlated with the formation of the bicyclic aziridinium intermediate **41** and thus the piperidine **42** and pyrrolidine methyl ethers **43** by application of the steady-state approximation (compare Chapter 2.2).



Scheme 11: Thorpe-Ingold effect for the methanolysis of 3-chlorobutylpiperidines **40** via bicyclic aziridinium ions **41**.

The results of these examinations are depicted in Scheme 11 and show that the introduction of sterically demanding substituents, such as methyl and phenyl groups, accelerate the methanolysis compared to the unsubstituted 3-chloropiperidine ( $\text{R} = \text{H}$ ). This increase in reaction rate can be explained by compression of the internal angle  $\theta$  due to the increased steric repulsion of the introduced substituents, which is commonly known as the Thorpe-Ingold effect (compare Chapter 1.4). Contrarily, the internal angle is increased if strained cycloalkyl rings, like cyclopropane and cyclobutane, are chosen as substituents. The small bond angles in these substituents cause readjustment of the remaining carbon bonds, resulting in larger internal  $\theta$  angles and therefore a decrease in the rate of aziridinium ion formation. These angular distortion effects have been confirmed by single crystal XRD as well as DFT calculations for the examined 3-chloropiperidine derivatives.<sup>[81]</sup> Accordingly, a linear correlation between the internal  $\theta$  angle and the rate of methanolysis  $k_1$  was observed, which was also reflected by the experimentally determined Gibbs free energies of activation  $\Delta G^\ddagger$  (see Chapter 4.3). Therefore, adoption of this effect would represent another possibility, beyond the exchange of nitrogen substituents, to fine-tune the reactivity of 3-chloropiperidines for their application as DNA alkylating agents.

## 2.4. Summary and Perspective

In the present work, various 3-chloropiperidine derivatives were synthesized as cyclic analogues of nitrogen mustards and their reactivity as well as their reaction mechanism were studied in detail. These compounds efficiently alkylated DNA in previous studies, just as their acyclic nitrogen mustard analogues. The reaction mechanism of these compounds was confirmed to proceed *via* highly electrophilic bicyclic aziridinium ions, which could be isolated and their structure as well as their reactivity were studied. These investigations confirmed, that the reactive intermediate is readily consumed by attack of different nucleophiles, like imidazole as a model compound for DNA nucleobases. Therefore, the formation of the bicyclic aziridinium ion has been verified as the rate-determining step of the DNA alkylation mechanism. Further evaluation confirmed, that the reaction rate of 3-chloropiperidines with a guanine nucleophile was reduced in comparison to an aliphatic half-mustard, which is most likely due to the increased ring strain of the bicyclic aziridinium intermediate (compare Chapter 2.2 and Chapter 4.2). The reactivity of 3-chloropiperidines towards DNA was shown to depend on their respective nitrogen substituent as well as the C5 piperidine ring substituents and the absolute configuration of the chlorine leaving group, leading to in-depth structure-reactivity relationship studies (compare Chapter 2.3).

Consequently, different methods for the synthesis of such derivatives have been used, such as initial construction of the 3-chloropiperidine moiety or rearrangement of existing aza-heterocycles (compare Chapter 2.1). Both methods make use of the equilibrium between the bicyclic aziridinium ion and the 3-chloropiperidine to achieve a clean transformation to the desired heterocycle (compare Scheme 3 and Scheme 5). The synthesis of *bis*-3-chloropiperidine derivatives is commonly carried out by an established bidirectional procedure, including the construction of an unsaturated diamine linker which is converted to the *bis*-*N*-chloroamine and subsequently cyclized to the bridged *bis*-3-chloropiperidine (compare Scheme 6 and Chapter 4.1). This strategy has been used to obtain several derivatives of these alkylating agents connected by aliphatic linkers as well as substituted aromatic compounds and various lysine esters and amides. A similar approach was used for the synthesis of C5 substituted 3-chloropiperidines, which combines the chlorination and cyclization steps in a copper(II) catalyzed one-pot procedure (compare Scheme 7 and Chapter 4.3). In contrast, the synthesis of optically active 3-chloropiperidines is achieved by stereoconvergent ring expansion of naturally occurring heterocycles, such as enantiopure proline derivatives (compare Scheme 8).

Structure-activity relationship studies of the synthesized 3-chloropiperidines were carried out by two different approaches, the first being our well-established *in vitro* DNA cleavage assay (compare Figure 5a and Chapter 2.3). This method evaluates the reactivity of these alkylating agents in terms of their ability to convert a supercoiled DNA plasmid into the open circular form, resulting from DNA strand breaks after alkylation. Examination of *bis*-3-chloropiperidines with various linker structures revealed, that the reactivity of these compounds is strongly influenced by the electronic nature of the linker as well as the steric hindrance provided by different additional substituents and their relative orientation. Sterically demanding substituents or an unfavorable orientation of the 3-chloropiperidine moieties reduces their alkylating activity (compare Figure 5a), while the length or rigidity of the linker has a minor effect. Furthermore, electron-withdrawing substituents, such as aromatic linkers, also reduced the activity of these compounds, similar to the reduced reactivity of aromatic nitrogen mustards compared

to their aliphatic analogues (compare Chapter 1.1). This effect was further enhanced by the introduction of additional electron-withdrawing substituents to the aromatic linker (compare Figure 6). In addition, these *bis*-3-chloropiperidines with aromatic linker structures as well as those with bridging lysine esters and amides, containing appended aromatic substituents, showed an impressive cytotoxicity, in most cases much higher than Chlorambucil, especially against pancreatic cancer cells (see Chapter 4.1). In-depth biological studies later showed, that this phenomenon is attributed to an insufficient cellular response of this specific cell line against the alkylation of their cellular DNA by these aromatic 3-chloropiperidines.

During such DNA cleavage studies on monofunctional 3-chloropiperidines a significant effect of the C5 *gem*-methylation of the piperidine heterocycle was noticed, initiating detailed kinetic studies to explain this particular issue. Therefore, a new NMR kinetic method was established which utilizes the fact, that the formation of the reactive aziridinium ion is the rate-determining step for the reaction of 3-chloropiperidines with nucleophiles (compare Scheme 9). The consumption of the 3-chloropiperidine was monitored by <sup>1</sup>H-NMR and the resulting first order kinetics could be compared, showing similar results to the aforementioned DNA cleavage assays. These investigations verified, that the geminal methyl groups in C5 position accelerate the formation of the bicyclic aziridinium intermediate, and therefore the reaction rate of the alkylation *via* the geminal dialkyl effect (see Chapter 4.2). More specific, the observed rate enhancement was confirmed to be the result of an angle dependent Thorpe-Ingold effect by additional kinetic studies, in which this effect could be separated from competing conformational effects and validated by single crystal XRD as well as DFT calculations (see Chapter 4.3). Accordingly, a new structure-activity relationship was established using different *gem*-substituents at the C5 carbon of the 3-chloropiperidine ring to decrease or increase the reaction rate, compared to the unsubstituted homologue (compare Scheme 11).

In conclusion, our studies confirm the proposed reaction mechanism of 3-chloropiperidines with nucleophiles and show their potential application as cyclic analogues of nitrogen mustards. Their ability to efficiently alkylate DNA, even against different cancer cell lines, combined with their accessible synthesis and the possibility to fine-tune their reactivity, using various nitrogen and piperidine ring substituents, makes them promising candidates for the development of new anticancer drugs.

### 3. References

- [1] R. K. Singh, S. Kumar, D. N. Prasad, T. R. Bhardwaj, *European journal of medicinal chemistry* **2018**, *151*, 401.
- [2] B. A. Chabner, T. G. Roberts, *Nature Reviews Cancer* **2005**, *5*, 65.
- [3] a) E. Chu, V. T. DeVita, *Physicians' cancer chemotherapy drug manual 2015*, Jones & Bartlett Learning, Burlington, MA, **2015**; b) D. Fu, J. A. Calvo, L. D. Samson, *Nature Reviews Cancer* **2012**, *12*, 104.
- [4] M. R. P. D. Alison (Ed.) *The Cancer Handbook*, John Wiley & Sons Inc, Chichester, UK, **2004**.
- [5] K. O. Alfarouk, C.-M. Stock, S. Taylor, M. Walsh, A. K. Muddathir, D. Verduzco, A. H. H. Bashir, O. Y. Mohammed, G. O. Elhassan, S. Harguindey et al., *Cancer cell international* **2015**, *15*, 71.
- [6] C. Avendaño, J. C. Menéndez, *Medicinal chemistry of anticancer drugs*, Elsevier Science Ltd, Amsterdam, **2015**.
- [7] R. Airley, *Cancer chemotherapy*, J. Wiley, Chichester, West Sussex, Hoboken, NJ, **2009**.
- [8] K. W. Kohn, *Cancer research* **1996**, *56*, 5533.
- [9] L. P. Bignold, *Anticancer research* **2006**, *26*, 1327.
- [10] A. Gilman, F. S. Phillips, *Science* **1946**, *103*, 409.
- [11] a) A. Gilman, *The American Journal of Surgery* **1963**, *105*, 574; b) L. S. Goodman, M. M. Wintrobe, *Journal of the American Medical Association* **1946**, *132*, 126.
- [12] L. O. Jacobson, C. L. Spurr, *Journal of the American Medical Association* **1946**, *132*, 263.
- [13] a) G. A. R. Kon, W. C. J. Ross, *Nature* **1948**, *162*, 824; b) W. C. J. Ross, *The Journal of organic chemistry* **1949**, *183*; c) J. L. Everett, W. C. J. Ross, *The Journal of organic chemistry* **1949**, 1972.
- [14] J. L. Everett, J. J. Roberts, W. C. J. Ross, *The Journal of organic chemistry* **1953**, 2386.
- [15] a) F. Bergel, J. A. Stock, *The Journal of organic chemistry* **1954**, 2409; b) W. Ozegowski, D. Krebs, M. Wunderwald, *Journal für Praktische Chemie* **1963**, *20*, 166; c) W. Ozegowski, D. Krebs, *Journal für Praktische Chemie* **1965**, *29*, 18; d) W. Ozegowski, M. Wunderwald, D. Krebs, *Journal für Praktische Chemie* **1959**, *9*, 54.
- [16] a) F. Bergel, V. C. E. Burnop, J. A. Stock, *The Journal of organic chemistry* **1955**, *0*, 1223; b) L. F. Larionov, A. S. Khokhlov, E. N. Shkodinskaja, O. S. Vasina, V. I. Troosheikina, M. A. Novikova, *The Lancet* **1955**, *266*, 169; c) W. Ozegowski, D. Krebs, *Journal für Praktische Chemie* **1963**, *20*, 178.
- [17] O. M. Friedman, A. M. Seligman, *Journal of the American Chemical Society* **1954**, *76*, 655.
- [18] O. M. Colvin, *Current pharmaceutical design* **1999**, *5*, 555.
- [19] a) H. Arnold, F. Bourseaux, N. Brock, *Nature* **1958**, *181*, 931; b) N. Brock, *Cancer* **1996**, *78*, 542; c) O. M. Friedman, I. Wodinsky, A. Myles, *Cancer treatment reports* **1976**, *60*, 337.
- [20] a) C. Fenselau, M.-N. N. Kan, S. S. Rao, A. Myles, O. M. Friedman, M. Colvin, *Cancer research* **1977**, *37*, 2538; b) T. K. Chang, G. F. Weber, C. L. Crespi, D. J. Waxman, *Cancer research* **1993**, *53*, 5629.
- [21] P. A. Dockham, M.-O. Lee, N. E. Sladek, *Biochemical Pharmacology* **1992**, *43*, 2453.
- [22] M. Colvin, R. B. Brundrett, M.-N. N. Kan, I. Jardine, C. Fenselau, *Cancer research* **1976**, *36*, 1121.
- [23] a) J. S. Fruton, W. H. Stein, *The Journal of organic chemistry* **1946**, *11*, 571; b) J. S. Fruton, W. H. Stein, M. Bergmann, *The Journal of organic chemistry* **1946**, *11*, 559; c) S. Moore, W. H. Stein, J. S. Fruton, *The Journal of organic chemistry* **1946**, *11*, 675.
- [24] C. Golumbic, J. S. Fruton, M. Bergmann, *The Journal of organic chemistry* **1946**, *11*, 518.
- [25] M. J. Lind, *Medicine* **2016**, *44*, 20.
- [26] C. C. Price, *Annals of the New York Academy of Sciences* **1958**, *68*, 663.
- [27] C. E. Williamson, B. Witten, *Cancer research* **1967**, *27*, 33.
- [28] a) G. P. Warwick, *Cancer research* **1963**, *23*, 1315; b) L. H. Hurley, *Nature Reviews Cancer* **2002**, *2*, 188; c) C. C. Price, H. Akimoto, R. Ho, *The Journal of organic chemistry* **1973**, *38*, 1538; d) C. C. Price, M.-T. L. Yip, *Journal of Biological Chemistry* **1974**, *249*, 6849.
- [29] a) P. Brookes, P. D. Lawley, *The Biochemical journal* **1961**, *80*, 496; b) N. Kondo, A. Takahashi, K. Ono, T. Ohnishi, *Journal of nucleic acids* **2010**, *2010*, 543531; c) M. R. Osborne, D. E. V. Wilman, P. D. Lawley, *Chemical research in toxicology* **1995**, *8*, 316.
- [30] a) Q. Dong, D. Barsky, M. E. Colvin, C. F. Melius, S. M. Ludeman, J. F. Moravek, O. M. Colvin, D. D. Bigner, P. Modrich, H. S. Friedman, *Proceedings of the National Academy of Sciences of the United States of America* **1995**, *92*, 12170; b) J. T. Millard, S. Raucher, P. B. Hopkins, *Journal of the American Chemical Society* **1990**, *112*, 2459; c) S. M. Rink, M. S. Solomon, M. J. Taylor, S. B. Rajur, L. W. McLaughlin, P. B. Hopkins, *Journal of the American Chemical Society* **1993**, *115*, 2551; d) G. B. Bauer, L. F. Povirk, *Nucleic Acids Research* **1997**, *25*, 1211.
- [31] a) K. S. Gates, *Chemical research in toxicology* **2009**, *22*, 1747; b) K. S. Gates, T. Nooner, S. Dutta, *Chemical research in toxicology* **2004**, *17*, 839.

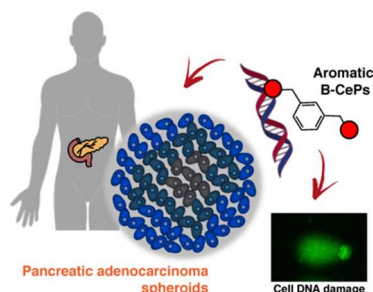
- [32] a) C. J. O'Connor, W. A. Denny, J.-Y. Fan, G. L. Gravatt, B. A. Grigor, D. J. McLennan, *Journal of the Chemical Society, Perkin Transactions 2* **1991**, 1933; b) W. R. Owen, P. J. Stewart, *Journal of pharmaceutical sciences* **1979**, *68*, 992; c) D. C. Chatterji, R. L. Yeager, J. F. Gallelli, *Journal of pharmaceutical sciences* **1982**, *71*, 50.
- [33] E. Watson, P. Dea, K. K. Chan, *Journal of pharmaceutical sciences* **1985**, *74*, 1283.
- [34] A. Polavarapu, J. A. Stillabower, S. G. W. Stubblefield, W. M. Taylor, M.-H. Baik, *The Journal of organic chemistry* **2012**, *77*, 5914.
- [35] a) B. Neog, S. Sinha, P. K. Bhattacharyya, *Computational and Theoretical Chemistry* **2013**, *1018*, 19; b) Z. Ul-Haq, J. D. Madura (Eds.) *Frontiers in computational chemistry*, Bentham Science Publ, Sharjah, UAE, **2015**; c) P. K. Bhattacharyya, S. Sinha, N. Sarmah, B. C. Deka in *Frontiers in computational chemistry* (Eds.: Z. Ul-Haq, J. D. Madura), Bentham Science Publ, Sharjah, UAE, **2015**, pp. 121–186; d) O. Larrañaga, A. de Cózar, F. P. Cossío, *ChemPhysChem* **2017**, *18*, 3390; e) D. J. Mann, *The journal of physical chemistry A* **2010**, *114*, 4486.
- [36] A. Paasche, M. Arnone, R. F. Fink, T. Schirmeister, B. Engels, *The Journal of organic chemistry* **2009**, *74*, 5244.
- [37] a) J. Ranjith, H.-J. Ha, *Molecules* **2021**, *26*; b) T. H. Chuang, K. B. Sharpless, *Organic letters* **2000**, *2*, 3555.
- [38] J. Dolfen, N. N. Yadav, N. De Kimpe, M. D'hooghe, H.-J. Ha, *Advanced Synthesis & Catalysis* **2016**, *358*, 3485.
- [39] a) L. Macha, M. D'hooghe, H.-J. Ha, *Synthesis* **2019**, *51*, 1491; b) R. Akhtar, S. A. R. Naqvi, A. F. Zahoor, S. Saleem, *Molecular diversity* **2018**, *22*, 447; c) I. E. Głowacka, A. Trocha, A. E. Wróblewski, D. G. Piotrowska, *Beilstein journal of organic chemistry* **2019**, *15*, 1722.
- [40] S. Y. Yun, S. Catak, W. K. Lee, M. D'hooghe, N. de Kimpe, V. van Speybroeck, M. Waroquier, Y. Kim, H.-J. Ha, *Chemical communications* **2009**, 2508.
- [41] Y.-H. Lam, K. N. Houk, J. Cossy, D. G. Prado, A. Cochi, *Helvetica chimica acta* **2012**, *95*, 2265.
- [42] a) H.-J. Ha, J.-H. Jung, W. K. Lee, *Asian Journal of Organic Chemistry* **2014**, *3*, 1020; b) S. Stanković, M. D'hooghe, S. Catak, H. Eum, M. Waroquier, V. van Speybroeck, N. de Kimpe, H.-J. Ha, *Chemical Society reviews* **2012**, *41*, 643.
- [43] H. Goossens, D. Hertsen, K. Mollet, S. Catak, M. D'hooghe, F. de Proft, P. Geerlings, N. de Kimpe, M. Waroquier, V. van Speybroeck in *Topics in Heterocyclic Chemistry, Vol. 38* (Eds.: F. de Proft, P. Geerlings), Springer Berlin Heidelberg; Imprint; Springer, Berlin, Heidelberg, **2014**, pp. 1–34.
- [44] E. B. Boydas, G. Tanriver, M. D'hooghe, H.-J. Ha, V. van Speybroeck, S. Catak, *Organic & biomolecular chemistry* **2018**, *16*, 796.
- [45] a) M. D'hooghe, S. Catak, S. Stanković, M. Waroquier, Y. Kim, H.-J. Ha, V. van Speybroeck, N. de Kimpe, *European Journal of Organic Chemistry* **2010**, *2010*, 4920; b) M. D'hooghe, V. van Speybroeck, M. Waroquier, N. de Kimpe, *Chemical communications* **2006**, 1554.
- [46] A. Cochi, D. G. Pardo, J. Cossy, *European Journal of Organic Chemistry* **2012**, *2012*, 2023.
- [47] J. Cossy, C. Dumas, D. G. Pardo, *European Journal of Organic Chemistry* **1999**, *1999*, 1693.
- [48] D. Gomez Pardo, J. Cossy, *Chemistry* **2014**, *20*, 4516.
- [49] J. Choi, N. N. Yadav, H.-J. Ha, *Asian Journal of Organic Chemistry* **2017**, *6*, 1292.
- [50] S. Rioton, A. Orliac, Z. Antoun, R. Bidault, D. Gomez Pardo, J. Cossy, *Organic letters* **2015**, *17*, 2916.
- [51] N. de Kimpe, M. Boelens, J. Contreras, *Tetrahedron Letters* **1996**, *37*, 3171.
- [52] a) A. J. Kirby in *Advances in Physical Organic Chemistry*, Elsevier, **1980**, pp. 183–278; b) B. Capon, S. P. McManus (Eds.) *Neighboring Group Participation*, Springer US, Boston, MA, **1976**; c) M. E. Jung, *Synlett* **1999**, 1999, 843.
- [53] M. E. Jung, G. Piizzi, *Chemical reviews* **2005**, *105*, 1735.
- [54] M. J. O'Neill, T. Riesebeck, J. Cornella, *Angewandte Chemie (International Edition)* **2018**, *57*, 9103.
- [55] E. Brenna, F. Distanti, F. G. Gatti, G. Gatti, *Catalysis Science & Technology* **2017**, *7*, 1497.
- [56] a) R. M. Beesley, C. K. Ingold, J. F. Thorpe, *Journal of the Chemical Society, Transactions* **1915**, *107*, 1080; b) C. K. Ingold, J. F. Thorpe, *The Journal of organic chemistry* **1928**, *0*, 1318; c) C. K. Ingold, S. Sako, J. F. Thorpe, *Journal of the Chemical Society, Transactions* **1922**, *121*, 1177; d) C. K. Ingold, *Journal of the Chemical Society, Transactions* **1921**, *119*, 305.
- [57] a) J. L. Derissen, *Acta Crystallographica Section B Structural Crystallography and Crystal Chemistry* **1970**, *26*, 901; b) J. Jager, T. Graafland, H. Schenk, A. J. Kirby, J. B. F. N. Engberts, *Journal of the American Chemical Society* **1984**, *106*, 139; c) A. J. Kirby, G. J. Lloyd, *Journal of the Chemical Society, Perkin Transactions 2* **1976**, 1753; d) H. Nilsson, L. Smith, *Zeitschrift für Physikalische Chemie* **1933**, *166A*, 136.
- [58] P. von Ragué Schleyer, *Journal of the American Chemical Society* **1961**, *83*, 1368.
- [59] a) T. C. Bruice, U. K. Pandit, *Proceedings of the National Academy of Sciences of the United States of America* **1960**, *46*, 402; b) T. C. Bruice, U. K. Pandit, *Journal of the American Chemical Society* **1960**, *82*, 5858.
- [60] M. E. Jung, *Synlett* **1990**, *1990*, 186.

- [61] a) A. L. Parrill, D. P. Dolata, *Tetrahedron Letters* **1994**, 35, 7319; b) A. L. Parrill, D. P. Dolata, *Journal of Molecular Structure: THEOCHEM* **1996**, 370, 187.
- [62] a) S. Milstien, L. A. Cohen, *Proceedings of the National Academy of Sciences of the United States of America* **1970**, 67, 1143; b) S. Milstien, L. A. Cohen, *Journal of the American Chemical Society* **1972**, 94, 9158; c) R. T. Borchardt, L. A. Cohen, *Journal of the American Chemical Society* **1972**, 94, 9175.
- [63] a) C. Danforth, A. W. Nicholson, J. C. James, G. M. Loudon, *Journal of the American Chemical Society* **1976**, 98, 4275; b) R. E. Winans, C. F. Wilcox, *Journal of the American Chemical Society* **1976**, 98, 4281.
- [64] a) R. D. Bach, O. Dmitrenko, *The Journal of organic chemistry* **2002**, 67, 3884; b) R. D. Bach, O. Dmitrenko, *The Journal of organic chemistry* **2002**, 67, 2588; c) S. M. Bachrach, *The Journal of organic chemistry* **2008**, 73, 2466; d) A. L. Ringer, D. H. Magers, *The Journal of organic chemistry* **2007**, 72, 2533.
- [65] N. L. Allinger, V. Zalkow, *The Journal of organic chemistry* **1960**, 25, 701.
- [66] a) M. S. Newman, W. J. Broger, J. B. LaPidus, A. Tye, *Journal of medicinal chemistry* **1972**, 15, 1003; b) T. T. Talele, *Journal of medicinal chemistry* **2018**, 61, 2166; c) C. Toniolo, M. Crisma, F. Formaggio, C. Peggion, *Biopolymers* **2001**, 60, 396; d) E. Asante-Appiah, J. Seetharaman, F. Sicheri, D. S. Yang, W. W. Chan, *Biochemistry* **1997**, 36, 8710; e) W. T. Ashton, R. M. Sisco, Y. T. Yang, J.-L. Lo, J. B. Yudkovitz, K. Cheng, M. T. Goulet, *Bioorganic & medicinal chemistry letters* **2001**, 11, 1723; f) M. Kuwahara, Y. Kawano, M. Kajino, Y. Ashida, A. Miyake, *Chemical & pharmaceutical bulletin* **1997**, 45, 1447.
- [67] P. G. Sammes, D. J. Weller, *Synthesis* **1995**, 1995, 1205.
- [68] a) J. M. Karle, I. L. Karle, *Journal of the American Chemical Society* **1972**, 94, 9182; b) M. Caswell, G. L. Schmir, *Journal of the American Chemical Society* **1980**, 102, 4815.
- [69] a) M. P. Dillon, H. Cai, H. Maag, *Bioorganic & medicinal chemistry letters* **1996**, 6, 1653; b) K. L. Amsberry, A. E. Gerstenberger, R. T. Borchardt, *Pharmaceutical research* **1991**, 8, 455; c) D. Shan, M. G. Nicolaou, R. T. Borchardt, B. Wang, *Journal of pharmaceutical sciences* **1997**, 86, 765; d) B. Testa, J. M. Mayer, *Drug metabolism reviews* **1998**, 30, 787.
- [70] a) S. W. Mamber, A. B. Mikkilineni, E. J. Pack, M. P. Rosser, H. Wong, Y. Ueda, S. Forenza, *The Journal of pharmacology and experimental therapeutics* **1995**, 274, 877; b) Y. Ueda, J. D. Matiskella, A. B. Mikkilineni, V. Farina, J. O. Knipe, W. C. Rose, A. M. Casazza, D. M. Vyas, *Bioorganic & medicinal chemistry letters* **1995**, 5, 247; c) Y. Ueda, A. B. Mikkilineni, J. O. Knipe, W. C. Rose, A. M. Casazza, D. M. Vyas, *Bioorganic & medicinal chemistry letters* **1993**, 3, 1761.
- [71] R. B. Greenwald, Y. H. Choe, C. D. Conover, K. Shum, D. Wu, M. Royzen, *Journal of medicinal chemistry* **2000**, 43, 475.
- [72] C. F. Hammer, S. R. Heller, J. H. Craig, *Tetrahedron* **1972**, 28, 239.
- [73] T. Helbing, M. Georg, F. Stöhr, C. Carraro, J. Becker, B. Gatto, R. Göttlich, *European Journal of Organic Chemistry* **2021**, 2021, 5905.
- [74] C. O. Gitterman, E. L. Rickes, D. E. Wolf, J. Madas, S. B. Zimmerman, T. H. Stoudt, T. C. Demny, *The Journal of antibiotics* **1970**, 23, 305.
- [75] I. Zuravka, R. Roesmann, A. Susic, W. Wende, A. Pingoud, B. Gatto, R. Göttlich, *ChemMedChem* **2014**, 9, 2178.
- [76] A. Susic, I. Zuravka, N.-K. Schmitt, A. Miola, R. Göttlich, D. Fabris, B. Gatto, *ChemMedChem* **2017**, 12, 1471.
- [77] I. Zuravka, R. Roesmann, A. Susic, R. Göttlich, B. Gatto, *Bioorganic & medicinal chemistry* **2015**, 23, 1241.
- [78] I. Zuravka, A. Susic, B. Gatto, R. Göttlich, *Bioorganic & medicinal chemistry letters* **2015**, 25, 4606.
- [79] T. Helbing, C. Carraro, A. Francke, A. Susic, M. de Franco, V. Gandin, R. Göttlich, B. Gatto, *ChemMedChem* **2020**, 15, 2040.
- [80] C. Carraro, L. Bonaguro, J. Schulte-Schrepping, A. Horne, M. Oestreich, S. Warnat-Herresthal, T. Helbing, M. de Franco, K. Haendler, S. Mukherjee et al., *eLife* **2022**, 11.
- [81] T. Helbing, M. Kirchner, J. Becker, R. Göttlich, *European Journal of Organic Chemistry* **2022**.
- [82] C. Carraro, A. Francke, A. Susic, F. Kohl, T. Helbing, M. de Franco, D. Fabris, R. Göttlich, B. Gatto, *ACS Medicinal Chemistry Letters* **2019**, 10, 552.
- [83] M. Noack, R. Göttlich, *European Journal of Organic Chemistry* **2002**, 2002, 3171.
- [84] K. C. Brannock, *Journal of the American Chemical Society* **1959**, 81, 3379.
- [85] C. Carraro, T. Helbing, A. Francke, I. Zuravka, A. Susic, M. de Franco, V. Gandin, B. Gatto, D. R. Göttlich, *ChemMedChem* **2021**, 16, 860.
- [86] R. Göttlich, *Synthesis* **2000**, 2000, 1561.
- [87] J. Helaja, R. Göttlich, *Chemical communications* **2002**, 720.
- [88] R. Göttlich, M. Noack, *Tetrahedron Letters* **2001**, 42, 7771.
- [89] W. Li, G.-Q. Liu, B. Cui, L. Zhang, T.-T. Li, L. Li, L. Duan, Y.-M. Li, *RSC Advances* **2014**, 4, 13509.
- [90] G. Yin, T. Wu, G. Liu, *Chemistry* **2012**, 18, 451.
- [91] a) R.-L. Li, G.-Q. Liu, W. Li, Y.-M. Wang, L. Li, L. Duan, Y.-M. Li, *Tetrahedron* **2013**, 69, 5867; b) G.-Q. Liu, W. Li, Y.-M. Li, *Advanced Synthesis & Catalysis* **2013**, 355, 395-402.

- [92] a) F. Liu, K. M. Worthy, L. Bindu, A. Giubellino, D. P. Bottaro, R. J. Fisher, T. R. Burke, *Organic & biomolecular chemistry* **2007**, *5*, 367; b) Z.-J. Liu, X. Lu, G. Wang, L. Li, W.-T. Jiang, Y.-D. Wang, B. Xiao, Y. Fu, *Journal of the American Chemical Society* **2016**, *138*, 9714; c) X. Qi, C. Chen, C. Hou, L. Fu, P. Chen, G. Liu, *Journal of the American Chemical Society* **2018**, *140*, 7415; d) C. J. Maddocks, K. Ermanis, P. A. Clarke, *Organic letters* **2020**, *22*, 8116.
- [93] a) M. A. Casely-Hayford, K. Pors, L. H. Patterson, C. Gerner, S. Neidle, M. Searcey, *Bioorganic & medicinal chemistry letters* **2005**, *15*, 653; b) M. A. Casely-Hayford, K. Pors, C. H. James, L. H. Patterson, J. A. Hartley, M. Searcey, *Organic & biomolecular chemistry* **2005**, *3*, 3585.
- [94] K. Pors, S. D. Shnyder, P. H. Teesdale-Spittle, J. A. Hartley, M. Zloh, M. Searcey, L. H. Patterson, *Journal of medicinal chemistry* **2006**, *49*, 7013.
- [95] R. C. Fuson, C. L. Zirkle, *Journal of the American Chemical Society* **1948**, *70*, 2760.
- [96] M. A. Wijdeven, J. Willemsen, F. P. J. T. Rutjes, *European Journal of Organic Chemistry* **2010**, *2010*, 2831.
- [97] a) Y. Du, A. Yu, J. Jia, Y. Zhang, X. Meng, *Chemical communications* **2017**, *53*, 1684; b) S. B. D. Jarvis, A. B. Charette, *Organic letters* **2011**, *13*, 3830; c) L. Micouin, T. Varea, C. Riche, A. Chiaroni, J.-C. Quirion, H.-P. Husson, *Tetrahedron Letters* **1994**, *35*, 2529; d) A. I. Subota, S. V. Ryabukhin, A. O. Gorlova, O. O. Grygorenko, D. M. Volochnyuk, *Journal of Fluorine Chemistry* **2019**, *224*, 61; e) L. Zhou, D. W. Tay, J. Chen, G. Y. C. Leung, Y.-Y. Yeung, *Chemical communications* **2013**, *49*, 4412; f) A. Bari, A. Iqbal, Z. A. Khan, S. A. Shahzad, M. Yar, *Synthetic Communications* **2020**, *50*, 2572.
- [98] M. A. Graham, M. Thornton-Pett, C. M. Rayner, A. H. Wadsworth, *Chemical communications* **2001**, 966.
- [99] P. Y. Lee, J. Costumbrado, C.-Y. Hsu, Y. H. Kim, *Journal of visualized experiments: JoVE* **2012**.
- [100] P. H. Johnson, L. I. Grossman, *Biochemistry* **1977**, *16*, 4217.
- [101] a) N. Jalani, S. Kothari, K. K. Banerji, *International Journal of Chemical Kinetics* **1996**, *28*, 165; b) B. Varghese, S. Kothari, K. K. Banerji, *International Journal of Chemical Kinetics* **1999**, *31*, 245.

## 4. Publications

### 4.1. Aromatic Linkers Unleash the Antiproliferative Potential of 3-Chloropiperidines Against Pancreatic Cancer Cells



**As keen as mustard:** Aromatic 3-chloropiperidines designed to improve the therapeutic potential of mustard-based DNA alkylating agents have been synthesized and evaluated. These small molecules exhibited a marked anti-proliferative effect preferentially against BxPC-3 pancreatic adenocarcinoma cells in 2D and 3D cultures, thus demonstrating themselves to be promising candidates for the further development of sustainable chemotherapeutics active against pancreatic tumors.

#### Reference

Tim Helbing, Caterina Carraro, Alexander Francke, Alice Susic, Michele De Franco, Valentina Gandin, Richard Göttlich, Barbara Gatto, *ChemMedChem* **2020**, *15*, 2040. (doi: 10.1002/cmdc.202000457)

Tim Helbing and Caterina Carraro contributed equally to this work.

© 2020 The Authors. Published by Wiley – VCH Verlag GmbH & Co. KGaA, Weinheim.

Reproduced with permission of the copyright owners.

Special Collection

# Aromatic Linkers Unleash the Antiproliferative Potential of 3-Chloropiperidines Against Pancreatic Cancer Cells

Tim Helbing<sup>+</sup>,<sup>[a]</sup> Caterina Carraro<sup>+</sup>,<sup>[b]</sup> Alexander Francke,<sup>[a]</sup> Alice Sosic,<sup>[b]</sup> Michele De Franco,<sup>[b]</sup> Valentina Gandin,<sup>[b]</sup> Richard Göttlich,<sup>\*[a]</sup> and Barbara Gatto<sup>\*[b]</sup>

In this study, we describe the synthesis and biological evaluation of a set of *bis*-3-chloropiperidines (B-CePs) containing rigid aromatic linker structures. A modification of the synthetic strategy also enabled the synthesis of a pilot *tris*-3-chloropiperidine (Tri-CeP) bearing three reactive *meta*-chloropiperidine moieties on the aromatic scaffold. A structure–reactivity relationship analysis of B-CePs suggests that the arrangement of the reactive units affects the DNA alkylating activity, while also revealing correlations between the electron

density of the aromatic system and the reactivity with biologically relevant nucleophiles, both on isolated DNA and in cancer cells. Interestingly, all aromatic 3-chloropiperidines exhibited a marked cytotoxicity and tropism for 2D and 3D cultures of pancreatic cancer cells. Therefore, the new aromatic 3-chloropiperidines appear to be promising contenders for further development of mustard-based anticancer agents aimed at pancreatic cancers.

## Introduction

Recent efforts in the search for targeted anticancer agents have led to the discovery of promising candidates that interfere with different carcinogenic pathways. Nevertheless, persistent drawbacks undermine the development of these drugs, such as the rapid emergence of resistance mechanisms and the onerous manufacturing costs, especially for biologics.<sup>[1]</sup> Consequently, “old” chemotherapeutics still represent a valid choice in first-line treatments.<sup>[2]</sup> Among the most diffused alternatives, nitrogen mustards (NMs), such as those depicted in Figure 1a) represent one of the first class of alkylating anticancer agents which act by directly damaging DNA thus preferentially impairing replication and transcription in fast-dividing tumor cells.<sup>[2]</sup> Unfortunately, the therapeutic applicability of these drugs is limited by their scarce selectivity, which is frequently associated to tough side effects for patients.<sup>[2,3]</sup> Thus, efforts are required to identify new NM candidates with ameliorated efficacy and safety profiles. Seeking to improve the therapeutic

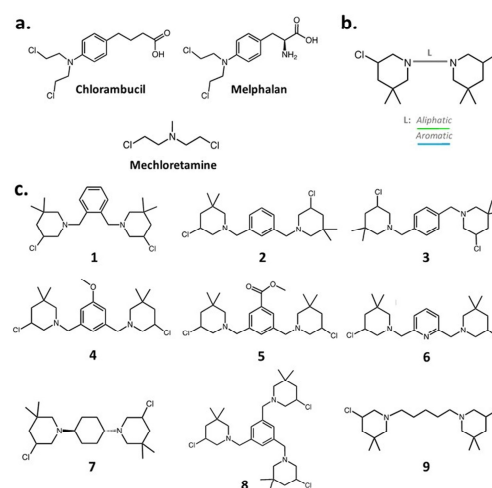


**Figure 1.** a) Chemical structure of chlorambucil, melphalan and mechlometamine. b) General structure of B-CePs. Different connecting linkers (L) are schematized with different colors. c) Chemical structures of the analyzed 3-chloropiperidines.

value of these economically sustainable antitumor agents, our studies focused on the development of *bis*-3-chloropiperidines (B-CePs) as a new class of revisited mustard-based alkylating agents (Figure 1b).<sup>[4]</sup>

In preceding works, we thoroughly investigated the mechanism of DNA alkylation by B-CePs. Thanks to their marked electrophilicity, these compounds efficiently react with nucleobases, forming mono- and bi-functional adducts preferentially with the N7 of guanines.<sup>[5]</sup> These base lesions rearrange into purinic sites leading to DNA cleavage,<sup>[5]</sup> with in vitro potencies

[a] T. Helbing,<sup>+</sup> A. Francke, Prof. Dr. R. Göttlich  
Institute of Organic Chemistry  
Justus Liebig University Giessen  
Heinrich-Buff-Ring 17, 35392 Giessen (Germany)  
E-mail: richard.goettlich@org.chemie.uni-giessen.de

[b] C. Carraro,<sup>+</sup> Dr. A. Sosic, M. De Franco, Prof. Dr. V. Gandin, Prof. Dr. B. Gatto  
Department of Pharmaceutical and Pharmacological Sciences  
University of Padova  
Via Francesco Marzolo 5, 35131 Padova (Italy)  
E-mail: barbara.gatto@unipd.it

<sup>†</sup> These authors contributed equally.

Supporting information for this article is available on the WWW under <https://doi.org/10.1002/cmdc.202000457>

This article belongs to the Special Collection “NMMC 2019: DCF-SCI 40th Anniversary”.

© 2020 The Authors. Published by Wiley-VCH GmbH. This is an open access article under the terms of the Creative Commons Attribution License, which permits use, distribution and reproduction in any medium, provided the original work is properly cited.

modulated by the chemistry of the linker connecting the two 3-chloropiperidine reactive centers.<sup>[4a,b]</sup> Along with potent derivatives characterized by aliphatic linkers, our previous studies examined the activity toward DNA of one B-CeP bearing a *para*-xylene linker (compound **3**, Figure 1c).<sup>[4b]</sup>

In vitro, the aromatic rigid linker reduced the DNA cleavage potency relative to the aliphatic analogues, an attribute worth to be further explored in the characterization of this class of compounds.<sup>[4b]</sup> Similarly, the classical nitrogen mustards bearing aromatic moieties (e. g., chlorambucil and melphalan, Figure 1a) possess a milder electrophilicity, which makes them less toxic drugs compared to aliphatic analogues (e. g., mechlorethamine, Figure 1a).<sup>[6]</sup>

From these premises, the present work aims to further investigate the chemical space and anticancer value of B-CePs by synthesizing and evaluating a series of derivatives bearing different linkers intended at modulating the compounds electrophilicity. The new set is called here for simplicity "aromatic B-CePs" as their characteristic feature is the presence of aromatic linkers connecting the two reactive moieties (Figure 1b). The chemical structure of test derivatives is depicted in Figure 1c. In detail, the set includes: i) derivatives with *ortho*-, *meta*- and *para*-xylene linker arrangements (compounds **1–3**) to reveal the effects of orientation and distance between reactive centers on the activity of B-CePs; ii) two exploratory derivatives containing electron-withdrawing functional groups, respectively bearing a methoxy group and a methyl ester function (compounds **4** and **5**) attached in *meta* position to minimize steric effects, in order to probe the possible influence of substituents on the aromatic system; moreover, iii) we incorporated a pyridine linker in compound **6** to study the influence of a heteroatom in the aromatic bridging linker; finally, iv) to probe the value of *tris*-3-chloropiperidines (Tri-CePs), we synthesized compound **8**, bearing three reactive moieties in *meta* on the aromatic scaffold, to explore the correlation between activity and number of reactive centers. For comparative purpose, we included in our analyses the previously synthesized *aliphatic* B-CePs **7**, possessing a rigid aliphatic cyclohexane linker, and **9**, bearing a flexible pentyl linker.<sup>[4b]</sup>

Aside from proposing novel accessible strategies to synthesize the described set of aromatic derivatives, the present work aims at extending their biological evaluation beyond the reactivity on model nucleic acids, investigating the effects of all compounds against different cancer cell types to gain evidence of biological activity and tropism toward different tumors. The remarkable cytotoxicity in the pancreatic tumor-derived cells prompted us to further explore the valuable biological activity of aromatic B-CePs. We therefore assessed the involvement of transporters in the uptake of B-CePs. Furthermore, we inspected their molecular mechanism of action by checking the presence in cells of genomic DNA lesions upon treatment. Finally, we demonstrated in 3D models of pancreatic cancer how the modulation of reactivity of the aromatic compounds is crucial for unleashing their antitumor potential.

## Results and Discussion

### Synthesis of *bis*- and *tris*-3-chloropiperidines

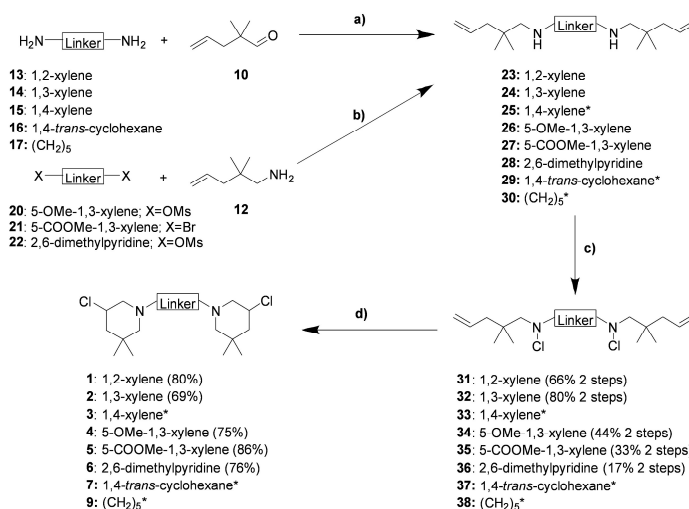
The synthetic strategy to obtain the *bis*-3-chloropiperidines **1–7** and **9** remained similar to our previously reported procedures,<sup>[4]</sup> but was adapted for the substituted B-CePs **4–6** to further extend the range of suitable precursors (Scheme 1). The synthesis of the final products **3**, **7** and **9** has already been described in our previous work.<sup>[4b]</sup> Starting with the diamines **13–17** and the functionalized aromatic building blocks **20–22** the desired product was always the corresponding unsaturated diamine **23–30**, which was prepared by two different strategies. For the synthesis of the *bis*-3-chloropiperidines with varying substitution pattern **1–3**, the preparation started with the corresponding aromatic diamines **13–15** which were converted to their secondary analogues **23–25** by a double reductive amination using 2,2-dimethylpent-4-enal **10** and sodium triacetoxyborohydride.<sup>[7]</sup> This strategy is well known and was also applied in the previous synthesis of the B-CePs **7** and **9**, starting from their corresponding diamines **16** and **17**.<sup>[4b]</sup> In contrast, the secondary diamines **26–28** were obtained by nucleophilic substitution of a suitable leaving group attached to the substituted aromatic linkers. For this reaction the aldehyde **10** was converted to the corresponding primary amine **12**, which was deprotonated using sodium hydride and then reacted with the brominated or mesylated aromatic precursors **20–22**. Afterwards, the secondary diamines **23–30** were treated with *N*-chlorosuccinimide (NCS) to obtain the unsaturated *bis*-*N*-chloroamines **31–38**. These products were then converted to the desired *bis*-3-chloropiperidines **1–7** and **9** by iodine catalyzed cyclization using tetrabutylammoniumiodide.<sup>[8]</sup>

Detailed synthetic procedures for the preparation of the precursors **10–13** and **18–22** from readily available starting materials can be found in the Supporting Information.

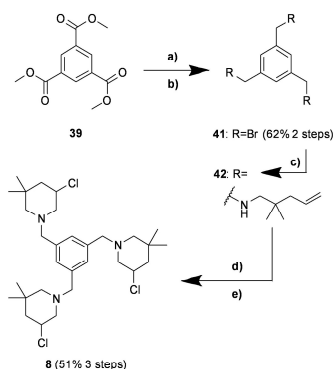
The brominated precursor **41** was synthesized by a two-step procedure from the readily available trimethyl 1,3,5-benzenetricarboxylate **39** (see the Supporting Information for details), which was then reacted with an excess of the unsaturated amine **12** to obtain the corresponding secondary triamine **42**. Afterwards, the known synthetic strategy for *bis*-3-chloropiperidines, involving the *N*-chlorination and cyclization, was adopted and applied to the trifunctional compound, providing the desired *tris*-3-chloropiperidine **8** in good yield (Scheme 2).

### Aromatic and aliphatic B-CePs exhibit different reactivity

The mechanism of DNA alkylation by B-CePs involves an intramolecular nucleophilic displacement of the chloride in 3-position, leading to the formation of the reactive aziridinium ion, which is readily attacked by nucleophiles such as water or nucleobases.<sup>[5]</sup> To support our hypothesis that the reactivity of B-CePs with nucleophiles is influenced by the nature of linker, we determined the kinetics of B-CePs consumption in aqueous



**Scheme 1.** Synthesis of *bis*-3-chloropiperidines 1–6. a) NaBH(OAc)<sub>3</sub>, AcOH, dry CH<sub>2</sub>Cl<sub>2</sub>, 0 °C to RT, 16–18 h; b) NaH, dry THF, 0 °C to RT, 20–22 h; c) NCS, dry CH<sub>2</sub>Cl<sub>2</sub>, 0 °C to RT, 2.5–3 h; d) TBAI (cat.), dry CHCl<sub>3</sub>, 60 °C (oil bath temperature), 2–2.5 h (inseparable diastereomeric mixture). \*The synthesis of compounds 3, 7 and 9 as well as their corresponding precursors has been described elsewhere.<sup>[4b]</sup>



**Scheme 2.** Synthesis of *tris*-3-chloropiperidine **8**. a) LAH, dry THF, 0 °C to RT to reflux, 18 h; b) PBr<sub>3</sub>, dry Et<sub>2</sub>O, 0 °C to RT, 24 h; c) 2,2-dimethylpent-4-en-1-amine **12**, dry CH<sub>2</sub>Cl<sub>2</sub>, 0 °C to RT, 68 h; d) NCS, dry CH<sub>2</sub>Cl<sub>2</sub>, 0 °C to RT, 2.5 h; e) TBAI (cat.), dry CHCl<sub>3</sub>, reflux, 4 h.

solution. We employed electrospray ionization mass spectrometry (ESI-MS) to monitor the formation of compounds hydrolysis products and intermediates over time. For the aromatic compounds, we analyzed **1** and **2** to investigate the influence of *ortho* and *meta* substitution and compared them with **7** and **9** to explore the effects of aliphatic linkers on the dynamics of B–CePs reactivity. Aqueous solutions of mentioned compounds were incubated at 37 °C and aliquots of the reaction mixtures were analyzed after different incubation times (0, 20, 40, 60, and 180 min and overnight) by ESI-MS. Graphs showing the

relative distribution of detected species (U=unreacted compound, N<sup>+</sup>=aziridinium ion, 2 N<sup>+</sup>=double aziridinium ion, OH=monohydroxylated, N<sup>+</sup>/OH=monohydroxylated/aziridinium ion, 2OH=dihydroxylated) over time are reported in Figure S1 in the Supporting Information. The kinetics of the reaction of aliphatic versus aromatic compounds was very different. Derivatives **7** and **9** were rapidly consumed in water, with the unreacted species coexisting with mono and dihydroxylated species formed at high rates already from 20 minutes of incubation. At 3 h both compounds were almost totally reacted. The reactivity of aromatic compounds was slower compared to the aliphatic analogues, as expected. Besides, we noted the slower kinetics of **1** compared to **2**. The N<sup>+</sup> species of **2** formed immediately and turned out to be rather stable, with the ratio between unreacted **2** and its N<sup>+</sup> ion almost preserved during the first hour of incubation, suggesting the presence of a pre-equilibrium; the dihydroxylated species formed from 60 min up to 3 h. Conversely, compound **1** started reacting with water only after 20 min of incubation leading to the formation of hydroxylated species. Interestingly, the 1 N<sup>+</sup> intermediate was never detected in time, attesting the different reactivity profile of the *ortho* compared to the *meta* analogue. Based on these findings, we proceeded with the evaluation of reactivity with biological macromolecules.

**Meta arrangement increases aromatic B-CePs reactivity with plasmid DNA**

In line with our precedent studies on 3-chloropiperidines, the new derivatives were initially evaluated for their ability to react with nucleic acids and induce DNA strand breaks.<sup>[4,9]</sup> The electrophoretic cleavage assay allows to visualize the compound-mediated conversion of the supercoiled plasmid substrate (SC) into its retarded nicked and linearized forms (OC = open circular, L = linearized). In detail, the pBR322 plasmid was incubated with increasing concentrations of test compounds for 3 h at 37 °C and reaction products were run on agarose gel. The bar chart in Figure 2 reports the EC<sub>50</sub> values of test compounds in ascending order. For the sake of clarity, final EC<sub>50</sub>s of the test derivatives are detailed in Table S1.

With the exception of compounds **1** and **8**, test derivatives exhibited EC<sub>50</sub> values below 5 μM, thus demonstrating to efficiently cleave DNA *in vitro*. In line with the previous observations for **3** with a different substrate,<sup>[4b]</sup> the new results confirm that aromatic linkers (blue bars in Figure 2) decrease the DNA cleavage potency of B-CePs: only the aliphatic compounds **9** and **7** (green bars in Figure 2) possess potencies below 1 μM.

A comparison between the isomers **1**, **2** and **3**, respectively bearing *ortho*-, *meta*- and *para*-xylene linkers, allowed to evaluate the influence of different substitution patterns on the reactivity of aromatic B-CePs. Resulting EC<sub>50</sub> values demonstrated that, while the *meta* and *para* substitutions conferred a similar potency to compounds **2** and **3**, the activity of the *ortho* positional isomer **1** toward DNA decreased consistently with the reduced reactivity with water. In that conditions, after the first hydroxylation of **1**, intramolecular hydrogen bonding interactions between the newly formed hydroxyl group and the nitrogen atoms of both chloropiperidine rings might reduce the reactivity of the second 3-chloropiperidine moiety. Such interactions cannot be established when increasing the distance between the two reactive groups as in the case of the *meta* isomer **2**. In addition, the restrained rotability and steric

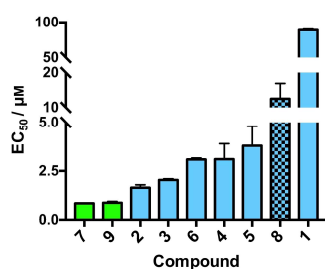


**Figure 2.** DNA cleavage EC<sub>50</sub> values of analyzed B-CePs. The supercoiled pBR322 plasmid was incubated with increasing concentrations of test compounds at 37 °C for 3 h in BPE buffer. EC<sub>50</sub> values were calculated by comparing the intensities of the supercoiled species band to the negative control as a function of compound concentration. Average EC<sub>50</sub> values and standard deviations result from two independent experiments. Green bars: aliphatic B-CePs; blue bars: aromatic B-CePs; blue checkered bar: Tri-CeP.

hindrance of **1** may prevent an efficient attack of guanine residues in DNA. Given the limited cleavage of **1** observed at 3 h, the reactivity of **1**, **2** and **3** was indeed investigated at the longer incubation time of 18 h. Resulting gel images are shown in Figure 3a (3 h) and b (18 h). Though much less reactive than its analogues, compound **1** demonstrated to extensively fragment the plasmid at the longer incubation time of 18 h, as clearly attested by the appearance of an intense smear. This suggests that the reaction with nucleic acids still occurs, although it needs time to achieve DNA cleavage compared to the *meta* and *para* isomers. Compounds **4** and **5**, tested to investigate the influence of substitution of the xylene linker, show higher EC<sub>50</sub> values than **2**, indicating that the insertion of the ether group and the ester substituent reduces the reactivity exhibited by the parent compound. Although there is no direct conjugation to the aromatic system in the case of the substituted B-CePs, the electronic nature of the aromatic system clearly influences the reactivity of the compounds, which decreases in presence of these electron withdrawing groups. As there is no direct conjugation between the piperidine-nitrogen and the aromatic system, the impact of substituents is limited to inductive effects. Such substituent effects are described by linear free energy relationships derived from the Hammett equation.<sup>[10]</sup> Though initially developed for substituent effects on the ionization of benzoic acid derivatives, they are also applicable to different organic reactions and have already been applied to aromatic nitrogen mustards.<sup>[11]</sup> The

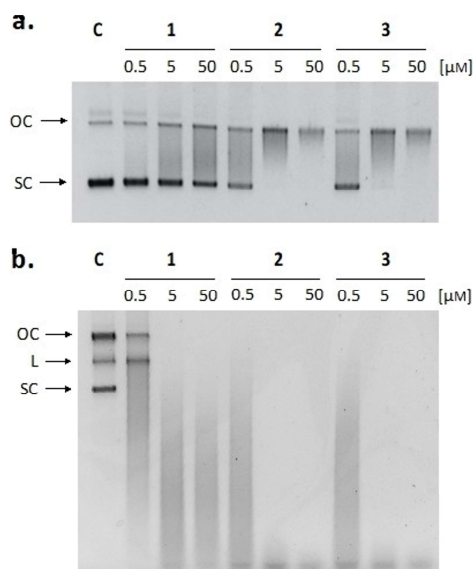


**Figure 3.** DNA cleavage assay for compounds **1**, **2** and **3**. DNA cleavage assay upon incubation with pBR322 after a) 3 and b) 18 h at 37 °C with increasing compound concentrations (0.5, 5, 50 μM). SC: supercoiled plasmid; L: linearized plasmid; OC: open circular plasmid; C: supercoiled pBR322 plasmid control.

correlation observed for the substituted B–CePs compared to compound **2** is not perfect, but similar to the reactivity of substituted benzylamines as nucleophiles.<sup>[12]</sup> This relationship seems to be comparable to our experiments, since the first step in the reaction of B–CePs is always the formation of an aziridinium ion, provided by a nucleophilic attack of the benzylic piperidine-nitrogen.

Accordingly, the introduction of a nitrogen heteroatom, reducing the electron density of the aromatic linker in **6**, also decreased the compounds reactivity when compared to analogue **2**. Unintuitively, also the third additional reactive moiety of the Tri-CeP **8** curtailed its reactivity compared to the bifunctional analogue **2**.

#### Aromatic linkers address B–CePs toxicity against pancreatic cancer cells

After analyzing the reactivity of compounds with water and with purified DNA, the biological value of compounds was assessed by the MTT assay on a panel of human cancer cell lines, namely colorectal adenocarcinoma HCT-15, pancreatic adenocarcinoma BxPC-3 and ovarian carcinoma 2008 cells. Table 1 reports the IC<sub>50</sub> values observed after 72 h of treatment with tested B–CePs along with previously determined IC<sub>50</sub> values of the reference nitrogen mustard chlorambucil (Chl).<sup>[9]</sup> For its poor solubility and compatibly with the use of maximum 0.5% DMSO in cell culture, compound **5** was not tested over 25 μM.

Of note, all derivatives demonstrated a valuable cytotoxicity against the three human tumor cell lines, in most cases improved compared to the reference drug chlorambucil.<sup>[9]</sup> Interestingly, results suggest a separate analysis for HCT-15 and 2008 compared to BxPC-3 tumor cells: in fact, B–CePs behaved similarly against colorectal and ovarian cancer cells, exhibiting IC<sub>50</sub> values between 1 and 20 μM, whereas the new set was one or two orders of magnitude more potent against the pancreatic cancer cells. Considering the former two cell lines, aromatic derivatives exhibit a positive correlation between cytotoxicity and reactivity. The poorly reactive isomer **1** bearing the *ortho*-

xylene linker turned out to be less cytotoxic than its *meta*- and *para*-analogues **2** and **3**. The ether and ester substituents led to a decrease both in the reactivity and cytotoxicity of **4** and **5** compared to compound **2**, following the ranking **2** > **4** > **5**. Moreover, compound **2** resulted more cytotoxic and more reactive than its pyridine analogue **6**. Finally, the bifunctional agent **2** was also more cytotoxic than the trifunctional derivative **8**, always in line with cleavage results. However, when considering the aliphatic derivatives **7** and **9**, it is evident that the overall reactivity and cytotoxicity rankings do not match: unsurprisingly, this suggests that factors other than reactivity finally contribute to determine the cellular activity of B–CePs. When considering the aromatic series, we can conclude that for the colorectal and ovarian cancer models our results corroborate the mechanism of action of this class of alkylators and confirm the feasibility of modulating the activity of B–CePs by acting on the chemistry of the linker.

Results concerning the pancreatic cell line are quite divergent: very interestingly, all and only the *aromatic* derivatives showed nanomolar IC<sub>50</sub> values against pancreatic tumor cells, showing to be on average 200 times more toxic for BxPC-3 than chlorambucil, a difference not so evident considering HCT-15 and 2008 cells.

To highlight the unexpected tropism toward the pancreatic cancer cell line, the preferential activity index (P.A.I.) expressed as ratio between the IC<sub>50</sub> of each compound against 2008 or HCT-15 relative to BxPC-3 cells is reported in Figure 4.

Notably, we observe a marked selectivity for the pancreatic cell line (Figure 4), with the least DNA reactive compounds **1** and **8** among the most selective for BxPC-3 cells. On the other hand, the aliphatic compounds **7** and **9** (green bars in Figure 4) showed no different behavior throughout the screened panel, resulting in no selectivity and much higher IC<sub>50</sub> values for pancreatic cancer cells.

Given the encouraging cytotoxicity observed against the pancreatic cancer cell line, we proceeded to better characterize the biological profile of the tested compounds.

**Table 1.** MTT assay IC<sub>50</sub> values with the associated standard deviations on HCT-15, BxPC-3 and 2008 cells of test B–CePs on BxPC-3 cells after treatment for 72 h.

Compound	MTT IC <sub>50</sub> values/[μM]		
	HCT-15	2008	BxPC-3
<b>1</b>	23.8 ± 7.2	16.1 ± 5.6	0.4 ± 0.1
<b>2</b>	3.3 ± 1.1	2.8 ± 1.1	0.3 ± 0.2
<b>3</b>	3.0 ± 0.9	2.3 ± 0.3	0.4 ± 0.1
<b>4</b>	9.5 ± 2.7	4.0 ± 1.9	0.5 ± 0.2
<b>5</b>	> 25	> 25	0.4 ± 0.1
<b>6</b>	14.2 ± 2.2	10.7 ± 2.7	0.4 ± 0.1
<b>7</b>	3.2 ± 2.5	2.6 ± 0.8	5.5 ± 1.1
<b>8</b>	9.3 ± 2.9	14.3 ± 5.5	0.3 ± 0.2
<b>9</b>	6.8 ± 2.1	11.3 ± 2.2	9.4 ± 1.6
Chl <sup>[9]</sup>	49.7 ± 3.3	12.5 ± 2.1	75.3 ± 5.1

[a] Reference IC<sub>50</sub> values reported in our previous work<sup>[9]</sup> Chl: Chlorambucil. IC<sub>50</sub> values were calculated by a four-parameter logistic model.

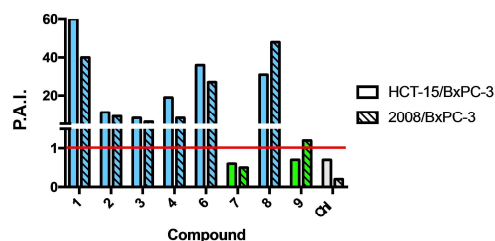


**Figure 4.** Preferential activity indexes of 3-chloropiperidines. P.A.I. are expressed as the ratio between the compound MTT IC<sub>50</sub> against HCT-15 and BxPC-3 cells (solid bars), as well as 2008 and BxPC-3 cells (dashed bars). Chl: Chlorambucil. Green bars: aliphatic B–CePs; blue bars: aromatic B–CePs; gray bars: Chl.

## B-CePs exploit transporter-mediated uptake

A modified MTT assay was performed on selected derivatives to investigate their mode of entry in BxPC-3 cells to disclose possible mechanisms of transporter-mediated uptake.<sup>[13]</sup> We analyzed the aromatic B-CePs 1, 2, 4, 6 together with compound 9 as representative of the aliphatic subset. The BxPC-3 selective trifunctional compound 8 was also examined. Given the almost equivalent reactivity and cytotoxicity profile between 2 and 3, the latter compound was not included in this analysis. Besides, being a non-optimal candidate for its poor solubility, compound 5 was not further investigated. Cells were seeded in two microplates and incubated for 5 h in parallel at 37 or 4 °C. Given the short incubation time, the adopted range of concentrations was increased compared to the IC<sub>50</sub> values obtained at 72 h. At the end of the incubation time the wells were rinsed with PBS, fresh medium was added and both microplates were incubated at 37 °C in the absence of compound. Finally, cell viability was assessed at 72 h and resulting curves are shown in Figure 5.

The differential viability resulting from the incubation of twin microplates at 37 or 4 °C allows to estimate the relative

contribution of transporters to the net intracellular accumulation of the compounds. The formazan absorbance of untreated controls was almost identical between plates incubated at 37 and 4 °C, suggesting that the sole initial temperature gap was not responsible for differences in viability, measured as metabolic state. At 37 °C (red line), both passive diffusion and transporter-mediated uptake could contribute to the net accumulation of cytotoxic agents in cells. On the other hand, the cytotoxicity observed at 4 °C (blue line) is almost exclusively a result of the passive diffusion of compounds across the cell membrane, since transporters are inhibited at low temperatures. A substantial drop in cell viability was observed upon treatment with all B-CePs derivatives at 37 °C compared to 4 °C (Figure 5), suggesting a key role for membrane transporters in determining intracellular accumulation of tested B-CePs. Nevertheless, the residual cytotoxicity observed at 4 °C demonstrates that compounds are also capable of passively diffusing through the cell membrane.

Interestingly, a comparable uptake profile was highlighted between 2 and 9, respectively aromatic and aliphatic analogues. This evidence confutes the hypothesis that the tropism toward BxPC-3 cells observed for aromatic but not aliphatic derivatives could depend on an enhanced cell penetration of the former. Results suggest that the pyridine linker enhances the intracellular accumulation of 6 by fostering its passive diffusion. Interestingly, the third reactive moiety of 8 apparently enhances its passive diffusion while clearly decreasing its transporter-mediated uptake compared to other bifunctional analogues.

## Aromatic B-CePs directly damage cellular DNA

In support of the activity observed on isolated DNA and as proof of principle of their mechanism of action, the alkaline single-cell gel electrophoresis (SCGE) assay was performed to evaluate potential genomic DNA lesions induced by B-CePs in cells.<sup>[14]</sup> The highly cytotoxic derivative 2 was chosen as representative of the aromatic B-CePs set. BxPC-3 cells were exposed for 6 h to 5 μM of compound 2: this short incubation time allows observing only direct compound-mediated DNA damage (DNA strand breaks, alkaline-labile sites), while excluding apoptotic fragmentation. Lesioned genomic DNA subjected to alkaline treatment and electrophoresis leads to the appearance of a characteristic comet tail upon staining with SYBR Green I. The same experiment was performed in presence of 0.5% DMSO and of the reference drug chlorambucil (Chl) at the concentration of 100 μM, representing the negative and positive controls respectively. Figure 6 shows the results of the SCGE assay: Figure 6a reports the relative percentage of comets, that is, the number of cells forming a comet relative to the total number of cells detected in two randomly captured fields from two independent experiments per each condition, while Figure 6b reports representative images of the comets in each condition.

Compound 2 harshly damages cellular DNA: in fact, upon 6 h of incubation with 5 μM of compound 2, at least one third of treated cells gave rise to a fragmented comet. This

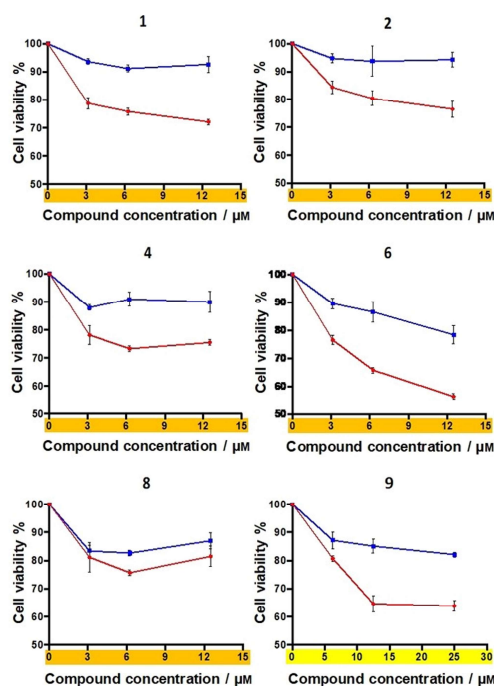
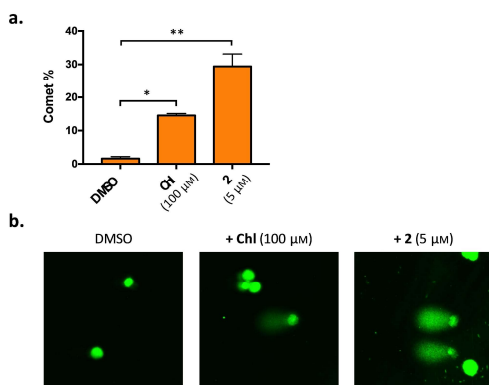


Figure 5. BxPC-3 cell viability upon exposure to increasing concentrations of selected compounds (3 to 12 μM of rigid derivatives 1, 2, 4, 6, 8 and 10 to 25 μM of 9) for 5 h at 37 °C (●) or 4 °C (◻), followed by a gentle rinse of wells with PBS and addition of fresh RPMI medium. The MTT assay was performed at 72 h.



**Figure 6.** An alkaline SCGE assay was performed on BxPC-3 cells upon incubation with DMSO 0.5%, chlorambucil (Chl) and compound 2 for 6 h at the indicated concentrations. a) The relative percentage of comets (number of cells forming a comet/total number of cells) detected in two randomly captured fields from two independent experiments per condition. b) Representative images (40x) of treated samples (including negative and positive controls) with comets are also reported. Paired t-test: \*  $p < 0.05$ , \*\*  $p < 0.001$ .

phenomenon was much reduced in case of the positive control chlorambucil: even at the much higher concentration of 100  $\mu\text{M}$ , only 15% of cells nuclei got damaged by the drug, and the damage was less severe, as attested by the representative images reported in Figure 6b. Overall, these cellular evidences endorse the mechanism of action of this class of DNA alkylators and justify the significant difference in cytotoxicity observed between our new set of derivatives and chlorambucil.

### 3-Chloropiperidines exhibit remarkable cytotoxicity against pancreatic cancer spheroids

In light of the promising cytotoxicity observed against BxPC-3 2D monolayer cultures, the activity of the aromatic B-CePs was further evaluated on 3D BxPC-3 spheroids, a more sophisticated model for the *in vitro* screening of therapeutics that better approximates the milieu and hypoxic core of solid tumors.<sup>[15]</sup> The acidic phosphatase assay (APH) was performed to assess viability of BxPC-3 spheroids grown in 96-well round-bottom microplates for two days and then incubated with selected compounds for 72 h.<sup>[16]</sup> The APH  $\text{IC}_{50}$  values for test derivatives are reported in Table 2.

Aromatic B-CePs confirmed their cytotoxicity also against BxPC-3 spheroids. Passing from 2D to 3D cultures, we can appreciate more pronounced inter-compound differences: in spheroids, compound 1 bearing the *ortho*-xylene linker was the most cytotoxic, followed by 4, bearing the *meta*-methoxy xylene linker, and by the new Tri-CeP agent 8. Compounds 2, 3 and 6 exhibited  $\text{IC}_{50}$  values over 100  $\mu\text{M}$ , a relevant result considering that chlorambucil was completely inactive up to the maximum tested concentration of 200  $\mu\text{M}$ . To understand

**Table 2.** BxPC-3 3D cultures cytotoxicity.

Compound	APH $\text{IC}_{50}$ values/ $[\mu\text{M}]$	Compound	APH $\text{IC}_{50}$ values/ $[\mu\text{M}]$
	BxPC-3		BxPC-3
1	40.1 $\pm$ 7.6	4	46.2 $\pm$ 0.6
2	122.4 $\pm$ 5.7	6	112.7 $\pm$ 2.4
3	133.1 $\pm$ 4.4	8	68.2 $\pm$ 4.6
Chl	inactive		

APH assay  $\text{IC}_{50}$  values with the associated standard deviations of selected compounds on BxPC-3 cancer cell 3D cultures after treatment for 72 h.  $\text{IC}_{50}$  values were calculated by a four-parameter logistic model. Chl: Chlorambucil, totally inactive at the maximum tested concentration (200  $\mu\text{M}$ ).

this result, we should reason about the requisites necessary for compounds to be effective against spheroids. Being three-dimensional, these systems are constituted by stratified cell layers and we can speculate that B-CePs must efficiently penetrate them while keeping their reactivity intact for a sufficient time. In this sense, a lower or delayed reactivity and a good uptake profile turn out to be crucial for the biological activity of these new set of alkylators in 3D models. Compound 1 was the least reactive with nucleophiles but could demonstrate effective time-dependent DNA damaging activity (Figure 3b). Compound 8 showed also a restrained reactivity at the DNA cleavage assay but it demonstrated to almost exclusively enter cells by passive diffusion, a slow and less efficient process. Noteworthy, 1 and 8 were highlighted to be among the most selective against the pancreatic cancer cell line (Figure 4), thus showing to be promising leads for upgraded studies as anticancer agents for pancreatic tumors. Although more reactive than 1 and 8, the methyl-ether compound 4 showed a valuable activity against spheroids: this result might depend on the ability of the ether function to hamper potential self-stacking interactions between aromatic molecules, thus increasing the efficiency of spheroid penetration.

## Conclusions

This study highlighted the anticancer potential of a new set of 3-chloropiperidines designed to improve the efficacy of mustard-based chemotherapeutics obtained through a convenient synthetic strategy. Different linker substituents and substitution patterns demonstrated to modulate the reactivity of B-CePs toward isolated DNA. Most interestingly, *meta*- and *para*-xylene isomers demonstrated to provide a similar and efficient potency of alkylation on isolated DNA, while the *ortho* analogue and B-CePs incorporating electron withdrawing substituents on the aromatic linker exhibited a delayed reactivity. Noteworthy, we demonstrated for the first time the potent antiproliferative effect of B-CePs on a panel of tumor cell lines. In the case of aromatic B-CePs, a clear correlation between reactivity and cytotoxicity was observed against ovarian 2008 and colorectal HCT-15 cancer cells. Unexpectedly, aromatic but not aliphatic linkers confer to B-CePs nanomolar toxicities against pancreatic BxPC-3 cells, resulting into valuable indexes of preferential activity for this cancer cell line. As proof

of principle of their mechanism of action, the representative aromatic derivative **2** demonstrated to damage cellular DNA to a higher extent compared to chlorambucil even at a much lower concentration. The tropism toward pancreatic cancer cells is exceptionally relevant considering the aggressiveness of this tumor type and recalls what observed with monofunctional 3-chloropiperidines (M-CePs) against the same cell line.<sup>[9]</sup>

In this study we also investigated the new trifunctional 3-chloropiperidine **8**, which showed a valuable activity against the advanced model of pancreatic 3D spheroid cultures, most likely by virtue of its lower reactivity, a feature shared with the low reactive B-CeP **1**. This attests that restrained reactivity and good uptake are determinants for the effectiveness of 3-chloropiperidines in this model, a precious knowledge for the potential development of such compounds against solid tumors.

To conclude, the empowered anticancer features of aromatic B-CePs compared to aliphatic analogues provide a versatile starting point for the advanced synthesis of such compounds. This exclusivity seems not to rely on differences in the intracellular accumulation of aromatic compared to aliphatic compounds, since both showed a very similar uptake profile. Nevertheless, studies are ongoing to reveal which distinctive mechanisms prior or following DNA damage are responsible for the unexpected activity of aromatic B-CePs against BxPC-3 pancreatic cancer cells. Preferential targeting by nitrogen mustards has recently been reported for chlorambucil against BRCA 1/2-deficient tumors, thus demonstrating that even agents commonly known as *aspecific* could exhibit cancer type tropisms.<sup>[17]</sup> In this sense, we plan to employ an omic approach to elucidate the molecular determinants of sensitivity for aromatic 3-chloropiperidines against BxPC-3 cells. Perturbations of the transcriptional profile and chromatin accessibility state will be evaluated upon cell stimulation with selected derivatives. This signature-driven strategy may open new perspectives in the refinement and exploration of the mechanism of action of these new chemical entities, facilitating the mindful repositioning of B-CePs as potential therapeutics.

## Experimental Section

### Materials and Methods

**MS studies.** The formation of B-CePs reactive species upon incubation at 37 °C in water was followed in time by ESI-MS as reported previously.<sup>[6a]</sup> A 80 μM solution of test compounds was prepared in MilliQ water from 1 mM DMSO stocks and incubated at 37 °C for 3 h. Small samples were taken after 0, 20, 40, 60 and 180 min, diluted 1:10 with methanol, and analyzed by ESI-MS. Measurements were performed in positive ion mode using a Xevo G2-XS Qtof instrument (Waters).

**Cleavage assay.** The ability of compounds to cleave the supercoiled plasmid pBR322 (Inspiralis Ltd) was investigated at the electrophoretic cleavage assay. The assay was performed following previously reported materials and protocols.<sup>[4a,b]</sup> B-CePs dilutions were freshly prepared from a 10 mM DMSO stock in Milli-Q water, resulting in a 0.5% DMSO concentration in the final reaction volume. Diversely, a 5 mM DMSO stock was prepared in the case of

the poorly soluble compound **5**, resulting in a final 1% DMSO concentration in the assay volume. EC<sub>50</sub> values were calculated considering the intensity of the supercoiled plasmid band at increasing compound concentrations expressed as percentage compared to the untreated control. Experiments were performed in duplicate to calculate average values and standard deviations.

**Cell cultures.** Colon (HCT-15) and pancreatic (BxPC-3) carcinoma cell lines were purchased from American Type Culture Collection (ATCC). The human ovarian 2008 cancer cell line was kindly provided by G. Marverti (Department of Biomedical Science, University of Modena and Reggio Emilia, Modena, Italy). Cell lines were maintained in logarithmic phase at 37 °C in a 5% carbon dioxide atmosphere using RPMI 1640 medium (Euroclone) containing 10% fetal calf serum (FCS, Euroclone), antibiotics (50 units/mL penicillin and 50 μg/mL streptomycin), and 2 mM L-glutamine.

**MTT assay.** The 72 h MTT assay was performed following previously reported materials and protocols.<sup>[9,18]</sup> Test compounds were dissolved in DMSO and added at defined concentrations to the cell growth medium to a final solvent concentration of 0.5%, which had no detectable effect on cell killing. A modified MTT assay was employed to investigate the uptake of test compounds. BxPC-3 cells were incubated either in the absence or presence of the compound for 5 h at 37 or 4 °C in parallel microplates. At the end of the incubation, fresh RPMI was added to wells replacing the medium containing the compound. Microplates were then incubated both at 37 °C up to 72 h and the MTT assay was performed. The method was validated in this modified version using cisplatin as positive internal control (Figure S2). This drug is known to exploit transporters to enter cells.<sup>[13,19]</sup>

**Alkaline single-cell gel electrophoresis.** The alkaline SCGE assay allowed to investigate the possible direct damage of genomic DNA induced by B-CePs on BxPC-3 cells. Experiments were performed following a previously reported protocol with only minor modifications.<sup>[20]</sup> 3 × 10<sup>5</sup> cells were seeded in 25 cm<sup>2</sup> flasks and incubated after 24 h with the defined concentration of compound or 0.5% DMSO for 6 h. Subsequently, cells were washed in PBS, harvested, centrifuged and resuspended at 1 × 10<sup>5</sup> in 1% low melting point agarose (LMPA, Trevigen). Pretreated comet slides (Trevigen) were spotted with 50 μL of cells-LMPA mixture and allowed to set at 4 °C for 30 min. Slides were immersed in lysis buffer (Trevigen) for 45 min, then incubated for 20 min in an alkaline electrophoresis solution (1 mM EDTA, 300 mM NaOH) followed by alkaline electrophoresis (1 V/cm) at 4 °C for 30 min. Slides were then washed twice in deionized H<sub>2</sub>O, fixed in 70% ethanol for 5 min and air-dried. DNA was stained with SYBR Green I for 10 min at 4 °C. Slides were examined at 5x and 40x magnification in a Zeiss LSM 800 confocal microscope using the Zeiss ZEN 2.3 software system. The relative % of comets (no. cells forming a comet/ total no. of cells) detected in two randomly captured fields (including at least 250 cells/field) from two independent experiments per condition was analyzed.

**Acid phosphatase (APH) assay.** The APH assay was employed to assess cell viability of spheroids treated with test compounds following previously reported protocols.<sup>[16]</sup> BxPC-3 cells were seeded (1.5 × 10<sup>3</sup> cells/well) in phenol red-free RPMI medium (Euroclone) containing antibiotics and L-glutamine (as previously specified) as well as 10% FCS and 20% methyl cellulose in round-bottom non-tissue culture treated 96 well-plates (Greiner Bio-one). After 72 h from seeding, spheroids were treated at the defined concentration of compound freshly dissolved in DMSO to a final solvent concentration of 0.5%, which had no detectable effect on cell killing. Upon 72 h of incubation, spheroids were incubated with 100 μL of the assay buffer for 3 h at 37 °C (0.1 M sodium acetate, 0.1% Triton-X-100, supplemented with ImmunoPure *p*-nitrophenyl

phosphate by Sigma). Subsequently, 10  $\mu\text{L}$  of 1 M NaOH were added before measuring the absorbance of each well at 405 nm (BioRad 680 microplate reader). Compounds  $\text{IC}_{50}$  values were extrapolated applying a four-parameter logistic (4-PL) model and average values of two experimental replicates were reported.

## Chemistry

All solvents were purified by distillation prior to use and in case of anhydrous solvents dried and stored under nitrogen atmosphere. Commercially available reagents were used as supplied if not stated different. Synthesis using anhydrous solvents were carried out under Schlenk conditions. For purification by flash column chromatography silica gel 60 (Merck) was used.  $^1\text{H}$  and  $^{13}\text{C}$  NMR spectra were recorded at Bruker Avance II 200 spectrometer ( $^1\text{H}$  at 200 MHz;  $^{13}\text{C}$  at 50 MHz) and Bruker Avance II 400 spectrometer ( $^1\text{H}$  at 400 MHz;  $^{13}\text{C}$  at 100 MHz) in deuterated solvents. Chemical shifts were determined by reference to the residual solvent signals. High-resolution ESI mass spectra were recorded in methanol using a ESI-microTOF spectrometer (Bruker Daltonics) in positive ion mode. All elemental analysis (CHN) were performed on a Thermo FlashEA-1112 series instrument. NMR spectra of all final products, as well as the synthetic procedures of the precursors 10–13, 18–22 and 40–43 are included in the Supporting Information. The synthesis of compounds 3, 7 and 9 as well as their corresponding precursors has been described elsewhere.<sup>[4b]</sup>

## Synthetic procedures

### General procedure A: Synthesis of diamines (23–24)

Under a nitrogen atmosphere 2,2-dimethylpent-4-enal (10; 2.1–2.4 equiv) as well as the corresponding diamine were dissolved in anhydrous dichloromethane (10 mL/mmol of diamine) and sodium triacetoxyborohydride (2.6–3 equiv) was added portion wise at 0 °C, followed by acetic acid (2.2–2.4 equiv). The mixture was stirred at room temperature for 16–18 h and was then quenched by the addition of 20% NaOH solution. The phases were separated and the aqueous layer was extracted three times with dichloromethane. The combined organic extracts were washed with brine, followed by distilled water and dried over  $\text{MgSO}_4$ . The solvent was removed under reduced pressure and the crude product was obtained, which was used in the next step without further purification.

### 1,2-Bis-[(2,2-dimethylpent-4-enyl)aminomethyl]benzene (23)

Was prepared according to the general procedure A from 1,2-bis(aminomethyl)benzene (13; 0.71 g, 5.23 mmol) and 2,2-dimethylpent-4-enal (10; 1.41 g, 12.55 mmol) yielding the title compound as a pale red oil (1.50 g, 4.58 mmol).  $^1\text{H}$  NMR (400 MHz,  $\text{CDCl}_3$ ):  $\delta$  = 7.33–7.29 (m, 2H), 7.26–7.22 (m, 2H), 5.84–5.74 (m, 2H), 5.03–4.96 (m, 4H), 3.83 (s, 4H), 2.41 (s, 4H), 2.01 (d,  $J$  = 7.5 Hz, 4H), 0.89 (s, 12H) ppm;  $^{13}\text{C}$  NMR (101 MHz,  $\text{CDCl}_3$ ):  $\delta$  = 139.21, 135.65, 129.78, 127.19, 116.96, 60.33, 52.93, 44.86, 34.54, 25.69 ppm; HRMS (ESI):  $m/z$  calcd for  $\text{C}_{22}\text{H}_{37}\text{N}_2^+$ : 329.2951; found: 329.2950 [ $M+H$ ] $^+$ .

### 1,3-Bis-[(2,2-dimethylpent-4-enyl)aminomethyl]benzene (24)

Was prepared according to the general procedure A from 1,3-bis(aminomethyl)benzene (14; 1.03 g, 7.56 mmol) and 2,2-dimethylpent-4-enal (10; 1.75 g, 15.60 mmol) yielding the title compound as a colorless oil (2.18 g, 6.64 mmol).  $^1\text{H}$  NMR (200 MHz,  $\text{CDCl}_3$ ):  $\delta$  = 7.42–7.28 (m, 4H), 5.90–5.65 (m, 2H), 5.11–4.93 (m, 4H), 4.13 (s, 4H), 2.93 (s, 4H), 2.08 (d,  $J$  = 7.2 Hz, 4H), 0.95 (s, 12H) ppm;  $^{13}\text{C}$  NMR

(50 MHz,  $\text{CDCl}_3$ ):  $\delta$  = 137.79, 135.33, 130.18, 128.80, 128.39, 117.43, 73.42, 70.49, 45.03, 35.75, 25.95 ppm; HRMS (ESI):  $m/z$  calcd for  $\text{C}_{27}\text{H}_{37}\text{N}_2^+$ : 329.2951; found: 329.2958 [ $M+H$ ] $^+$ .

### General procedure B: Synthesis of diamines (26–28)

Under a nitrogen atmosphere sodium hydride (2.8 equiv) was suspended in anhydrous tetrahydrofuran (10 mL/100 mg of sodium hydride) and 2,2-dimethylpent-4-en-1-amine (12; 2.4 equiv) was added dropwise at 0 °C. The mixture was stirred at 0 °C for 30 min and the corresponding dibromide or *bis*-mesylate, dissolved in anhydrous tetrahydrofuran (2 mL/mmol of dibromide/*bis*-mesylate), was added dropwise at 0 °C. Afterwards the mixture was stirred for 1 h at 0 °C and for an additional 20 h at room temperature. The reaction was then quenched by the addition of 10% NaOH solution. The phases were separated and the aqueous layer was extracted three times with ethyl acetate. The combined organic extracts were washed with distilled water, followed by brine and dried over  $\text{MgSO}_4$ . The solvent was removed under reduced pressure and the crude product was obtained, which was used in the next step without further purification.

### 5-Methoxy-1,3-bis-[(2,2-dimethylpent-4-enyl)aminomethyl]benzene (26)

Was prepared according to the general procedure B from 5-methoxy-1,3-bis-[(methylsulfonyloxy)methyl]benzene (20; 2.50 g, 7.71 mmol) and 2,2-dimethylpent-4-en-1-amine (12; 2.09 g, 18.46 mmol) yielding the title compound as a yellow oil (2.71 g, 7.55 mmol).  $^1\text{H}$  NMR (400 MHz,  $\text{CDCl}_3$ ):  $\delta$  = 6.92 (s, 1H), 6.84 (s, 2H), 5.81–5.73 (m, 2H), 5.03–4.98 (m, 4H), 3.82–3.81 (m, 7H), 2.40 (s, 4H), 2.04–2.02 (m, 4H), 0.91 (s, 12H) ppm;  $^{13}\text{C}$  NMR (101 MHz,  $\text{CDCl}_3$ ):  $\delta$  = 160.04, 135.39, 120.61, 117.19, 112.60, 59.35, 55.42, 54.41, 44.72, 34.37, 25.57 ppm; HRMS (ESI):  $m/z$  calcd for  $\text{C}_{23}\text{H}_{39}\text{N}_2\text{O}^+$ : 359.3057; found: 359.3053 [ $M+H$ ] $^+$ .

### Methyl 3,5-bis-[(2,2-dimethylpent-4-enyl)aminomethyl]benzoate (27)

Was prepared according to the general procedure B from 3,5-bis-(bromomethyl)benzoic acid methyl ester (21; 1.17 g, 3.63 mmol) and 2,2-dimethylpent-4-en-1-amine (12; 0.99 g, 8.72 mmol) yielding the title compound as a yellow oil (1.38 g, 3.56 mmol).  $^1\text{H}$  NMR (400 MHz,  $\text{CDCl}_3$ ):  $\delta$  = 7.89–7.85 (m, 2H), 7.58–7.53 (m, 1H), 5.83–5.73 (m, 2H), 5.03–4.97 (m, 4H), 3.91 (s, 3H), 3.83 (s, 4H), 2.35 (s, 4H), 2.02 (d,  $J$  = 7.5 Hz, 4H), 0.89 (s, 12H) ppm;  $^{13}\text{C}$  NMR (101 MHz,  $\text{CDCl}_3$ ):  $\delta$  = 167.45, 141.33, 135.60, 132.53, 130.33, 127.93, 117.01, 59.67, 54.34, 52.22, 44.76, 34.50, 25.67 ppm; HRMS (ESI):  $m/z$  calcd for  $\text{C}_{24}\text{H}_{39}\text{N}_2\text{O}_2^+$ : 387.3006; found: 387.3008 [ $M+H$ ] $^+$ .

### 2,6-Bis-[(2,2-dimethylpent-4-enyl)aminomethyl]pyridine (28)

Was prepared according to the general procedure B from 2,6-bis-[(methylsulfonyloxy)methyl]pyridine (22; 1.29 g, 4.39 mmol) and 2,2-dimethylpent-4-en-1-amine (12; 1.19 g, 10.53 mmol) yielding the title compound as a yellow oil (1.41 g, 4.28 mmol).  $^1\text{H}$  NMR (400 MHz,  $\text{CDCl}_3$ ):  $\delta$  = 7.58 (t,  $J$  = 7.6 Hz, 1H), 7.18 (d,  $J$  = 7.6 Hz, 2H), 5.85–5.74 (m, 2H), 5.03–4.98 (m, 4H), 3.88 (s, 4H), 2.39 (s, 4H), 2.03 (d,  $J$  = 7.5 Hz, 4H), 0.91 (s, 12H) ppm;  $^{13}\text{C}$  NMR (101 MHz,  $\text{CDCl}_3$ ):  $\delta$  = 159.67, 136.80, 135.59, 120.33, 117.00, 60.16, 56.03, 44.82, 34.50, 25.62 ppm; HRMS (ESI):  $m/z$  calcd for  $\text{C}_{27}\text{H}_{36}\text{N}_3^+$ : 330.2904; found: 330.2901 [ $M+H$ ] $^+$ .

**General procedure C: Synthesis of bis-N-chloroamines (31–36)**

Under a nitrogen atmosphere the crude unsaturated diamine was dissolved in anhydrous dichloromethane (10 ml/mmol of diamine) and freshly recrystallized *N*-chlorosuccinimide (2.4 equiv) was added portion wise at 0 °C. The mixture was stirred at 0 °C for 30 min and for an additional 2–2.5 h at room temperature. The solvent was removed under reduced pressure and the crude product was purified by flash column chromatography.

**1,2-Bis-[N-chloro(2,2-dimethylpent-4-enyl)aminomethyl]benzene (31)**

Was prepared according to the general procedure C from 1,2-bis-[(2,2-dimethylpent-4-enyl)aminomethyl]benzene (**23**; 1.48 g, 4.49 mmol) and purified by flash column chromatography (pentane/TBME 20:1), yielding the title compound as a pale yellow oil (1.35 g, 4.10 mmol, 66% over 2 steps). <sup>1</sup>H NMR (400 MHz, CDCl<sub>3</sub>): δ = 7.39–7.35 (m, 2H), 7.32–7.28 (m, 2H), 5.78–5.66 (m, 2H), 5.02–4.95 (m, 4H), 4.28 (s, 4H), 2.94 (s, 4H), 2.03 (d, *J* = 7.4 Hz, 4H), 0.92 (s, 12H) ppm; <sup>13</sup>C NMR (101 MHz, CDCl<sub>3</sub>): δ = 136.74, 135.22, 130.86, 127.92, 117.41, 73.59, 67.96, 45.19, 35.61, 26.03 ppm; HRMS (ESI): *m/z* calcd for C<sub>22</sub>H<sub>36</sub>Cl<sub>2</sub>N<sub>2</sub><sup>+</sup>: 397.2172; found: 397.2170 [*M* + H]<sup>+</sup>.

**1,3-Bis-[N-chloro(2,2-dimethylpent-4-enyl)aminomethyl]benzene (32)**

Was prepared according to the general procedure C from 1,3-bis-[(2,2-dimethylpent-4-enyl)aminomethyl]benzene (**24**; 1.47 g, 4.48 mmol) and purified by flash column chromatography (pentane/TBME 10:1), yielding the title compound as a colorless oil (1.63 g, 4.10 mmol, 80% over 2 steps). <sup>1</sup>H NMR (400 MHz, CDCl<sub>3</sub>): δ = 7.38–7.30 (m, 4H), 5.83–5.71 (m, 2H), 5.05–4.97 (m, 4H), 4.13 (s, 4H), 2.93 (s, 4H), 2.08 (d, *J* = 7.6 Hz, 4H), 0.95 (s, 12H) ppm; <sup>13</sup>C NMR (50 MHz, CDCl<sub>3</sub>): δ = 137.79, 135.33, 130.18, 128.81, 128.40, 117.43, 73.42, 70.49, 45.02, 35.75, 25.95 ppm; HRMS (ESI): *m/z* calcd for C<sub>22</sub>H<sub>36</sub>Cl<sub>2</sub>N<sub>2</sub><sup>+</sup>: 397.2172; found: 397.2178 [*M* + H]<sup>+</sup>.

**5-Methoxy-1,3-bis-[N-chloro(2,2-dimethylpent-4-enyl)aminomethyl]benzene (34)**

Was prepared according to the general procedure C from 5-Methoxy-1,3-bis-[(2,2-dimethylpent-4-enyl)aminomethyl]benzene (**26**; 1.54 g, 4.28 mmol) and purified by flash column chromatography (pentane/TBME 20:1), yielding the title compound as a pale yellow oil (827 mg, 1.93 mmol, 44% over 2 steps). <sup>1</sup>H NMR (400 MHz, CDCl<sub>3</sub>): δ = 6.94–6.92 (m, 1H), 6.88–6.86 (m, 2H), 5.82–5.71 (m, 2H), 5.03–5.02 (m, 2H), 5.01–4.97 (m, 2H), 4.09 (s, 4H), 3.82 (s, 3H), 2.91 (s, 4H), 2.07 (d, *J* = 7.4 Hz, 4H), 0.94 (s, 12H) ppm; <sup>13</sup>C NMR (101 MHz, CDCl<sub>3</sub>): δ = 159.74, 139.19, 135.33, 122.34, 117.41, 114.18, 73.44, 70.50, 55.43, 45.07, 35.75, 25.98 ppm; HRMS (ESI): *m/z* calcd for C<sub>23</sub>H<sub>36</sub>Cl<sub>2</sub>N<sub>2</sub>O<sup>+</sup>: 449.2097; found: 449.2100 [*M* + Na]<sup>+</sup>.

**Methyl 3,5-bis-[N-chloro(2,2-dimethylpent-4-enyl)aminomethyl]benzoate (35)**

Was prepared according to the general procedure C from methyl 3,5-bis-[(2,2-dimethylpent-4-enyl)aminomethyl]benzoate (**27**; 1.37 g, 3.55 mmol) and purified by flash column chromatography (pentane/TBME 10:1), yielding the title compound as a colorless oil (546 mg, 1.20 mmol, 33% over 2 steps). <sup>1</sup>H NMR (400 MHz, CDCl<sub>3</sub>): δ = 7.95 (d, *J* = 1.5 Hz, 2H), 7.62–7.60 (m, 1H), 5.04–5.03 (m, 2H), 5.00 (d, *J* = 5.4 Hz, 2H), 4.15 (s, 4H), 3.93 (s, 3H), 2.94 (s, 4H), 2.08 (d, *J* = 7.5 Hz, 4H), 0.95 (s, 12H) ppm; <sup>13</sup>C NMR (101 MHz, CDCl<sub>3</sub>): δ =

167.00, 138.31, 135.24, 134.59, 130.44, 129.90, 117.52, 73.71, 69.99, 52.35, 45.06, 35.83, 25.95 ppm; HRMS (ESI): *m/z* calcd for C<sub>24</sub>H<sub>37</sub>Cl<sub>2</sub>N<sub>2</sub>O<sub>2</sub><sup>+</sup>: 455.2227; found: 455.2231 [*M* + H]<sup>+</sup>.

**2,6-Bis-[N-chloro(2,2-dimethylpent-4-enyl)aminomethyl]pyridine (36)**

Was prepared according to the general procedure C from 2,6-bis-[(2,2-dimethylpent-4-enyl)aminomethyl]pyridine (**28**; 1.31 g, 3.98 mmol) and purified by flash column chromatography (pentane/TBME 10:1), yielding the title compound as a colorless oil (284 mg, 0.71 mmol, 17% over 2 steps). <sup>1</sup>H NMR (400 MHz, CDCl<sub>3</sub>): δ = 7.73 (t, *J* = 7.7 Hz, 1H), 7.47 (d, *J* = 7.7 Hz, 2H), 5.82–5.72 (m, 2H), 5.03–4.97 (m, 4H), 4.28 (s, 4H), 3.01 (s, 4H), 2.07 (d, *J* = 7.5 Hz, 4H), 0.94 (s, 12H) ppm; <sup>13</sup>C NMR (101 MHz, CDCl<sub>3</sub>): δ = 156.85, 137.11, 135.25, 122.34, 117.51, 73.96, 71.93, 44.97, 35.85, 25.85 ppm; HRMS (ESI): *m/z* calcd for C<sub>21</sub>H<sub>34</sub>Cl<sub>2</sub>N<sub>3</sub><sup>+</sup>: 398.2125; found: 398.2126 [*M* + H]<sup>+</sup>.

**General procedure D: Synthesis of bis-3-chloropiperidines (1–6)**

Under a nitrogen atmosphere the appropriate *bis-N*-chloroamine was dissolved in anhydrous chloroform (10 mL/mmol of *bis-N*-chloroamine) and tetrabutylammonium iodide (10 mol%) was added. The mixture was heated to 60 °C (oil bath temperature) for 2–2.5 h and the solvent was removed under reduced pressure. The product was purified by flash column chromatography. The resulting bis-3-chloropiperidines were obtained as an inseparable mixture of diastereomers.

**1,2-Bis-[(3-chloro-5,5-dimethylpiperidin-1-yl)methyl]benzene (1)**

Was prepared according to the general procedure D from 1,2-bis-[N-chloro(2,2-dimethylpent-4-enyl)aminomethyl]benzene (**31**; 1.34 g, 3.36 mmol) and purified by flash column chromatography (pentane/TBME 20:1), yielding the title compound as a pale yellow oil (1.07 g, 2.69 mmol, 80%). <sup>1</sup>H NMR (400 MHz, CDCl<sub>3</sub>): δ = 7.32–7.26 (m, 2H), 7.24–7.19 (m, 2H), 4.09–3.98 (m, 2H), 3.74 (d, *J* = 13.1 Hz, 1H), 3.59 (q, *J* = 13.2 Hz, 2H), 3.43 (d, *J* = 13.1 Hz, 1H), 3.13–3.03 (m, 2H), 2.42–2.32 (m, 2H), 2.00–1.89 (m, 4H), 1.83–1.75 (m, 2H), 1.36 (t, *J* = 12.3 Hz, 2H), 1.04 (d, *J* = 7.4 Hz, 6H), 0.91 (s, 6H) ppm; <sup>13</sup>C NMR (101 MHz, CDCl<sub>3</sub>): δ = 137.46, 130.32, 127.08, 77.16, 65.59, 61.74, 60.04, 54.36, 48.49, 33.60, 29.45, 25.52 ppm; HRMS (ESI): *m/z* calcd for C<sub>22</sub>H<sub>35</sub>Cl<sub>2</sub>N<sub>2</sub><sup>+</sup>: 397.2172; found: 397.2175 [*M* + H]<sup>+</sup>; elemental analysis calcd (%) for C<sub>22</sub>H<sub>34</sub>Cl<sub>2</sub>N<sub>2</sub>: C 66.49; H 8.62; N 7.05; found: C 66.23; H 8.54; N 6.72.

**1,3-Bis-[(3-chloro-5,5-dimethylpiperidin-1-yl)methyl]benzene (2)**

Was prepared according to the general procedure D from 1,3-bis-[N-chloro(2,2-dimethylpent-4-enyl)aminomethyl]benzene (**32**; 950 mg, 2.39 mmol) and purified by flash column chromatography (pentane/TBME 10:1), yielding the title compound as a pale yellow oil (651 mg, 1.64 mmol, 69%). <sup>1</sup>H NMR (400 MHz, CDCl<sub>3</sub>): δ = 7.27–7.15 (m, 4H), 4.16–4.06 (m, 2H), 3.58–3.43 (m, 4H), 3.20–3.12 (m, 2H), 2.43–2.35 (m, 2H), 2.04–1.92 (m, 4H), 1.76 (dd, *J* = 10.9, 6.7 Hz, 2H), 1.35 (t, *J* = 12.3 Hz, 2H), 1.06 (d, *J* = 2.8 Hz, 6H), 0.89 (d, *J* = 1.5 Hz, 6H) ppm; <sup>13</sup>C NMR (101 MHz, CDCl<sub>3</sub>): δ = 138.61, 129.15, 128.25, 127.58, 64.69, 62.43, 62.08, 54.36, 48.56, 33.53, 29.43, 25.27 ppm; HRMS (ESI): *m/z* calcd for C<sub>22</sub>H<sub>35</sub>Cl<sub>2</sub>N<sub>2</sub><sup>+</sup>: 397.2172; found: 397.2176 [*M* + H]<sup>+</sup>.

#### 5-Methoxy-1,3-bis-[(3-chloro-5,5-dimethylpiperidin-1-yl)methyl]benzene (4)

Was prepared according to the general procedure D from 5-methoxy-1,3-bis-[N-chloro(2,2-dimethylpent-4-enyl)aminomethyl]benzene (34; 1.31 g, 3.06 mmol) and purified by flash column chromatography (pentane/TBME 10:1), yielding the title compound as a pale orange oil (981 mg, 2.29 mmol, 75%). <sup>1</sup>H NMR (400 MHz, CDCl<sub>3</sub>): δ = 6.84–6.80 (m, 1H), 6.80–6.75 (m, 2H), 4.17–4.06 (m, 2H), 3.80 (s, 3H), 3.56–3.37 (m, 4H), 3.20–3.11 (m, 2H), 2.43–2.34 (m, 2H), 2.05–1.91 (m, 4H), 1.78–1.70 (m, 2H), 1.35 (t, *J* = 12.3 Hz, 2H), 1.07 (s, 6H), 0.89 (s, 6H) ppm; <sup>13</sup>C NMR (101 MHz, CDCl<sub>3</sub>): δ = 159.87, 140.21, 121.37, 112.77, 77.16, 64.64, 62.33, 55.34, 54.36, 48.51, 33.52, 29.42, 25.27 ppm; HRMS (ESI): *m/z* calcd for C<sub>23</sub>H<sub>37</sub>Cl<sub>2</sub>N<sub>2</sub>O<sup>+</sup>: 427.2278; found: 427.2281 [*M* + H]<sup>+</sup>; elemental analysis calcd (%) for C<sub>23</sub>H<sub>36</sub>Cl<sub>2</sub>N<sub>2</sub>O: C 64.63; H 8.49; N 6.55; found: C 64.96; H 8.29; N 6.62.

#### Methyl 3,5-bis-[(3-chloro-5,5-dimethylpiperidin-1-yl)methyl]-benzoate (5)

Was prepared according to the general procedure D from methyl 3,5-bis-[N-chloro(2,2-dimethylpent-4-enyl)aminomethyl]benzoate (35; 514 mg, 1.13 mmol) and purified by flash column chromatography (pentane/TBME 10:1), yielding the title compound as a pale yellow oil (447 mg, 0.98 mmol, 86%). <sup>1</sup>H NMR (400 MHz, CDCl<sub>3</sub>): δ = 7.87–7.82 (m, 2H), 7.48 (d, *J* = 7.8 Hz, 1H), 4.10 (s, 2H), 3.92 (s, 3H), 3.61–3.46 (m, 4H), 3.18–3.09 (m, 2H), 2.36 (t, *J* = 9.9 Hz, 2H), 2.06–1.92 (m, 4H), 1.80–1.73 (m, 2H), 1.35 (t, *J* = 12.3 Hz, 2H), 1.06 (d, *J* = 3.3 Hz, 6H), 0.89 (s, 6H) ppm; <sup>13</sup>C NMR (101 MHz, CDCl<sub>3</sub>): δ = 167.33, 139.19, 133.65, 130.36, 128.82, 77.16, 64.68, 62.01, 54.18, 52.27, 48.45, 33.53, 29.40, 25.25 ppm; HRMS (ESI): *m/z* calcd for C<sub>24</sub>H<sub>37</sub>Cl<sub>2</sub>N<sub>2</sub>O<sub>2</sub><sup>+</sup>: 455.2227; found: 455.2228 [*M* + H]<sup>+</sup>.

#### 2,6-Bis-[(3-chloro-5,5-dimethylpiperidin-1-yl)methyl]-pyridine (6)

Was prepared according to the general procedure D from 2,6-bis-[N-chloro(2,2-dimethylpent-4-enyl)aminomethyl]pyridine (36; 240 mg, 0.60 mmol) and purified by flash column chromatography (pentane/TBME 3:1), yielding the title compound as a pale yellow oil (183 mg, 0.46 mmol, 76%). <sup>1</sup>H NMR (400 MHz, CDCl<sub>3</sub>): δ = 7.64 (t, *J* = 7.7 Hz, 1H), 7.34 (d, *J* = 7.1 Hz, 2H), 4.19–4.10 (m, 2H), 3.76–3.59 (m, 4H), 3.19 (d, *J* = 8.5 Hz, 2H), 2.40 (d, *J* = 10.9 Hz, 2H), 2.14 (t, *J* = 10.6 Hz, 2H), 1.98–1.86 (m, 4H), 1.37 (t, *J* = 12.3 Hz, 2H), 1.09 (s, 6H), 0.90 (s, 6H) ppm; <sup>13</sup>C NMR (101 MHz, CDCl<sub>3</sub>): δ = 158.30, 137.07, 121.00, 64.79, 63.95, 62.18, 54.02, 48.26, 33.53, 29.39, 25.30 ppm; HRMS (ESI): *m/z* calcd for C<sub>21</sub>H<sub>34</sub>Cl<sub>2</sub>N<sub>3</sub><sup>+</sup>: 398.2125; found: 398.2124 [*M* + H]<sup>+</sup>.

#### 1,3,5-Tris-[(2,2-dimethylpent-4-enyl)aminomethyl]benzene (42)

Under a nitrogen atmosphere 1,3,5-tris-(bromomethyl)benzene (41; 1.00 g, 2.81 mmol) was dissolved in anhydrous dichloromethane (60 mL) and 2,2-dimethylpent-4-en-1-amine (12; 1.90 g, 16.78 mmol) was added dropwise at 0 °C. The mixture was stirred at room temperature for 68 h and was then quenched by the addition of distilled water (50 mL). The layers were separated, the organic phase washed with brine and was then dried over MgSO<sub>4</sub>. The solvent was removed under reduced pressure and the crude product was obtained as a yellow oil, which was used in the next step without further purification (1.17 g, 2.59 mmol). <sup>1</sup>H NMR (400 MHz, CDCl<sub>3</sub>): δ = 7.16 (s, 3H), 5.84–5.74 (m, 3H), 5.00 (d, *J* = 13.5 Hz, 6H), 3.78 (s, 6H), 2.37 (s, 6H), 2.02 (d, *J* = 7.5 Hz, 6H), 0.89 (s, 18H) ppm; <sup>13</sup>C NMR (101 MHz, CDCl<sub>3</sub>): δ = 141.07, 135.72, 126.21, 116.89, 59.88, 54.81, 44.78, 34.50, 25.67 ppm; HRMS (ESI): *m/z* calcd for C<sub>30</sub>H<sub>52</sub>N<sub>3</sub><sup>+</sup>: 454.4156; found: 454.4154 [*M* + H]<sup>+</sup>.

#### 1,3,5-Tris-[N-chloro-(2,2-dimethylpent-4-enyl)aminomethyl]benzene (43)

Under a nitrogen atmosphere 1,3,5-tris-[(2,2-dimethylpent-4-enyl)aminomethyl]benzene (42; 1.13 g, 2.49 mmol) was dissolved in anhydrous dichloromethane (80 mL) and freshly recrystallized *N*-chlorosuccinimide (1.10 g, 8.22 mmol) was added portion wise at 0 °C. The mixture was stirred at 0 °C for 30 min and for an additional 2 h at room temperature. The solvent was removed under reduced pressure and the crude product was purified by flash column chromatography (pentane/TBME 10:1). The product was obtained as a colorless oil (1.09 g, 1.95 mmol, 75% over 2 steps). <sup>1</sup>H NMR (400 MHz, CDCl<sub>3</sub>): δ = 7.32–7.27 (m, 3H), 5.81–5.71 (m, 3H), 5.03–4.97 (m, 6H), 4.12 (s, 6H), 2.92 (s, 6H), 2.06 (d, *J* = 7.5 Hz, 6H), 0.94 (s, 18H) ppm; <sup>13</sup>C NMR (101 MHz, CDCl<sub>3</sub>): δ = 137.84, 135.34, 129.73, 117.43, 77.16, 73.37, 70.39, 45.06, 35.75, 25.96 ppm; HRMS (ESI): *m/z* calcd for C<sub>30</sub>H<sub>48</sub>Cl<sub>3</sub>N<sub>3</sub>Na<sup>+</sup>: 578.2806; found: 578.2806 [*M* + H]<sup>+</sup>.

#### 1,3,5-Tris-[(3-chloro-5,5-dimethylpiperidin-1-yl)methyl]-benzene (8)

Under a nitrogen atmosphere 1,3,5-Tris-[N-chloro-(2,2-dimethylpent-4-enyl)aminomethyl]benzene (43; 1.03 g, 1.85 mmol) was dissolved in anhydrous chloroform (20 mL) and tetrabutylammonium iodide (81 mg, 14 mol%) was added. The mixture was heated to reflux for 4 h and the solvent was removed under reduced pressure. The product was purified by flash column chromatography (pentane/TBME 10:1) and was obtained as a pale yellow oil (0.70 g, 1.26 mmol, 68%). <sup>1</sup>H NMR (400 MHz, CDCl<sub>3</sub>): δ = 7.14–7.06 (m, 3H), 4.14–4.06 (m, 3H), 3.56–3.40 (m, 6H), 3.19–3.11 (m, 3H), 2.41–2.33 (m, 3H), 2.03–1.91 (m, 6H), 1.74 (dt, *J* = 11.0, 5.4 Hz, 3H), 1.34 (t, *J* = 12.3 Hz, 3H), 1.05 (t, *J* = 3.1 Hz, 9H), 0.89 (s, 9H) ppm; <sup>13</sup>C NMR (101 MHz, CDCl<sub>3</sub>): δ = 138.51, 128.02, 64.66, 62.41, 62.10, 54.39, 48.53, 33.53, 29.44, 25.31 ppm; HRMS (ESI): *m/z* calcd for C<sub>30</sub>H<sub>48</sub>Cl<sub>3</sub>N<sub>3</sub><sup>+</sup>: 556.2987; found: 556.2988 [*M* + H]<sup>+</sup>; elemental analysis calcd (%) for C<sub>30</sub>H<sub>48</sub>Cl<sub>3</sub>N<sub>3</sub>: C 64.68; H 8.69; N 7.44; found: C 64.58; H 8.52; N 7.44.

### Acknowledgements

A.S. received funding from the European Union's Horizon 2020 Research and Innovation programme under the Marie Skłodowska-Curie grant agreement no. 751931. Open access funding enabled and organized by Projekt DEAL.

### Conflict of Interest

The authors declare no conflict of interest.

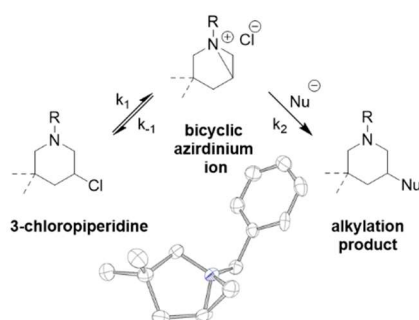
**Keywords:** alkylating agents · aromatic chloropiperidines · DNA damage · pancreatic cancer spheroids · structure-activity relationships

- [1] a) N. Saijo, *Cancer Res.* **2012**, *44*, 1–10; b) M. Huang, A. J. Shen, J. Ding, M. Y. Geng, *Trends Pharmacol. Sci.* **2014**, *35*, 41–50.
- [2] B. A. Chabner, T. G. Roberts Jr., *Nat. Rev. Cancer* **2005**, *5*, 65–72.
- [3] R. K. Singh, S. Kumar, D. N. Prasad, T. R. Bhardwaj, *Eur. J. Med. Chem.* **2018**, *151*, 401–433.
- [4] a) I. Zuravka, R. Roesmann, A. Sosic, R. Gottlich, B. Gatto, *Bioorg. Med. Chem.* **2015**, *23*, 1241–1250; b) I. Zuravka, R. Roesmann, A. Sosic, W.

- Wende, A. Pingoud, B. Gatto, R. Gottlich, *ChemMedChem* **2014**, *9*, 2178–2185; c) I. Zuravka, A. Susic, B. Gatto, R. Gottlich, *Bioorg. Med. Chem. Lett.* **2015**, *25*, 4606–4609.
- [5] A. Susic, I. Zuravka, N. K. Schmitt, A. Miola, R. Gottlich, D. Fabris, B. Gatto, *ChemMedChem* **2017**, *12*, 1471–1479.
- [6] a) A. Polavarapu, J. A. Stillabower, S. G. Stubblefield, W. M. Taylor, M. H. Baik, *J. Org. Chem.* **2012**, *77*, 5914–5921; b) R. B. Silverman, M. W. Holladay, *The Organic Chemistry of Drug Design and Drug Action*, 3rd ed., Elsevier, Amsterdam, **2014**.
- [7] K. C. Brannock, *J. Am. Chem. Soc.* **1959**, *81*, 3379–3383.
- [8] M. Noack, R. Göttlich, *Eur. J. Org. Chem.* **2002**, *2002*, 3171–3178.
- [9] C. Carraro, A. Francke, A. Susic, F. Kohl, T. Helbing, M. De Franco, D. Fabris, R. Gottlich, B. Gatto, *ACS Med. Chem. Lett.* **2019**, *10*, 552–557.
- [10] L. P. Hammett, *J. Am. Chem. Soc.* **1937**, *59*, 96–103.
- [11] C. J. O'Connor, W. A. Denny, J. Y. Fan, G. L. Gravatt, B. A. Grigor, D. J. McLennan, *J. Chem. Soc. Perkin Trans. 2* **1991**, 1933–1939.
- [12] B. Varghese, S. Kothari, K. K. Banerji, *Int. J. Chem. Kinet.* **1999**, *31*, 245–252.
- [13] C. Bolzati, D. Carta, V. Gandin, C. Marzano, N. Morellato, N. Salvatore, M. Cantore, N. A. Colabufo, *J. Biol. Inorg. Chem.* **2013**, *18*, 523–538.
- [14] D. W. Fairbairn, P. L. Olive, K. L. O'Neill, *Mutat. Res.* **1995**, *339*, 37–59.
- [15] R. Edmondson, J. J. Broglie, A. F. Adcock, L. Yang, *Assay Drug Dev. Technol.* **2014**, *12*, 207–218.
- [16] V. Gandin, C. Ceresa, G. Esposito, S. Indraccolo, M. Porchia, F. Tisato, C. Santini, M. Pellei, C. Marzano, *Sci. Rep.* **2017**, *7*, 13936. 10.1038/s41598-017-13698-1.
- [17] E. M. Tacconi, S. Badie, G. De Gregoriis, T. Reisländer, X. Lai, M. Porru, C. Folio, J. Moore, A. Kopp, J. Baguna Torres, D. Sneddon, M. Green, S. Dedic, J. W. Lee, A. S. Batra, O. M. Rueda, A. Bruna, C. Leonetti, C. Caldas, B. Cornelissen, L. Brino, A. Ryan, A. Biroccio, M. Tarsounas, *EMBO Mol. Med.* **2019**, *11*, e9982.
- [18] a) D. Montagner, V. Gandin, C. Marzano, A. Erxleben, *J. Inorg. Biochem.* **2015**, *145*, 101–107; b) M. C. Alley, D. A. Scudiero, A. Monks, M. L. Hursey, M. J. Czerwinski, D. L. Fine, B. J. Abbott, J. G. Mayo, R. H. Shoemaker, M. R. Boyd, *Cancer Res.* **1988**, *48*, 589–601.
- [19] F. Arnesano, M. Losacco, G. Natile, *Eur. J. Inorg. Chem.* **2013**, 2701–2711. 10.1002/ejic.201300001.
- [20] C. Marzano, S. M. Sbovata, V. Gandin, D. Colavito, E. Del Giudice, R. A. Michelin, A. Venzo, R. Seraglia, F. Benetollo, M. Schiavon, R. Bertani, *J. Med. Chem.* **2010**, *53*, 6210–6227.

Manuscript received: June 27, 2020  
Accepted manuscript online: August 3, 2020  
Version of record online: September 15, 2020

## 4.2. Understanding the Alkylation Mechanism of 3-Chloropiperidines – NMR Kinetic Studies and Isolation of Bicyclic Aziridinium Ions



In this research, we analyzed the alkylation mechanism of 3-chloropiperidines by isolation of the proposed intermediate aziridinium ions and NMR kinetic investigations. The bicyclic structure of these predicted intermediates was confirmed by single crystal XRD, while the kinetic analysis revealed remarkable reactivity differences between the gem-methylated compounds and their corresponding non-methylated analogues.

### Reference

Tim Helbing, Mats Georg, Fabian Stöhr, Caterina Carraro, Jonathan Becker, Barbara Gatto, Richard Göttlich, *European Journal of Organic Chemistry* **2021**, 2021, 5905. (doi: 10.1002/ejoc.202101072)

Cover Feature in *European Journal of Organic Chemistry* 44/2021. (doi: 10.1002/ejoc.202101371)

© 2021 The Authors. *European Journal of Organic Chemistry* published by Wiley – VCH Verlag GmbH & Co. KGaA, Weinheim.

Reproduced with permission of the copyright owners.



# Understanding the Alkylation Mechanism of 3-Chloropiperidines – NMR Kinetic Studies and Isolation of Bicyclic Aziridinium Ions

Tim Helbing,<sup>[a]</sup> Mats Georg,<sup>[a]</sup> Fabian Stöhr,<sup>[a, b]</sup> Caterina Carraro,<sup>[c]</sup> Jonathan Becker,<sup>[b]</sup> Barbara Gatto,<sup>[c]</sup> and Richard Göttlich<sup>\*[a]</sup>

The present study describes the kinetic analysis of the 3-chloropiperidine alkylation mechanism. These nitrogen mustard-based compounds are expected to react via a highly electrophilic bicyclic aziridinium ion, which is readily attacked by nucleophiles. Halide abstraction using silver salts with weakly coordinating anions lead to the isolation of these proposed intermediates, whereas their structure was confirmed by single crystal XRD. Kinetic studies of the aziridinium ions also

revealed notable reactivity differences of the C5 gem-methylated compounds and their unmethylated counterparts. The observed reactivity trends were also reflected by NMR studies in aqueous solution and DNA alkylation experiments of the related 3-chloropiperidines. Therefore, the underlying Thorpe-Ingold effect might be considered as another option to adjust the alkylation activity of these compounds.

## Introduction

Since many years alkylating agents serve as therapeutic agents for the treatment of cancer.<sup>[1]</sup> Amongst these therapeutic alkylating agents, nitrogen mustards like mechlorethamine and chlorambucil (Figure 1a) represent one of the first clinically applied chemotherapeutics which are used in cancer treatment.<sup>[2]</sup> Their simple but effective molecular mode of action involves the formation of an electrophilic aziridinium ion by intramolecular displacement of a chloride, which is then readily attacked by nucleophiles such as the guanine base in DNA.<sup>[3]</sup> The resulting covalent adducts eventually lead to depurination and strand cleavage, potentially followed by apoptosis of the cancer cell.<sup>[4]</sup> Despite the fact that there are numerous other promising candidates for the treatment of cancer and that alkylating agents suffer from severe side effects, these compounds continue to be an important class of

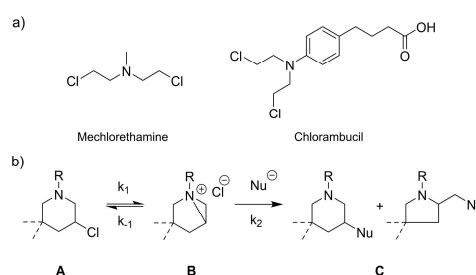


**Figure 1.** a) Structures of the nitrogen mustards mechlorethamine and chlorambucil. b) General structure of a 3-chloropiperidine **A** in equilibrium with the corresponding aziridinium ion **B**, which is attacked by a nucleophile forming the alkylation products **C**.

[a] T. Helbing, M. Georg, F. Stöhr, Prof. Dr. R. Göttlich  
Institute of Organic Chemistry,  
Justus Liebig University Giessen  
Heinrich-Buff-Ring 17, 35392 Giessen, Germany  
E-mail: richard.göttlich@org.chemie.uni-giessen.de  
https://www.uni-giessen.de/fbz/fb08/Inst/organische-chemie/  
AGGoettlich

[b] F. Stöhr, J. Becker  
Institute of Inorganic and Analytical Chemistry,  
Justus Liebig University Giessen  
Heinrich-Buff-Ring 17, 35392 Giessen, Germany

[c] C. Carraro, Prof. Dr. B. Gatto  
Department of Pharmaceutical and Pharmacological Sciences,  
University of Padova  
Via Francesco Marzolo 5, 35131 Padova, Italy

Supporting information for this article is available on the WWW under  
https://doi.org/10.1002/ejoc.202101072

© 2021 The Authors. European Journal of Organic Chemistry published by  
Wiley-VCH GmbH. This is an open access article under the terms of the  
Creative Commons Attribution License, which permits use, distribution and  
reproduction in any medium, provided the original work is properly cited.

therapeutics in today's clinical use. Consequently, our working group developed 3-chloropiperidines as cyclic analogues of nitrogen mustards, whose simple and easily modifiable synthesis led to a broad set of compounds.<sup>[5]</sup> These novel compounds also demonstrated to be effective DNA alkylating agents with different *in vitro* potencies, confirmed to be preferentially attacked by the *N*<sup>2</sup>-position of the guanine nucleobase.<sup>[6]</sup>

In our previous studies on monofunctional 3-chloropiperidines (Figure 1b, **A**) we noticed that the two methyl groups attached in the 5-position of the piperidine ring highly effect the reactivity of the 3-chloropiperidines in comparison to their respective unmethylated analogues.<sup>[7]</sup> This observation seemed to be worth a detailed examination, since the gem-methylation resulted from our original synthesis and should accelerate the cyclisation *via* Thorpe-Ingold effect.<sup>[8]</sup> Hence, in the present work we focused on analysing the kinetics of the underlying alkylation reaction while also taking a closer look at the

intermediate bicyclic aziridinium ion **B**. The regioselective ring opening reactions of these intermediates proved to be useful for various synthetic applications and have been studied intensively.<sup>[9]</sup> We therefore investigated the reaction of the four 3-chloropiperidines **1–4** as well as the reference compound 2-chloroethyl diethylamine **5** (Figure 2) in aqueous solution and the presence of 2'-desoxyguanosine as a nucleophile by NMR spectroscopy. The selected series of compounds cover electronic effects induced by different substituents on the piper-

idine nitrogen as well as the impact of ring methylation in 5-position. Beside these aqueous solution studies, we also isolated the corresponding aziridinium ions of these compounds, which are expected to be the intermediates of the alkylation reaction and studied their respective reactivity with different nucleophiles. These experiments also led to the crystallization of some of the aziridinium ions, confirming the bicyclic structure of the proposed reaction intermediate by single crystal XRD.

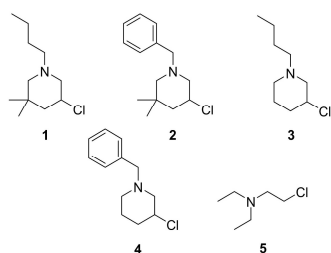
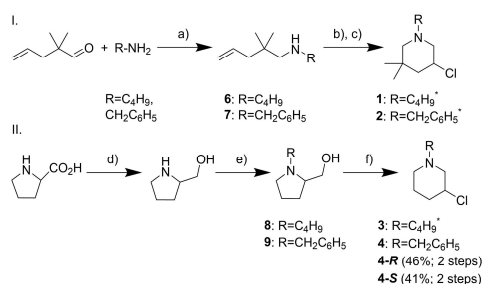
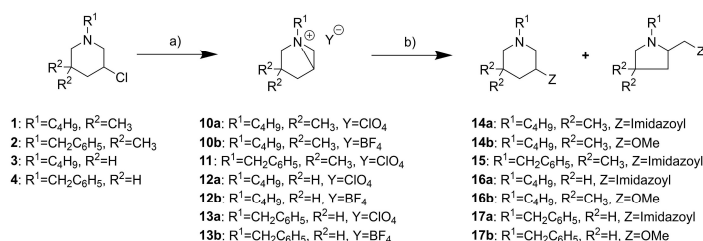


**Figure 2.** Structures of the analysed 3-chloropiperidines **1–4** and the half-mustard 2-chloroethyl diethylamine **5** used as a reference compound.



**Scheme 1.** Synthesis of 3-chloropiperidines **1–4**. a)  $\text{NaBH}(\text{OAc})_3$ ,  $\text{AcOH}$ , dry  $\text{CH}_2\text{Cl}_2$ ,  $0^\circ\text{C}$  to RT; b)  $\text{NCS}$ , dry  $\text{CH}_2\text{Cl}_2$ ,  $0^\circ\text{C}$  to RT; c)  $\text{TBAI}$  (cat.), dry  $\text{CHCl}_3$ ,  $60^\circ\text{C}$  (inseparable diastereomeric mixture); d)  $\text{LiAlH}_4$ , dry THF,  $0^\circ\text{C}$  to reflux; e) butyl iodide,  $\text{K}_2\text{CO}_3$ , dry THF, reflux (**8**) or  $\text{NEt}_3$ , dry THF, RT (**9**); f)  $\text{SOCl}_2$ , pyridine, dry  $\text{CH}_2\text{Cl}_2$ ,  $0^\circ\text{C}$  to RT (**3**) or  $\text{MsCl}$ ,  $\text{DIPEA}$ , dry  $\text{CH}_2\text{Cl}_2$ ,  $0^\circ\text{C}$  to RT (**4**). \*The synthesis of compounds **1**, **2** and **3** has been described elsewhere.<sup>[7,8,10]</sup>



**Scheme 2.** Synthesis of aziridinium ions from 3-chloropiperidines **1–4** and subsequent reaction with nucleophiles. a)  $\text{AgClO}_4$  or  $\text{AgBF}_4$ , dry Acetone; b) Imidazole or  $\text{MeOH}$ , dry  $\text{CD}_3\text{CN}$ , RT or  $50^\circ\text{C}$ .

unmethylated piperidines. Therefore, the reactions of **1** and **3** with silver tetrafluoroborate in deuterated acetone were studied by NMR spectroscopy. Small aliquots of the solution were taken after appropriate points in time, mixed with dibenzyl ether as an internal standard and filtered to remove the precipitated silver chloride. This analysis confirmed that the conversion of both reactions is almost quantitative (> 95%). According to these measurements the aziridinium ion formation of the methylated piperidine **1** was completed in less than one hour while the reaction of the unmethylated compound **3** with AgBF<sub>4</sub> took roughly 24 h until the starting material was not detectable anymore. This last sample still showed small amounts of silver chloride precipitating even after 24 h, indicating that the reaction was not finished. A possible explanation for the accelerated aziridinium ion formation might be an amplification of the neighbouring group effect, induced by the angle contraction arising from the gem-methylation in 5-position, just as the previously mentioned faster cyclization of gem-methylated *N*-chloroamines.

Similarly, we noticed a fast aziridinium ion formation for 3-chloropiperidine **2**, although prolonged stirring resulted in the formation of a complex and inseparable mixture of compounds including an oxazolidinium salt by solvolysis reaction (confirmed by HRMS), as previously reported for other reactive aziridinium salts.<sup>[12]</sup> Therefore, the reaction was stopped after one hour and remaining starting material was removed by precipitation of the product with diethyl ether. Although the aziridinium ion **11** could be isolated under these conditions, a similar side reaction took place after a couple of hours with the NMR solvent (CD<sub>3</sub>CN).<sup>[13]</sup> If the counter ion was changed to BF<sub>4</sub><sup>-</sup>, the crude product showed additional decomposition visible by colourization, and was therefore excluded in further studies.

Since the aziridinium ions **10** and **11** could be isolated as colourless solids we also tried to crystallize these compounds. Vapour diffusion crystallization with diethyl ether finally led to crystals of **10a** and **11** suitable for structure determination by single crystal XRD (Figure 3). Primarily the obtained crystal structures confirm the bicyclic structure of the aziridinium ion proposed as the intermediate of the reaction of our 3-chloropiperidines with nucleophiles, while the structure of **11** is congruent with an already described aziridinium ion obtained by a different method.<sup>[14]</sup> Furthermore, the boat-like structures of these intermediates match the computational calculations

for C4 fluorinated bicyclic aziridinium ions obtained from the corresponding prolinol derivatives.<sup>[15]</sup> Comparison of the two structures also allows assumptions about the reactivity of the benzyl substituted aziridinium ion **11** compared to the butyl analogue **10a**. Although **10a** in crystalline state exhibits whole molecule disorder (see Table S4-S7 for details), the length of the newly formed bond between the piperidine nitrogen and C3 is shorter compared to the benzyl aziridinium ion **11** (Figure 3). This difference in bond length, and therefore in bond strength, might be a first explanation for the fast decomposition of compound **11**, while also indicating a higher reactivity compared to the butyl analogue **10a**. Although we tested multiple anions and conditions, we were not able to crystallize the unmethylated aziridinium ions **12** and **13** to strengthen our estimation of a correlation between reactivity and bond length observed in accessible aziridinium ion crystal structures.

Next, to further explore the previously mentioned reactivity hypothesis we started to study the reaction of the aziridinium ions **10**–**13** with nucleophiles, choosing imidazole and methanol as model compounds for biologically relevant nucleophiles. The aziridinium ions obtained above were dissolved in deuterated acetonitrile and reacted with two equivalents of the corresponding nucleophile to obtain a mixture of the piperidine and pyrrolidine adducts **14**–**17** (Scheme 2). This mixture was directly analysed in the NMR and after aqueous workup also by GC-MS to determine the ratio of five-membered to six-membered ring product. The corresponding anion (ClO<sub>4</sub><sup>-</sup> and BF<sub>4</sub><sup>-</sup>) did not influence the reactivity of the aziridinium ions with nucleophiles in our experiments. Moreover, comparative samples of these compounds were obtained from the corresponding 3-chloropiperidines by reaction with an excess of the according nucleophile (see Supporting Information for details). In both, the reaction of the aziridinium ions with the nucleophiles and the direct alkylation reactions of the 3-chloropiperidines, we observed a strong preference of the gem-methylated compounds **14** and **15** (or **1** and **2** respectively) for the piperidine adduct, while the unmethylated compounds **16** and **17** (or **3** and **4** respectively) generally preferred the pyrrolidine adduct. Overall, the regiochemistry of ring opening reactions of bicyclic aziridinium ions is dependent on several factors such as the attacking nucleophile<sup>[16]</sup> as well as substituents<sup>[17]</sup> and has also been studied intensively under theoretical aspects.<sup>[18,19]</sup> In line with our results, the ring opening of gem-methylated bicyclic aziridinium ions favours the thermodynamic six-membered piperidine product,<sup>[20]</sup> while the unmethylated compounds typically prefer the kinetic five-membered pyrrolidine product with the exact ratio depending on the aforementioned aspects.

In addition to the bicyclic aziridinium ions derived from our 3-chloropiperidines, we synthesised the aziridinium ions **18a** and **18b** of the half-mustard 2-chloroethyl diethylamine **5** and reacted them with two equivalents of imidazole and methanol respectively (Scheme 3). This enabled a direct comparison with a reference compound known to undergo alkylation reactions via the aziridinium ion **18**.<sup>[21]</sup> Again, comparative samples of the alkylation products were synthesised from 2-chloroethyl diethyl-

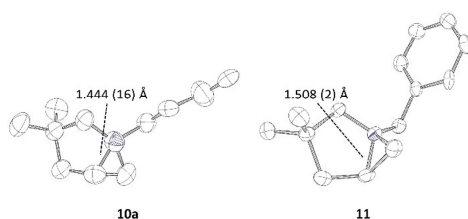


Figure 3. Molecular structures of the bicyclic aziridinium ions **10a** and **11** derived from single crystal structures. Hydrogens and ClO<sub>4</sub><sup>-</sup> anions are omitted for clarity, ellipsoids are drawn at 50% probability.



**Scheme 3.** Synthesis of the aziridinium ion of 2-chloroethyl diethylamine **5** and subsequent reaction with nucleophiles. a) AgClO<sub>4</sub> or AgBF<sub>4</sub>, dry Acetone; b) Imidazole or MeOH, dry CD<sub>3</sub>CN, RT or 50 °C.

amine **5** and the corresponding nucleophiles (see Supporting Information for details).

While the reaction of all aziridinium ions with imidazole occurred immediately at room temperature and according to NMR quantitatively (>95%), the compounds proved to be less reactive against methanol. After incubation of a sample of **10b** with two equivalents of methanol overnight at room temperature, only half of the aziridinium ion reacted with the alcohol. We therefore analysed that reaction at 50 °C for 16 h, recording an NMR spectrum every 30 mins. In this case only a small amount of the starting material remained, leading to a product mixture primarily containing the 3-methoxypiperidine product of **14b**. This approach was also applied to the different aziridinium ions **12b**, **13b** and **18b**, which enabled a direct comparison of their reactivity by plotting the natural logarithm of the integral from a distinct aziridinium ion signal  $\ln(Az^+)$  against the reaction time  $t$  (Figure 4). Due to the already observed instability, the aziridinium ion **11** had to be excluded in this analysis.

All methanolysis reactions seem to follow pseudo first order kinetics, as a reasonable linear regression was only possible in

case of a first order reaction. Even though, the different reaction behaviour with respect to methanol and imidazole as nucleophiles supports previous studies of 3-chloro-1-ethylpiperidine with various nucleophiles.<sup>[22]</sup> Nevertheless, this method allowed a comparison of the bicyclic aziridinium ions **10b**, **12b** and **13b** as well as the half-mustard based reference aziridinium ion **18b** by determining their respective rate constants from the slope of the linear regression. The most remarkable difference is again noticed between the C-5 gem-methylated aziridinium ion **10b** ( $t_{1/2}$  = 507 min) and the corresponding unmethylated analogue **12b** ( $t_{1/2}$  = 12583 min) since their respective half-lives vary by two orders of magnitude. As already observed for the formation of the aziridinium ions, the methylated compounds react much faster than the unmethylated analogues. Once again, the gem-methylation could be the reason. Due to the boat-like structure of the aziridinium ions the methyl groups in 5-position induce additional strain into the bicyclic system, thus favouring a ring opening reaction resulting in a more reactive aziridinium ion. On one hand, this explains the higher reactivity of the bicyclic compound **10b** compared with the monocyclic half-mustard reference **18b**, although the difference in rate constants is not as outstanding as compared to the unmethylated aziridinium ions **12b** and **13b**. On the other hand, the aziridinium ions **12b** and **13b** were expected to be more reactive than the reference compound **18b** due to their bicyclic character, which is apparently not the case in our kinetic studies. These findings suggest that the unmethylated aziridinium ions are also quite stable towards hydrolysis, while their fast reaction with imidazole shows that they are still able to alkylate nitrogen nucleophiles efficiently. Looking to support these results we dissolved a sample of the most reactive aziridinium ion **10b**

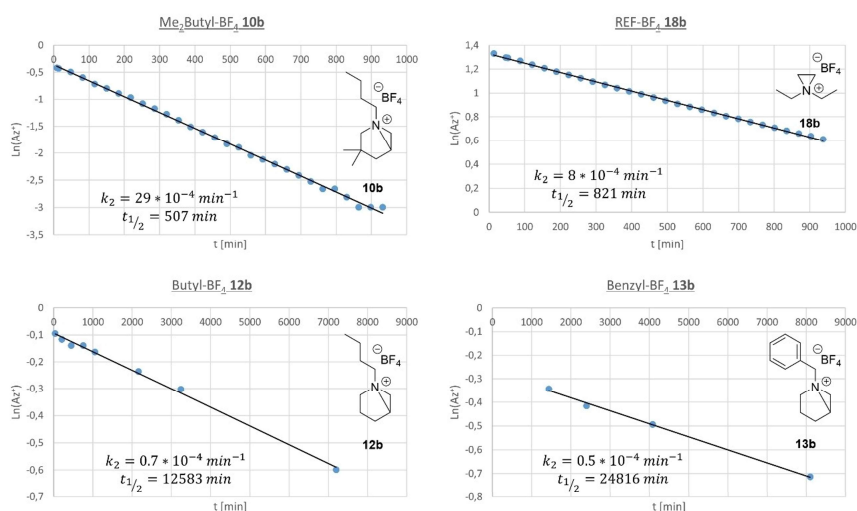
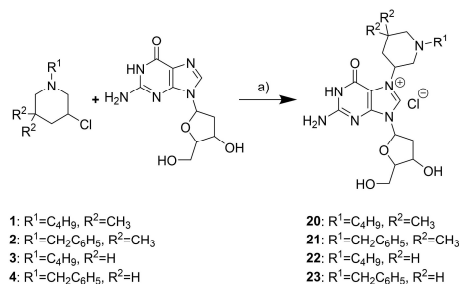


**Figure 4.** Reaction of aziridinium ions **10b**, **12b**, **13b** and **18b** with methanol at 50 °C observed in the NMR. The natural logarithm of the integral from a distinct aziridinium ion signal  $\ln(Az^+)$  is plotted against the reaction time  $t$  and from the slope of the linear regressions the reaction rate constants  $k_2$  are determined.

and the least reactive compound **13b** in methanol (0.1 M) and added two equivalents of imidazole. GC/MS analysis of the product mixture showed a 3:1 preference for the imidazole product of **10b**, while the reaction of **13b** with imidazole was favoured by a factor of 13:1.

To further explore this striking reactivity difference, we chose to directly measure the reaction rate of an alkylation reaction for the 3-chloropiperidines **1–4** in aqueous solution. We therefore studied the reaction of these compounds in the NMR using one equivalent of 2'-desoxyguanosine (Scheme 4) in



**Scheme 4.** Alkylation reaction of 3-chloropiperidines **1–4** with 2'-desoxyguanosine to the alkylation products **20–23**. a) 50 °C, 1:1 DMSO-*d*<sub>6</sub>/phosphate buffered D<sub>2</sub>O (pH = 7.4).

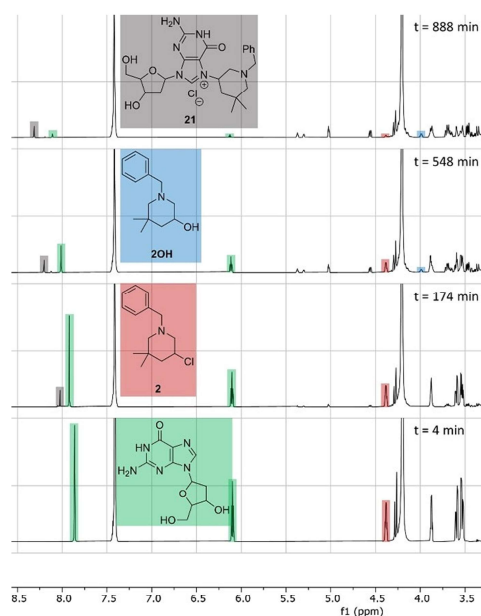


**Figure 5.** NMR spectra recorded at different times during the reaction of 3-chloropiperidine **2** with 2'-desoxyguanosine at 50 °C in a 1:1 mixture of DMSO-*d*<sub>6</sub> and phosphate buffered D<sub>2</sub>O (pH = 7.4).

a 1:1 mixture of DMSO-*d*<sub>6</sub> and phosphate buffered D<sub>2</sub>O (pH = 7.4). The reaction mixture was heated to 50 °C and analysed for 16 h, recording an NMR spectrum every 30 mins. Figure 5 shows sections of four different recorded <sup>1</sup>H-NMR spectra over the course of the reaction. In the initial spectrum, recorded after four minutes, distinct signals of the 3-chloropiperidine **2** (red) and 2'-desoxyguanosine (green) are visible. After roughly three hours (t = 174 min) these signals significantly decrease in intensity and an additional signal of the alkylation product **21** (grey) is visible. Over the course of reaction (t = 548 and 888 min) the signals of the starting material and the 2'-desoxyguanosine constantly decrease in intensity, while the signal of the alkylation product stays rather constant, a consequence of the increased acidity of the C-8 proton as a result of the alkylation, which undergoes exchange with the deuterated solvent.<sup>[23]</sup> In addition, small signals of the corresponding hydrolysis side product **20H** start to appear, increasing in intensity very slowly and staying low even after 16 h, again showing that the *N*-alkylation reaction is much faster compared to the hydrolysis of the 3-chloropiperidines.

This experiment was repeated with the 3-chloropiperidines **1**, **3** and **4**, while the consumption of the starting material was monitored by referencing the integration to the residual DMSO signal. The natural logarithm of one distinct 3-chloropiperidine signal *Ln(Cl)* was plotted against the reaction time *t*. From the slope of the linear regression the rate constant *k*, was determined (Figure 6). All reactions follow first order kinetics regarding the 3-chloropiperidine, as the first step of their alkylation reaction is the formation of the corresponding aziridinium ion, which is rapidly consumed afterwards, implementing the steady state approximation (*k*<sub>2</sub> ≫ *k*<sub>-1</sub>). For the unmethylated compounds **3** (*t*<sub>1/2</sub> = 3306 min) and **4** (*t*<sub>1/2</sub> = 1728 min) the reaction was again much slower compared to their methylated analogues **1** (*t*<sub>1/2</sub> = 708 min) and **2** (*t*<sub>1/2</sub> = 423 min), as apparent from their respective half-lives and the reduced consumption of the starting materials after 16 h of reaction time (Table S2). The rate constants of the methylated 3-chloropiperidines **1** and **2** were only determined in the first half of the reaction time. After this point the rapid consumption of the aziridinium ion seems to become inconsistent due to the lower concentration of available nitrogen nucleophile, which might also explain the appearance of the hydrolysis side product **20H** solely after eight to nine hours of incubation. Nonetheless, the reactivity trend we previously observed in the consumption kinetics of the aziridinium ions **10b**, **12b** and **13b**, as well as our estimations from their crystal structures and formation rate of aziridinium ions appear to match the alkylation reactions of the 3-chloropiperidines **1–4** in aqueous solution. The *N*-benzyl substitution seems to accelerate the reaction compared to the corresponding *N*-butyl compounds while the gem-methylation in 5-position again results in a much faster consumption of the starting material. Accordingly, the double ring methylation increased the reactivity of **1** and **2** also with plasmid DNA after 8 h of incubation at 37 °C (Figure S3), in line with previous observations at different incubation times.<sup>[7]</sup> When analysing a complex model nucleophile as in the case of plasmid DNA, the *N*-benzyl substitution slightly accelerated the reactivity of the unmethylated analogue **4** while this effect was not seen in the case of **2**.

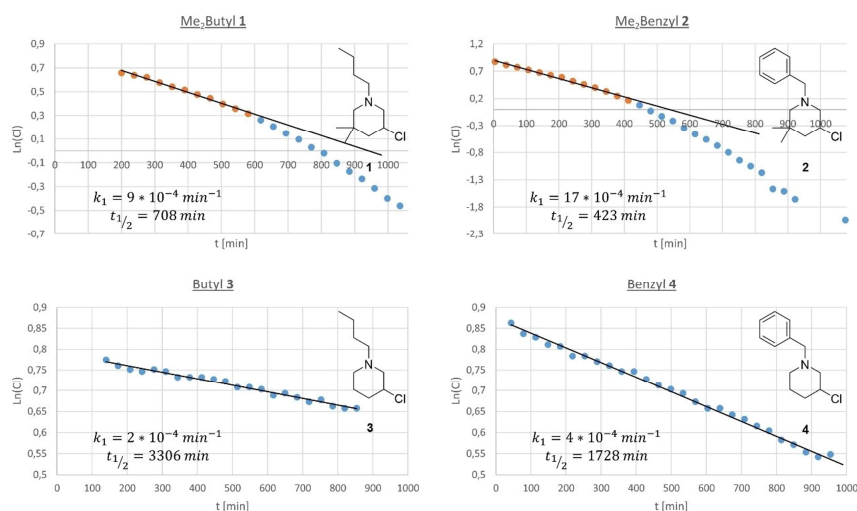


Figure 6. Reaction of 3-chloropiperidines 1–4 with 2'-desoxyguanosin at 50 °C observed in the NMR. The natural logarithm of the integral from a distinct aziridinium ion signal  $\text{Ln}(C)$  is plotted against the reaction time  $t$  and from the slope of the linear regressions the reaction rate constants  $k_1$  are determined.

To get a final validation for our established NMR-method we repeated the aqueous reaction kinetic using the reference compound 5 and 2'-desoxyguanosine as a nucleophile. Since the reaction of its corresponding nitrogen mustard analogue mechlorethamine with nucleophiles in aqueous solution is known to proceed rapidly<sup>[24]</sup> and studies of the half-mustard derivative 5 with different nucleophiles in DMF show fast first-order rate constants,<sup>[25]</sup> therefore the reaction is expected to be a suitable comparison in our case. Indeed, the observed half-life ( $t_{1/2} = 286$  min) was lower compared to our 3-chloropiperidines 1–4 and after already 15 h reaction time no starting material could be detected (Figure 7). Furthermore, we observed a behaviour similar to the reactions of the gem-methylated 3-chloropiperidines 1 and 2. After a considerable amount of alkylation product 24 has built up, the reaction seemed to not follow first order kinetics anymore. This might be a consequence of the increasing chloride concentration, which can compete with the 2'-desoxyguanosine as a nucleophile. This results in a fast equilibrium between the starting material and the aziridinium ion, changing the kinetic behaviour.<sup>[18]</sup> Since we also observed this change in kinetics for the more reactive gem-methylated 3-chloropiperidines 1 and 2, these findings support the applicability of this method for mustard based alkylating agents.

## Conclusion

In conclusion, we developed a fast and easy method for the initial estimation of the reactivity of our 3-chloropiperidines by NMR spectroscopy, demonstrated by the reactions of com-

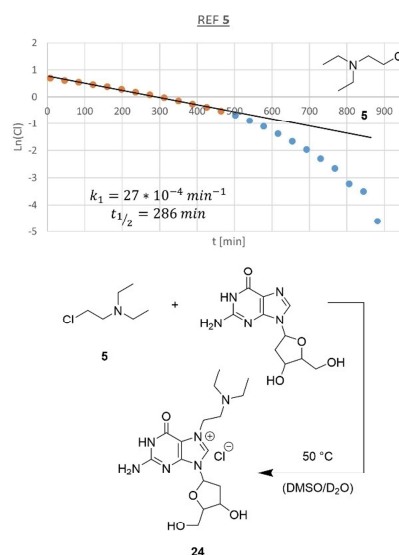


Figure 7. Reaction of 2-chloroethyl diethylamine 5 with 2'-desoxyguanosin to the alkylation product 24 observed in the NMR at 50 °C in a 1:1 mixture of DMSO- $d_6$ /phosphate buffered  $D_2O$  (pH = 7.4). Plotted is the natural logarithm of the integral from a distinct signal  $\text{Ln}(C)$  against the reaction time  $t$ , from the slope of the linear regression the reaction rate constant  $k_1$  was determined.

pounds 1–4 in aqueous solution with 2'-desoxyguanosine as a nucleophile. Accordingly, the alkylation activity of these compounds is significantly increased by C-5 gem-methylation, as also suggested by results with model DNA.<sup>[7]</sup> The *N*-substitution has a lower influence on the reactivity and is affected by the complexity of the structure and the context of the examined nucleophile. We could also demonstrate that these reactions follow first order kinetics and behave similar to the known half-mustard 2-chloroethyl diethylamine 5 in aqueous solution. Furthermore, we were able to isolate the corresponding aziridinium ions of the 3-chloropiperidines 1–4 and yet obtained crystal structures of the two aziridinium salts 10a and 11, confirming their boat-like bicyclic structure and enabling a direct structure-activity comparison. Kinetic studies of these aziridinium ions again confirmed the higher reactivity of the C-5 gem-methylated compounds, while also demonstrating their ability to alkylate nitrogen nucleophiles efficiently. These results indicate that the Thorpe-Ingold effect induced by the gem-methylation seems to be more relevant for the reactivity of our 3-chloropiperidines than initially expected. Therefore, ongoing kinetic and computer chemical studies intent to reveal a possible correlation between the C-5 angle contraction and the alkylation activity of monofunctional 3-chloropiperidines.

## Experimental Section

All solvents were purified by distillation prior to use, in case of anhydrous solvents 100 mL AcroSeal™ bottles from ACROS Organics™ were used. Commercially available reagents were used as supplied if not stated different, reagents used in the glovebox were dried in advance using standard procedures. Synthesis using anhydrous solvents were carried out under Schlenk conditions or in a nitrogen-filled glovebox if specifically stated. For purification by flash column chromatography silica gel 60 (Merck) was used. <sup>1</sup>H and <sup>13</sup>C NMR spectra were recorded at the Bruker Avance II 400 and Avance III 400 spectrometer (<sup>1</sup>H at 400 MHz; <sup>13</sup>C at 100 MHz) in deuterated solvents. NMR kinetic experiments were carried out at the Bruker Avance III 600 spectrometer (<sup>1</sup>H at 600 MHz). <sup>1</sup>H chemical shifts were determined by reference to the residual solvent signals. High-resolution ESI mass spectra were recorded in methanol using a ESI-microTOF spectrometer (Bruker Daltonics) in positive ion mode. All GC/MS spectra were recorded at the Agilent 5977B GC/MSD instrument equipped with a 7820 A GC System. All elemental analysis (CHN) were performed on a Thermo FlashEA – 1112 series instrument. NMR spectra of the synthesized compounds 4-S, 4-R, 10a, 10b, 11, 12a, 12b, 13a and 13b as well as the synthetic procedures for the compounds 14–17 (obtained from the corresponding aziridinium ions and 3-chloropiperidines) are included in the supplementary information. The synthesis of compounds 1–3 as well as their corresponding precursors has been described elsewhere.<sup>[7,8,10]</sup>

### (3R)-1-benzyl-3-chloropiperidine (4-R)

Under a nitrogen atmosphere (S)-2-(hydroxymethyl)pyrrolidine (505 mg, 4.99 mmol) was dissolved in anhydrous THF (25 mL) and anhydrous triethylamine (0.78 mL, 5.63 mmol) was added. Afterwards benzyl bromide (0.48 mL, 4.04 mmol) was added dropwise at 0 °C and the mixture was stirred at room temperature for 21 h. The solvent was removed under reduced pressure, the crude product was redissolved in anhydrous DCM (25 mL) and anhydrous DIPEA

(2.1 mL, 12.06 mmol) was added. Afterwards freshly distilled methanesulfonyl chloride (0.63 mL, 8.14 mmol) was added dropwise at 0 °C. The mixture was stirred at 0 °C for 2 and for 18 h at room temperature. The mixture was then partitioned between brine and ethyl acetate (50 mL each) and the phases were separated. The aqueous phase was then extracted twice with ethyl acetate and the combined organic extracts were dried over MgSO<sub>4</sub>. The solvent was removed under reduced pressure and the crude product was purified by flash column chromatography (DCM/acetone 100:1) yielding the title compound as a colourless oil (390 mg, 1.86 mmol, 46%). [ $\alpha$ ]<sub>D</sub><sup>25</sup> = -18.6 ± 1.4 (c = 25 mg/mL, CHCl<sub>3</sub>); <sup>1</sup>H NMR (400 MHz, CDCl<sub>3</sub>)  $\delta$  = 7.34–7.26 (m, 5H, aromatic CH), 4.05–3.96 (m, 1H, CH), 3.55 (s, 2H, ArCH<sub>2</sub>), 3.05 (d, J = 11.1 Hz, 1H, CH<sub>2</sub>), 2.72 (d, J = 11.6 Hz, 1H, CH<sub>2</sub>), 2.25–2.07 (m, 3H, overlap CH<sub>2</sub>), 1.81–1.75 (m, 1H, CH<sub>2</sub>), 1.68–1.52 (m, 2H, CH<sub>2</sub>) ppm; <sup>13</sup>C NMR (101 MHz, CDCl<sub>3</sub>)  $\delta$  = 137.89, 129.17, 128.41, 127.32, 62.81, 61.37, 56.17, 52.92, 34.99, 24.90 ppm. HRMS (ESI): *m/z* calcd for C<sub>12</sub>H<sub>17</sub>ClN<sup>+</sup>: 210.1044; found: 210.1047 [M + H]<sup>+</sup>; elementary analysis calcd (%) for C<sub>12</sub>H<sub>16</sub>ClN: C 68.73, H 7.69, N 6.68; found: C 68.82, H 7.63, N 6.59.

### (3S)-1-benzyl-3-chloropiperidine (4-S)

Under a nitrogen atmosphere (R)-2-(hydroxymethyl)pyrrolidine (494 mg, 4.88 mmol) was dissolved in anhydrous THF (25 mL) and anhydrous triethylamine (0.79 mL, 5.70 mmol) was added. Afterwards benzyl bromide (0.49 mL, 4.12 mmol) was added dropwise at 0 °C and the mixture was stirred at room temperature for 64 h. The solvent was removed under reduced pressure, the crude product was redissolved in anhydrous DCM (25 mL) and anhydrous DIPEA (2.1 mL, 12.35 mmol) was added. Afterwards freshly distilled methanesulfonyl chloride (0.64 mL, 8.27 mmol) was added dropwise at 0 °C. The mixture was stirred at 0 °C for 2 and for 18 h at room temperature. The mixture was then partitioned between brine and ethyl acetate (50 mL each) and the phases were separated. The aqueous phase was then extracted twice with ethyl acetate and the combined organic extracts were dried over MgSO<sub>4</sub>. The solvent was removed under reduced pressure and the crude product was purified by flash column chromatography (DCM/acetone 100:1) yielding the title compound as a colourless oil (353 mg, 1.68 mmol, 41%). [ $\alpha$ ]<sub>D</sub><sup>25</sup> = +16.6 ± 2.6 (c = 25 mg/mL, CHCl<sub>3</sub>); <sup>1</sup>H NMR (400 MHz, CDCl<sub>3</sub>)  $\delta$  = 7.36–7.26 (m, 5H, aromatic CH), 4.05–3.96 (m, 1H, CH), 3.55 (s, 2H, ArCH<sub>2</sub>), 3.05 (d, J = 9.0 Hz, 1H, CH<sub>2</sub>), 2.72 (d, J = 11.4 Hz, 1H, CH<sub>2</sub>), 2.25–2.07 (m, 3H, overlap CH<sub>2</sub>), 1.82–1.75 (m, 1H, CH<sub>2</sub>), 1.68–1.50 (m, 2H, CH<sub>2</sub>) ppm; <sup>13</sup>C NMR (101 MHz, CDCl<sub>3</sub>)  $\delta$  = 137.89, 129.17, 128.41, 127.32, 62.81, 61.37, 56.17, 52.92, 34.99, 24.90 ppm. HRMS (ESI): *m/z* calcd for C<sub>12</sub>H<sub>17</sub>ClN<sup>+</sup>: 210.1044; found: 210.1051 [M + H]<sup>+</sup>; elementary analysis calcd (%) for C<sub>12</sub>H<sub>17</sub>Cl<sub>2</sub>N: C 58.55, H 6.96, N 5.69; found: C 58.87, H 6.77, N 5.71.

### 2-chloroethyl diethylamine (5)

To a solution of NaOH (20.0 g, 0.5 mol) in distilled water (80 mL) was added 2-chloroethyl diethylamine hydrochloride (17.21 g, 0.1 mol) dissolved in distilled water (20 mL) at 0 °C. The solution was stirred at room temperature for 15 min and then extracted three times with Et<sub>2</sub>O. The combined organic extracts were dried by stirring with MgSO<sub>4</sub> for 30 min and the solvent was removed under reduced pressure. The crude product was purified by vacuum distillation (47 °C at 30 mbar) over CaH<sub>2</sub> yielding the title compound as a colourless liquid (10.6 g, 78 mmol, 78%). <sup>1</sup>H NMR (400 MHz, CDCl<sub>3</sub>)  $\delta$  = 3.54–3.46 (m, 2H, CH<sub>2</sub>), 2.80–2.74 (m, 2H, CH<sub>2</sub>), 2.57 (q, J = 7.2 Hz, 4H, CH<sub>2</sub>), 1.03 (t, J = 7.2 Hz, 6H, CH<sub>3</sub>) ppm; <sup>13</sup>C NMR (101 MHz, CDCl<sub>3</sub>)  $\delta$  = 54.99, 47.74, 42.15, 11.96 ppm. HRMS (ESI): *m/z* calcd for

$C_6H_{10}ClN^+$ : 136.0888; found: 136.0886  $[M+H]^+$ ; These data are consistent with published data.<sup>[26]</sup>

#### General procedure for synthesis of aziridinium ions (10–13, 18)

Under a nitrogen atmosphere the corresponding 3-chloropiperidine/ $\beta$ -chloroethylamine (0.25–0.5 mmol) was weighed into a 10 mL schlenk tube, the tube was then evacuated and backfilled with nitrogen five times. After a final evacuation, the valve was closed and the schlenk tube transferred into a nitrogen-filled glovebox. Anhydrous acetone (0.25 mL/0.1 mmol of starting material) was added and a solution of the appropriate silver salt (1 eq., dried over  $P_2O_5$ ) in anhydrous acetone (0.25 mL/0.1 mmol of silver salt) was added. The mixture was stirred at room temperature under exclusion of light for the times indicated (monitored by TLC), afterwards filtered through a syringe filter (0.2  $\mu$ m PTFE) and the solvent was removed under high vacuum. The residue was dissolved in anhydrous DCM (0.5 mL/0.1 mmol starting material) and again filtered through a syringe filter (0.2  $\mu$ m PTFE). The solvent was removed under high vacuum and the crude product analysed by NMR spectroscopy.

#### 1-Butyl-5,5-dimethyl-1-azoniabicyclo[3.1.0]hexane perchlorate (10a)

Was prepared according to the general procedure (reaction time: 4 h) from 1-butyl-3-chloro-5,5-dimethylpiperidine (1; 102 mg, 0.5 mmol) and silver perchlorate (104 mg, 0.5 mmol) yielding the title compound as a colourless solid. Crystals for XRD analysis were obtained by vapour diffusion crystallization with DCM/ $Et_2O$ .  $^1H$  NMR (400 MHz,  $CD_3CN$ )  $\delta$  = 3.80–3.71 (m, 1H, CH), 3.52–3.44 (m, 1H,  $CH_2$ ), 3.38 (d,  $J$  = 12.3 Hz, 1H,  $CH_2$ ), 3.28 (d,  $J$  = 12.3 Hz, 1H,  $CH_2$ ), 3.16 (dd,  $J$  = 8.0, 4.1 Hz, 1H,  $N^+CH_2CH$ ), 3.06–3.02 (m, 1H,  $N^+CH_2CH$ ), 2.92–2.84 (m, 1H,  $CH_2$ ), 2.37 (dd,  $J$  = 13.7, 6.5 Hz, 1H,  $CH_2$ ), 1.94 (dd,  $J$  = 13.6, 2.7 Hz, 1H,  $CH_2$ ), 1.75–1.67 (m, 2H,  $CH_2$ ), 1.41–1.32 (m, 2H,  $CH_2$ ), 1.25 (s, 3H,  $CH_3$ ), 1.13 (s, 3H,  $CH_3$ ), 0.94 (t,  $J$  = 7.4 Hz, 3H,  $CH_3$ ) ppm;  $^{13}C$  NMR (101 MHz,  $CD_3CN$ )  $\delta$  = 68.87, 61.04, 56.65, 48.98, 45.06, 40.79, 29.75, 28.62, 28.07, 20.05, 13.88 ppm.

#### 1-Butyl-5,5-dimethyl-1-azoniabicyclo[3.1.0]hexane tetrafluoroborate (10b)

Was prepared according to the general procedure (reaction time: 4 h) from 1-butyl-3-chloro-5,5-dimethylpiperidine (1; 102 mg, 0.5 mmol) and silver tetrafluoroborate (97 mg, 0.5 mmol) yielding the title compound as a colourless solid.  $^1H$  NMR (400 MHz,  $CD_3CN$ )  $\delta$  = 3.80–3.71 (m, 1H, CH), 3.51–3.44 (m, 1H,  $CH_2$ ), 3.37 (d,  $J$  = 12.3 Hz, 1H,  $CH_2$ ), 3.27 (d,  $J$  = 12.3 Hz, 1H,  $CH_2$ ), 3.15 (dd,  $J$  = 8.0, 4.1 Hz, 1H,  $N^+CH_2CH$ ), 3.05–3.01 (m, 1H,  $N^+CH_2CH$ ), 2.92–2.83 (m, 1H,  $CH_2$ ), 2.37 (dd,  $J$  = 13.7, 6.5 Hz, 1H,  $CH_2$ ), 1.93 (dd,  $J$  = 13.5, 2.7 Hz, 1H,  $CH_2$ ), 1.74–1.67 (m, 2H,  $CH_2$ ), 1.41–1.32 (m, 2H,  $CH_2$ ), 1.24 (s, 3H,  $CH_3$ ), 1.13 (s, 3H,  $CH_3$ ), 0.94 (t,  $J$  = 7.4 Hz, 3H,  $CH_3$ ) ppm;  $^{13}C$  NMR (101 MHz,  $CD_3CN$ )  $\delta$  = 68.86, 61.04, 56.64, 48.99, 45.08, 40.80, 29.75, 28.62, 28.06, 20.06, 13.89 ppm.

#### 1-Benzyl-5,5-dimethyl-1-azoniabicyclo[3.1.0]hexane perchlorate (11)

Was prepared by a slight variation of the general procedure (reaction time: 1 h) from 1-benzyl-3-chloro-5,5-dimethylpiperidine (2; 71 mg, 0.3 mmol) and silver perchlorate (62 mg, 0.3 mmol). After filtration and removal of the solvent the crude product was dissolved in anhydrous DCM (1.5 mL) and added dropwise to

thoroughly stirred anhydrous  $Et_2O$  (6 mL). The solvent was decanted and the solid dried under high vacuum yielding the title compound as a colourless solid. Crystals for XRD analysis were obtained by vapour diffusion crystallization with DCM/ $Et_2O$ .  $^1H$  NMR (400 MHz,  $CD_3CN$ )  $\delta$  = 7.53–7.50 (m, 5H, aromatic CH), 4.55 (d,  $J$  = 13.7 Hz, 1H,  $ArCH_2$ ), 4.28 (d,  $J$  = 13.7 Hz, 1H,  $ArCH_2$ ), 3.96–3.90 (m, 1H, CH), 3.46 (d,  $J$  = 12.5 Hz, 1H,  $CH_2$ ), 3.34 (dd,  $J$  = 8.1, 4.3 Hz, 1H,  $N^+CH_2CH$ ), 3.18 (d,  $J$  = 12.3 Hz, 1H,  $CH_2$ ), 3.08 (dd,  $J$  = 6.4, 4.2 Hz, 1H,  $N^+CH_2CH$ ), 2.39 (dd,  $J$  = 13.8, 6.5 Hz, 1H,  $CH_2$ ), 1.99 (dd,  $J$  = 13.8, 2.3 Hz, 1H,  $CH_2$ ), 1.09 (s, 6H,  $CH_3$ ) ppm;  $^{13}C$  NMR (101 MHz,  $CD_3CN$ )  $\delta$  = 133.30, 131.50, 131.22, 130.42, 68.91, 63.49, 56.04, 48.30, 44.50, 40.96, 29.64, 28.35 ppm.

#### 1-Butyl-1-azoniabicyclo[3.1.0]hexane perchlorate (12a)

Was prepared according to the general procedure (reaction time: 72 h) from (3*R*)-1-butyl-3-chloropiperidine (3-*R*; 87 mg, 0.5 mmol) and silver perchlorate (104 mg, 0.5 mmol) yielding the title compound as a yellow oil.  $^1H$  NMR (400 MHz,  $CD_3CN$ )  $\delta$  = 3.63–3.54 (m, 2H, overlap CH and  $CH_2$ ), 3.42–3.34 (m, 2H,  $CH_2$ ), 3.31–3.23 (m, 1H,  $CH_2$ ), 3.08–3.00 (m, 1H,  $CH_2$ ), 2.97–2.88 (m, 2H,  $N^+CH_2CH$ ), 2.41–2.30 (m, 1H,  $CH_2$ ), 2.19–2.05 (m, 2H,  $CH_2$ ), 1.83–1.68 (m, 3H, overlap  $CH_2$ ), 1.37 (dq,  $J$  = 14.9, 7.4 Hz, 2H,  $CH_2$ ), 0.94 (t,  $J$  = 7.4 Hz, 3H,  $CH_3$ ) ppm;  $^{13}C$  NMR (101 MHz,  $CD_3CN$ )  $\delta$  = 58.94, 54.91, 53.54, 38.62, 28.31, 24.85, 20.96, 20.13, 13.86 ppm.

#### 1-Butyl-1-azoniabicyclo[3.1.0]hexane tetrafluoroborate (12b)

Was prepared according to the general procedure (reaction time: 120 h) from (3*R*)-1-butyl-3-chloropiperidine (3-*R*; 87 mg, 0.5 mmol) and silver tetrafluoroborate (97 mg, 0.5 mmol) yielding the title compound as an orange oil.  $^1H$  NMR (400 MHz,  $CD_3CN$ )  $\delta$  = 3.63–3.54 (m, 2H, overlap CH and  $CH_2$ ), 3.41–3.34 (m, 1H,  $CH_2$ ), 3.31–3.23 (m, 1H,  $CH_2$ ), 3.08–3.00 (m, 1H,  $CH_2$ ), 2.95–2.88 (m, 2H,  $N^+CH_2CH$ ), 2.40–2.30 (m, 1H,  $CH_2$ ), 2.19–2.05 (m, 2H,  $CH_2$ ), 1.83–1.67 (m, 3H, overlap  $CH_2$ ), 1.37 (dq,  $J$  = 15.2, 7.5 Hz, 2H,  $CH_2$ ), 0.94 (t,  $J$  = 7.3 Hz, 3H,  $CH_3$ ) ppm;  $^{13}C$  NMR (101 MHz,  $CD_3CN$ )  $\delta$  = 58.94, 54.89, 53.54, 38.60, 28.32, 24.84, 20.96, 20.14, 13.88 ppm.

#### 1-Benzyl-1-azoniabicyclo[3.1.0]hexane perchlorate (13a)

Was prepared according to the general procedure (reaction time: 120 h) from (3*R*)-1-benzyl-3-chloropiperidine (4-*R*; 52 mg, 0.25 mmol) and silver perchlorate (52 mg, 0.25 mmol) yielding the title compound as a yellow oil.  $^1H$  NMR (400 MHz,  $CD_3CN$ )  $\delta$  = 7.53–7.46 (m, 5H, aromatic  $CH_2$ ), 4.54 (d,  $J$  = 13.7 Hz, 1H,  $ArCH_2$ ), 4.33 (d,  $J$  = 13.6 Hz, 1H,  $ArCH_2$ ), 3.82–3.75 (m, 1H, CH), 3.43–3.29 (m, 2H,  $CH_2$ ), 3.12–3.07 (m, 1H,  $N^+CH_2CH$ ), 2.98–2.94 (m, 1H,  $N^+CH_2CH$ ), 2.40–2.29 (m, 1H,  $CH_2$ ), 2.22–2.16 (m, 1H,  $CH_2$ ), 2.07–1.99 (m, 1H,  $CH_2$ ), 1.80–1.70 (m, 1H,  $CH_2$ ) ppm;  $^{13}C$  NMR (101 MHz,  $CD_3CN$ )  $\delta$  = 131.51, 131.16, 130.41, 61.80, 55.19, 53.18, 37.89, 25.14, 20.76 ppm.

#### 1-Benzyl-1-azoniabicyclo[3.1.0]hexane tetrafluoroborate (13b)

Was prepared according to the general procedure (reaction time: 168 h) from (3*R*)-1-benzyl-3-chloropiperidine (4-*R*; 52 mg, 0.25 mmol) and silver tetrafluoroborate (49 mg, 0.25 mmol) yielding the title compound as an orange oil.  $^1H$  NMR (400 MHz,  $CD_3CN$ )  $\delta$  = 7.53–7.45 (m, 5H, aromatic CH), 4.52 (d,  $J$  = 13.6 Hz, 1H,  $ArCH_2$ ), 4.32 (d,  $J$  = 13.6 Hz, 1H,  $ArCH_2$ ), 3.81–3.74 (m, 1H, CH), 3.42–3.29 (m, 2H,  $CH_2$ ), 3.09 (dd,  $J$  = 7.8, 4.5 Hz, 1H,  $N^+CH_2CH$ ), 2.95 (dd,  $J$  = 6.4, 4.4 Hz, 1H,  $N^+CH_2CH$ ), 2.39–2.28 (m, 1H,  $CH_2$ ), 2.19 (dd,  $J$  = 13.9, 7.9 Hz, 1H,  $CH_2$ ), 2.07–1.99 (m, 1H,  $CH_2$ ), 1.80–1.70 (m, 1H,  $CH_2$ ) ppm;  $^{13}C$  NMR

(101 MHz, CD<sub>3</sub>CN)  $\delta$  = 131.51, 131.19, 131.16, 130.41, 61.79, 55.16, 53.18, 37.88, 25.13, 20.76 ppm.

### 1,1-Diethylaziridinium perchlorate (18a)

Was prepared according to the general procedure (reaction time: 2.5 h) from 2-chloroethyl diethylamine (5; 68 mg, 0.5 mmol) and silver perchlorate (104 mg, 0.5 mmol) yielding the title compound as a colourless solid. <sup>1</sup>H NMR (400 MHz, CD<sub>3</sub>CN)  $\delta$  = 3.13 (q, *J* = 7.2 Hz, 4H, CH<sub>2</sub>CH<sub>3</sub>), 2.92 (s, 4H, CH<sub>3</sub>), 1.27 (t, *J* = 7.2 Hz, 6H, CH<sub>2</sub>CH<sub>3</sub>) ppm; <sup>13</sup>C NMR (101 MHz, CD<sub>3</sub>CN)  $\delta$  = 53.61, 40.20, 9.90 ppm. These data are consistent with published data.<sup>[27]</sup>

### 1,1-Diethylaziridinium tetrafluoroborate (18b)

Was prepared according to the general procedure (reaction time: 2.5 h) from 2-chloroethyl diethylamine (5; 68 mg, 0.5 mmol) and silver tetrafluoroborate (97 mg, 0.5 mmol) yielding the title compound as a colourless solid. <sup>1</sup>H NMR (400 MHz, CD<sub>3</sub>CN)  $\delta$  = 3.12 (q, *J* = 7.2 Hz, 4H, CH<sub>2</sub>CH<sub>3</sub>), 2.91 (s, 4H, CH<sub>3</sub>), 1.27 (t, *J* = 7.2 Hz, 6H, CH<sub>2</sub>CH<sub>3</sub>) ppm; <sup>13</sup>C NMR (101 MHz, CD<sub>3</sub>CN)  $\delta$  = 53.62, 40.19, 9.89 ppm.

Deposition Numbers 2100817 (for 10a) and 2100818 (for 11) contain the supplementary crystallographic data for this paper. These data are provided free of charge by the joint Cambridge Crystallographic Data Centre and Fachinformationszentrum Karlsruhe Access Structures service [www.ccdc.cam.ac.uk/structures](http://www.ccdc.cam.ac.uk/structures).

### Acknowledgements

We thank Dr. Heike Hausmann for performing the AV600 NMR measurements. Open Access funding enabled and organized by Projekt DEAL.

### Conflict of Interest

The authors declare no conflict of interest.

**Keywords:** Alkylation · Antitumor agents · Aziridinium ions · Kinetics · Structure-Activity relationship

- [1] a) M. R. P. D. Alison (Ed.) *The Cancer Handbook*, John Wiley & Sons Inc, Chichester, UK, 2004; b) C. Avendaño, J. C. Menéndez, *Medicinal chemistry of anticancer drugs*, Elsevier Science Ltd, Amsterdam, 2015; c) R. K. Singh, S. Kumar, D. N. Prasad, T. R. Bhardwaj, *Eur. J. Med. Chem.* 2018, 151, 401.  
[2] a) K. W. Kohn, *Cancer Res.* 1996, 56, 5533; b) B. A. Chabner, T. G. Roberts, *Nature reviews. Cancer* 2005, 5, 65.

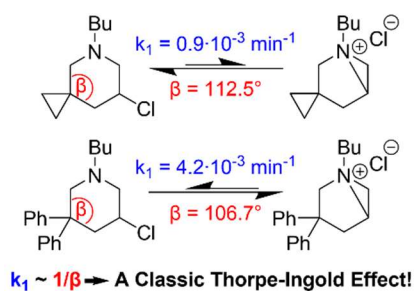
- [3] a) G. P. Warwick, *Cancer Res.* 1963, 23, 1315; b) L. H. Hurley, *Nat. Rev. Cancer* 2002, 2, 188.  
[4] a) K. S. Gates, T. Nooner, S. Dutta, *Chem. Res. Toxicol.* 2004, 17, 839; b) L. P. Bignold, *Anticancer Res.* 2006, 26, 1327.  
[5] a) I. Zuravka, R. Roesmann, A. Susic, W. Wende, A. Pingoud, B. Gatto, R. Göttlich, *ChemMedChem* 2014, 9, 2178; b) T. Helbing, C. Carraro, A. Francke, A. Susic, M. de Franco, V. Gandin, R. Göttlich, B. Gatto, *ChemMedChem* 2020, 15, 2040; c) C. Carraro, T. Helbing, A. Francke, I. Zuravka, A. Susic, M. de Franco, V. Gandin, B. Gatto, R. Göttlich, *ChemMedChem* 2021, 16, 860.  
[6] A. Susic, I. Zuravka, N.-K. Schmitt, A. Miola, R. Göttlich, D. Fabris, B. Gatto, *ChemMedChem* 2017, 12, 1471.  
[7] C. Carraro, A. Francke, A. Susic, F. Kohl, T. Helbing, M. de Franco, D. Fabris, R. Göttlich, B. Gatto, *ACS Med. Chem. Lett.* 2019, 10, 552.  
[8] M. Noack, R. Göttlich, *Eur. J. Org. Chem.* 2002, 3171.  
[9] a) S. Stanković, M. D'hooghe, S. Catak, H. Eum, M. Waroquier, V. van Speybroeck, N. de Kimpe, H.-J. Ha, *Chem. Soc. Rev.* 2012, 41, 643; b) J. Ranjith, H.-J. Ha, *Molecules* 2021, 26, 1774; c) H. Goossens, D. Hertsen, K. Mollet, S. Catak, M. D'hooghe, F. de Proft, P. Geerlings, N. de Kimpe, M. Waroquier, V. van Speybroeck in *Structure, Bonding and Reactivity of Heterocyclic Compounds* (Eds.: F. de Proft, P. Geerlings), Springer Berlin Heidelberg, Berlin, Heidelberg, 2014, pp. 1–34; d) J. Dolfen, N. N. Yadav, N. De Kimpe, M. D'hooghe, H.-J. Ha, *Adv. Synth. Catal.* 2016, 358, 3485.  
[10] R. Göttlich, *Synthesis* 2000, 1561.  
[11] K. C. Brannock, *J. Am. Chem. Soc.* 1959, 81, 3379.  
[12] N. J. Leonard, J. V. Paukstelis, L. E. Brady, *J. Org. Chem.* 1964, 29, 3383.  
[13] N. J. Leonard, L. E. Brady, *J. Org. Chem.* 1965, 30, 817.  
[14] M. A. Graham, M. Thornton-Pett, C. M. Rayner, A. H. Wadsworth, *Chem. Commun.* 2001, 966.  
[15] Y.-H. Lam, K. N. Houk, J. Cossy, D. G. Prado, A. Cochi, *Helv. Chim. Acta* 2012, 95, 2265.  
[16] a) M.-K. Ji, D. Hertsen, D.-H. Yoon, H. Eum, H. Goossens, M. Waroquier, V. van Speybroeck, M. D'hooghe, N. de Kimpe, H.-J. Ha, *Chem. Asian J.* 2014, 9, 1060; b) S. Y. Yun, S. Catak, W. K. Lee, M. D'hooghe, N. de Kimpe, V. van Speybroeck, M. Waroquier, Y. Kim, H.-J. Ha, *Chem. Commun.* 2009, 2508.  
[17] a) T.-X. Métro, B. Duthion, D. Gomez Pardo, J. Cossy, *Chem. Soc. Rev.* 2010, 39, 89; b) A. Cochi, D. G. Prado, J. Cossy, *Eur. J. Org. Chem.* 2012, 2012, 2023.  
[18] M. D'hooghe, S. Catak, S. Stanković, M. Waroquier, Y. Kim, H.-J. Ha, V. van Speybroeck, N. de Kimpe, *Eur. J. Org. Chem.* 2010, 2010, 4920.  
[19] E. B. Boydas, G. Tanriver, M. D'hooghe, H.-J. Ha, V. van Speybroeck, S. Catak, *Org. Biomol. Chem.* 2018, 16, 796.  
[20] N. de Kimpe, M. Boelens, J. Contreras, *Tetrahedron Lett.* 1996, 37, 3171.  
[21] a) C. C. Price, H. Akimoto, R. Ho, *J. Org. Chem.* 1973, 38, 1538; b) C. C. Price, M.-T. L. Yip, *J. Biol. Chem.* 1974, 249, 6849.  
[22] C. F. Hammer, S. R. Heller, J. H. Craig, *Tetrahedron* 1972, 28, 239.  
[23] K. S. Gates, *Chem. Res. Toxicol.* 2009, 22, 1747.  
[24] a) P. D. Bartlett, S. D. Ross, C. G. Swain, *J. Am. Chem. Soc.* 1947, 69, 2971; b) G. B. Bauer, L. F. Povirk, *Nucleic Acids Res.* 1997, 25, 1211; c) C. E. Williamson, B. Witten, *Cancer Res.* 1967, 27, 33; d) J. S. Fruton, W. H. Stein, *J. Org. Chem.* 1946, 11, 571.  
[25] H. Yang, F. C. Thyron, *Bull. Soc. Chim. Belg.* 1996, 105, 23.  
[26] M. S. Kharasch, P. G. Holton, W. Nudenberg, *J. Org. Chem.* 1954, 19, 1600.  
[27] N. J. Leonard, J. V. Paukstelis, *J. Org. Chem.* 1965, 30, 821.

Manuscript received: September 1, 2021

Revised manuscript received: September 28, 2021

Accepted manuscript online: September 29, 2021

### 4.3. Separation of the Thorpe-Ingold and Reactive Rotamer Effect by Using the Formation of Bicyclic Aziridinium Ions



A classic, angle dependent Thorpe-Ingold effect in the formation of bicyclic aziridinium ions is presented. Kinetic studies, backed up by SC-XRD and DFT calculations, reveal a linear correlation of the internal angle  $\beta$  with the rate constant  $k_1$ . Increased angles result in decreased rate constants and *vice versa*. The cyclic structure of the examined 3-chloropiperidines thereby excludes contribution of the reactive rotamer effect towards this cyclization.

#### Reference (Early View)

Tim Helbing, Michael Kirchner, Jonathan Becker, Richard Göttlich, *European Journal of Organic Chemistry* **2022**, e202200597. (doi: 10.1002/ejoc.202200597)

Tim Helbing and Michael Kirchner contributed equally to this work.

© 2022 The Authors. *European Journal of Organic Chemistry* published by Wiley – VCH Verlag GmbH & Co. KGaA, Weinheim.

Reproduced with permission of the copyright owners.

## VIP Very Important Paper

## Separation of the Thorpe–Ingold and Reactive Rotamer Effect by Using the Formation of Bicyclic Aziridinium Ions

Tim Helbing<sup>+</sup>,<sup>[a]</sup> Michael Kirchner<sup>+</sup>,<sup>[a]</sup> Jonathan Becker,<sup>[b]</sup> and Richard Göttlich<sup>\*,[a]</sup>

The geminal dialkyl effect is widely used in organic synthesis to promote cyclization reactions, although the exact origin of its rate enhancement remains unclear. In the present study, we demonstrate the applicability of this effect for the intramolecular formation of bicyclic aziridinium ions and assign it to angle contractions provided by introduction of sterically demanding substituents. Due to the cyclic structure of the examined 3-chloropiperidines the acceleration of this ring closure cannot be explained by an increased population of

reactive gauche rotamers and therefore agrees with the original Thorpe–Ingold theory. Furthermore, introduction of strained aliphatic rings resulted in internal angle expansions and were accompanied by a preliminary decrease of rate constants for the investigated aziridinium ion formation. These results lead to a linear correlation between internal angle and relative reaction rate, supported by computational and X-ray crystallographic structural data.

## Introduction

Intramolecular reactions can be accelerated by the introduction of a *gem*-substituent group in the carbon chain connecting two reactive centres. This is commonly known as the *gem*-disubstituent or *gem*-dialkyl effect.<sup>[1,2]</sup> Thorpe, Ingold and Beesley offered the first explanation of this rate enhancement, which was later termed the “Thorpe–Ingold effect”. According to their theory, the angle  $\alpha$  between two alkyl substituents is enlarged by increased steric repulsion compared to the unsubstituted homologue. Consequently, the opposite angle  $\beta$  is decreased to relieve steric strain moving the two reactive centres closer together, thus promoting cyclization (Figure 1a).<sup>[3]</sup> In 1960, Allinger and Zalkow concluded that the increased number of *gauche* interactions in *gem*-disubstituted acyclic compounds, compared to the corresponding cyclic system, reduces the enthalpy of activation  $\Delta H^\ddagger$ .<sup>[4]</sup> Furthermore, substitution restrains the rotational entropy in the open chain

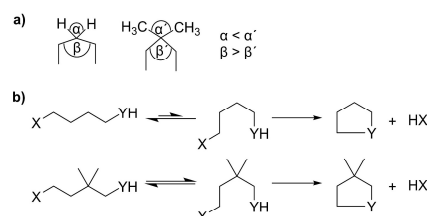


Figure 1. a) Compression of the  $\beta$  angle by introduction of geminal methyl groups known as the “Thorpe–Ingold effect”. b) Increase in the population of a reactive *gauche* rotamer, which readily undergoes cyclization, by *gem*-methylation known as the “reactive-rotamer effect”.

precursor more than in the cyclic product, resulting in a favourable entropy of activation  $\Delta S^\ddagger$  for the cyclization of *gem*-disubstituted compounds. Two years later, Schleyer calculated the contribution of the angle compression to the *gem*-dialkyl effect and mentioned that the small changes of the  $\beta$  angle cannot solely explain the experimentally observed enhancements of rate constants up to several orders of magnitude.<sup>[5]</sup> Therefore, Bruce and Pandit developed a different theory and associated the rate enhancements with an increased population of reactive *gauche* rotamers, which was later entitled the “reactive-rotamer effect”.<sup>[6]</sup> In these conformations, the two reactive centres are arranged properly for cyclization (Figure 1b). This concept is similar to the later developed theory of near attack conformers (NACs) by Bruce and Lightstone,<sup>[7–10]</sup> for which experimental evidence was given lately.<sup>[11]</sup> NACs represent ground state conformers, which are similar to the transition state in terms of geometry and orientation of the reactive centres, while still being separated by roughly 3 Å to ensure that bond formation as well as bond breaking has not occurred yet. This separation also represents the critical distance known from the spatiotemporal hypothesis of Menger,<sup>[12–17,18]</sup> which correlates distance between reactive

[a] T. Helbing,<sup>+</sup> M. Kirchner,<sup>+</sup> Prof. Dr. R. Göttlich  
Institute of Organic Chemistry  
Justus Liebig University Giessen  
Heinrich-Buff-Ring 17,  
35392 Giessen, Germany  
E-mail: richard.göttlich@org.chemie.uni-giessen.de  
https://www.uni-giessen.de/fbz/fb08/Inst/organische-chemie/  
AGGoettlich

[b] J. Becker  
Institute of Inorganic and Analytical Chemistry  
Justus Liebig University Giessen  
Heinrich-Buff-Ring 17,  
35392 Giessen, Germany

[†] These authors contributed equally to this work.

Supporting information for this article is available on the WWW under  
https://doi.org/10.1002/ejoc.202200597

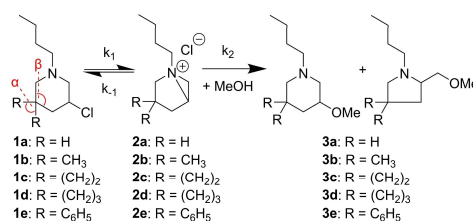
© 2022 The Authors. European Journal of Organic Chemistry published by Wiley-VCH GmbH. This is an open access article under the terms of the Creative Commons Attribution Non-Commercial NoDerivs License, which permits use and distribution in any medium, provided the original work is properly cited, the use is non-commercial and no modifications or adaptations are made.

centres with the reaction rate. The concept postulates that a reaction is accelerated by several orders of magnitude, if the reactive moieties are kept in proximity, less than the critical distance, for a sufficient time. The aforementioned theories, along with many others, have also been extensively discussed to explain the severe rate accelerations achieved in enzyme catalysed reactions.<sup>[19]</sup>

Although several articles have been published to support or discourage either the Thorpe-Ingold or the reactive rotamer effect, this subject remains challenging since both effects contribute to rate enhancements provided by *gem*-disubstitution and are therefore difficult to distinguish. For instance, Parrill and Dolata showed that there is no linear correlation between the population of reactive rotamers and the relative reaction rates, suggesting a "facilitated transition" hypothesis instead.<sup>[20]</sup> Contrarily, Jung and Gervay gave evidence for the reactive rotamer effect by examination of intramolecular Diels-Alder experiments, demonstrating an increase in rate constants even if strained rings, like cyclobutane or cyclopropane, were used as *gem*-substituents.<sup>[21]</sup> The small angles of these cyclic systems should lead to larger internal angles and would therefore retard the reaction if valency deviation effects were the dominant factors in the examined reaction. Several other theories have been published, for instance "stereopopulation control"<sup>[22–24]</sup> and "relief of ground-state strain",<sup>[25,26]</sup> both discussed as the origin of the "trimethyl lock effect". This conformational restriction, which represents a combination of the "buttressing effect"<sup>[27]</sup> and the *gem*-disubstituent effect, provides extreme rate enhancements and was first observed for the cyclization of methylated hydrocoumarinic acid derivatives.<sup>[22–26,28]</sup> Moreover, a reduction of ring strain energy by *gem*-disubstitution of small ring systems has been discussed.<sup>[29]</sup> Although, the detailed origin of rate enhancements by *gem*-disubstitution is still up for discussion, there are numerous examples of successful applications of the geminal dialkyl effect leading to accelerated reactions, increased yields and selectivity in cyclization reactions<sup>[2,30]</sup> as well as in ligand design.<sup>[31]</sup>

## Results and Discussion

In recent kinetic studies with substituted 3-chloropiperidines we noticed an enhanced reaction rate for the 5,5-dimethyl derivative **1b** compared to the corresponding unsubstituted compound **1a**.<sup>[32]</sup> The reaction of these compounds with nucleophiles proceeds *via* the highly electrophilic bicyclic aziridinium intermediate **2**, which is rapidly consumed by nucleophilic attack (Scheme 1). The observed increase in reaction rate is assumed to be the result of a *gem*-dialkyl effect, since a bicyclic system is obtained in the rate-determining formation of the aziridinium intermediate ( $k_1$ ), for which the steady state approximation ( $k_2 \gg k_{-1}$ ) can be applied. However, this rate acceleration cannot be explained by an increased population of reactive *gauche* conformers, since the cyclic structure of the 3-chloropiperidines already fixes the orientation of the reactive centres towards each other. Another explanation

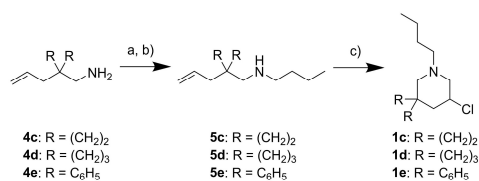


Scheme 1. Reaction mechanism of the examined 3-chloropiperidines **1a–e**, a mixture of the piperidine and pyrrolidine methyl ethers **3a–e** are formed by methanolysis of the intermediate bicyclic aziridinium ions **2a–e**.

would therefore be an angle contraction of the internal  $\beta$  angle, representing a classic Thorpe-Ingold effect, which could be studied separated from the reactive rotamer effect. If the hypothesis holds true for our 3-chloropiperidine system, it might be considered as a useful tool to modulate their reactivity as alkylating agents.<sup>[33]</sup> This would be of particular interest, since *gem*-dimethyl substitution has already been used to successfully improve the reactivity, stability or synthesis of various medical agents.<sup>[34]</sup>

In this study, we report for the first time a rate enhancement *via* distinct angle dependant Thorpe-Ingold effect for an intramolecular reaction in an already cyclic system. Furthermore, a preliminary deceleration of the examined solvolysis reaction, by introduction of strained cycloalkyl substituents, was observed. In the following, we will show a linear correlation between the internal  $\beta$  angle, provided by single crystal XRD and DFT<sup>[35]</sup> calculations, and the relative rate constant  $k_{rel}$  (with respect to the unsubstituted compound **1a**) observed in <sup>1</sup>H-NMR kinetic experiments of the 3-chloropiperidines **1a–e**. Furthermore, we demonstrate an analogous tendency for the experimentally determined Gibbs free energies of activation  $\Delta G^\ddagger$ . These results demonstrate, to the best of our knowledge, the first kinetic study about the contribution of the Thorpe-Ingold effect towards cyclization reactions separated from the reactive rotamer effect. Therefore, the novel *spiro* compounds **1c** and **1d** as well as the diphenyl derivative **1e** were synthesized from the corresponding unsaturated amines **4c–e**, which can be obtained by allylation and reduction of the corresponding nitriles, as described in literature.<sup>[36]</sup> The amine precursors were then alkylated by imine formation and subsequent reduction, followed by simultaneous *N*-chlorination and cyclization using copper(II)chloride<sup>[37,38]</sup> (Scheme 2). The synthesis of the 3-chloropiperidines **1a** and **1b** has already been described in our previous work.<sup>[39,40]</sup>

The reactivity of the obtained 3-chloropiperidines **1a–e** against methanol as an explorative nucleophile was examined by <sup>1</sup>H-NMR kinetic solvolysis experiments. The compounds were dissolved in methanol-*d*<sub>4</sub>, containing dibenzylether as an internal standard. The NMR tubes were heated to 50 °C for 7.5 h (except **1e**, which was incubated for only 2.5 h) in an oil bath and withdrawn for the measurements after an appropriate time. The consumption of the starting material, following the



**Scheme 2.** Synthesis of 3-chloropiperidines **1c–e**. a) *n*-butylaldehyde, MgSO<sub>4</sub>, DCM, RT; b) NaBH<sub>4</sub>, MeOH, 0 °C to RT; c) CuCl<sub>2</sub> · 2 H<sub>2</sub>O, THF, RT (**1c–d**) or CuCl<sub>2</sub>, THF, RT to reflux (**1e**).

mechanism depicted in Scheme 1, was monitored (Figures S1–S5) and the anticipated mixture of piperidine and pyrrolidine methyl ethers **3a–e** was confirmed by GC/MS (see supplementary Experimental Section). The observed regioselectivity in favour of the six-membered piperidine compound is in accordance with several other experimental and theoretical studies on ring expansion of bicyclic aziridinium ions.<sup>[41]</sup> Sterically demanding substituents in C5 position therefore result in a higher fraction of the thermodynamic piperidine product, compared to the corresponding unsubstituted compound. The first order rate constants of the examined solvolysis reactions were calculated by plotting the natural logarithm of the integral of the corresponding starting material 3-H signal  $\ln(3-H)$  (except **1e**, where an overlapping CH<sub>2</sub> signal was included in the integral) against the reaction time *t* (Table S1). As expected, we observed an increase in reactivity of the dimethyl derivative **1b** ( $k_{\text{rel}} = 1.56$ ) compared to the unsubstituted compound **1a**. The acceleration for the diphenyl derivative **1e** ( $k_{\text{rel}} = 2.38$ ) was even stronger, resulting in complete consumption of the starting material after approximately five hours. We also recognized a decreased reaction rate for compounds **1c** and **1d** in comparison to compound **1a**. This could be due to the strained cyclic substituents, as observed for the intramolecular catalytic activity of cycloalkyl-substituted malonic acid derivatives.<sup>[42]</sup> The decrease in reaction rate was more prominent for the cyclopropyl compound **1c** ( $k_{\text{rel}} = 0.53$ ) than for the cyclobutyl derivative **1d** ( $k_{\text{rel}} = 0.64$ ), suggesting a direct correlation of the internal  $\beta$  angle and the rate constant in our 3-chloropiperidine system, as originally proposed by the valency deviation theory of Thorpe and Ingold.<sup>[43]</sup> To show the robustness and reproducibility of

our kinetic method, we repeated the kinetic measurements at 50 °C for all compounds, performing the reaction at this temperature in the NMR spectrometer while also taking <sup>1</sup>H-NMR spectra more frequently (representative <sup>1</sup>H-NMR spectra shown in Figure S8) and obtained nearly the same rate constants (Table 1).

To confirm the assumed angle distortion by introduction of different substituents in 5-position, we crystallized several 3-chloropiperidine derivatives as their corresponding hydrochloride salts and analysed their structure *via* single crystal XRD. The respective angles  $\alpha$  and  $\beta$  (as depicted in Scheme 1), obtained from the crystal structures of the HCl salts of compounds **1a**, **1c** and **1e** (see Tables S2–S7 and S21–S2) are summarized in Table 1. Since a crystal structure of the dimethylated compound **1b** could not be obtained, the angles of the crystal structures of compounds **6a** and **6b** (see Tables S8–S20), which represent the *N*-benzyl substituted derivatives of **1a** and **1b**, were added. A similar effect resulting from *gem*-dimethylation can be assumed for the *N*-benzyl and *N*-butyl substituted derivatives, considering that the reaction of **1a** and **1b** as well as **6a** and **6b** with 2'-desoxyguanosine in aqueous solution provided similar relative rate constants in our previous work ( $k_{\text{rel}}(\mathbf{1b}/\mathbf{1a}) = 4.67$ ;  $k_{\text{rel}}(\mathbf{6b}/\mathbf{6a}) = 4.08$ ).<sup>[32]</sup> In addition, we obtained a relative rate constant of  $k_{\text{rel}} = 1.66$  in a separate kinetic study of **6a** and **6b** in methanol-d<sub>4</sub> at 50 °C (see Figure S6), which is comparable to the values of the respective *N*-butyl compounds reported in Table S1 and Table 1. Furthermore, we investigated the structure of the examined 3-chloropiperidine derivatives computationally using the orca program package (version 5.0.3.)<sup>[44]</sup> on the PCM(methanol)-PBEh-3c<sup>[45,46]</sup> level of theory, containing the corresponding modified def2-mSV(P) basis set<sup>[46,47]</sup> and confirmed the lowest energy conformers using the Crest program package.<sup>[48]</sup> The experimentally obtained as well as the calculated angles  $\alpha$  and  $\beta$  shown in Table 1 are in good agreement among each other, considering that the crystal structures were obtained from the corresponding hydrochloride salts. Moreover, both values show a good linear correlation ( $R^2_{\text{XRD}} = 0.98$  and  $R^2_{\text{DFT}} = 0.87$ ) between the internal  $\beta$  angle and the relative rate constant  $k_{\text{rel}}$  (Figure 2). An analogous correlation cannot be observed for the exocyclic  $\alpha$  angle (Figure S9), which is not surprising since  $\alpha$  and  $\beta$  show no direct linear relationship either (Figure S10). Nonetheless, introduction of substituents containing small  $\alpha$  angles lead to

**Table 1.** Rate constants  $k_1$  and relative rate constants  $k_{\text{rel}}$  for the solvolysis reactions of 3-chloropiperidines **1a–e** in methanol-d<sub>4</sub>. Bond angles  $\alpha$  and  $\beta$  in compounds **1a–e** derived from single crystal XRDs (hydrochloride salts), with their corresponding ESD-values in brackets, and DFT calculations. Activation parameters for compounds **1a–e** derived from the respective Arrhenius and Eyring plots. N/A = not available

	$k_1$ [10 <sup>-3</sup> min <sup>-1</sup> ] <sup>[a]</sup>	$k_{\text{rel}}$	$\alpha$ (XRD) [°]	$\alpha$ (DFT) [°]	$\beta$ (XRD) [°]	$\beta$ (DFT) [°]	$E_a$ [kcal/mol]	$\Delta H^\ddagger_{298}$ [kcal/mol]	$\Delta S^\ddagger_{298}$ [cal/(K <sup>o</sup> mol)]	$\Delta G^\ddagger_{298}$ [kcal/mol]
<b>1a</b>	1.66 ± 0.05	1	107.9 <sup>[b]</sup> 107.9 <sup>[b,c]</sup>	107.07	111.8 (3) 112.07 (14) <sup>[c]</sup>	110.95	18.03 ± 1.00	17.41 ± 1.00	-17.30 ± 3.21	22.56 ± 1.96
<b>1b</b>	2.97 ± 0.12	1.79	109.1 (2) <sup>[c]</sup>	109.12	109.35 (19) <sup>[c]</sup>	108.42	17.51 ± 0.91	16.88 ± 0.91	-17.62 ± 2.89	22.13 ± 1.77
<b>1c</b>	0.99 ± 0.01	0.54	60.06 (11)	60.30	113.28 (13)	112.49	17.11 ± 0.62	16.49 ± 0.62	-21.17 ± 2.00	22.80 ± 1.22
<b>1d</b>	1.44 ± 0.04	0.87	N/A	88.47	N/A	109.58	16.94 ± 1.01	16.31 ± 1.01	-21.36 ± 3.24	22.68 ± 2.35
<b>1e</b>	4.19 ± 0.13	2.52	110.2 (2)	107.57	107.54 (12)	106.66	17.28 ± 1.01	16.66 ± 1.02	-17.94 ± 3.25	22.01 ± 1.98

[a] Samples were incubated at 50 °C directly in the NMR spectrometer. [b]  $\angle_{\text{HCSH}}$  values derived geometrically from the positions of non-hydrogen substituents of C5. [c] Values obtained from the corresponding hydrochloride salts of the *N*-benzyl derivatives **6a** and **6b** (see Tables S8–S20).

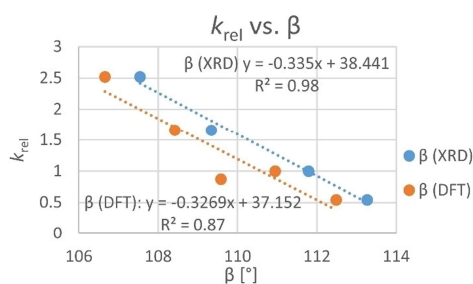


Figure 2. Linear correlation between the relative rate constants  $k_{rel}$  and the internal  $\beta$  angle, obtained by single crystal XRD and DFT calculations.

an increase of  $\beta$  and therefore retard the reaction, resulting in a lower relative rate constant, and *vice versa*, as originally proposed by Thorpe and Ingold. The obtained differences in rate constants are considerably smaller compared to reported systems in which the reactive rotamer effect is present,<sup>72</sup> but still show that angular distortion is capable of affecting the reaction rates. The change in the internal  $\beta$  angle is further accompanied by a slight change of the attack angle and distance of the nucleophilic nitrogen towards the electrophilic C3 centre, resulting from the geometrical distortion. Both are important factors to consider in a possible correlation following the spatiotemporal hypothesis.<sup>112–171</sup> The attack angle in the unsubstituted 3-chloropiperidine **1a** was calculated to be 142.85° (depicted in Figure S11), while the cyclopropyl substituted derivative **1c** performs the backside attack from an angle of 142.70° and the more reactive diphenyl compound **1e** attacks the leaving group C3 carbon from an angle of 143.28° (for other attack angles see Table S1). On the other hand, the cyclobutyl compound **1d** does not follow this trend, as its attack angle of 143° is closer to the angle of 180° typical for  $S_N2$  nucleophilic substitutions, but its reactivity is lower compared to compound **1a**. Moreover, the changes in NC3 distance (Table S1) compared to the unsubstituted compound **1a** (2.428 Å) are very small ( $\Delta r_{max} = 0.02$  Å), while still following a tendency similar to the NC3Cl attack angles. The nitrogen atom of the more reactive diphenyl compound **1e** is a little closer to the leaving-group C3 carbon (2.411 Å), while the distance for the cyclopropyl derivative **1c** was calculated to be 2.432 Å. Again, the less reactive cyclobutyl derivative **1d** represents an exception (2.422 Å). When also considering the mean absolute deviation of 0.009 Å for small first and second row molecules calculated by the PBEh-3c method,<sup>184</sup> we assumed that these small differences are no dominant factors in the examined solvolysis reaction of the substituted 3-chloropiperidines **1a–e**.

To understand the observed effect in more detail we also determined the activation parameters for compounds **1a–e**. Therefore, <sup>1</sup>H-NMR solvolysis experiments were performed between room temperature (22.5 °C) and 60 °C (oil bath temperature). The resulting rate constants (see Figures S12–S16) were then used to determine  $E_a$  (Arrhenius plots: Figures S17–S21)

and  $\Delta H^\ddagger$  as well as  $\Delta S^\ddagger$  (Eyring plots: Figures S22–S26), while  $\Delta G^\ddagger$  was calculated from these values (Table 1). The Gibbs free energies of activation  $\Delta G^\ddagger$  obtained from the Eyring plots reflect the general tendency of reactivity we observed in the initial kinetic experiments. Even though the differences in Gibbs free energies of activation  $\Delta\Delta G^\ddagger$  are smaller than expected from the relative rate constants, which can be attributed to the experimental error of roughly 2 kcal/mol. Interestingly all activation enthalpy  $\Delta H^\ddagger$  and activation energy  $E_a$  values are decreased when introducing substituents in 5-position, including the strained cycloalkyl moieties present in compounds **1c** and **1d**. In addition, the substitution of compounds **1b** and **1e** with more bulky groups just slightly increases the activation entropy  $\Delta S^\ddagger$  compared to the unsubstituted homologue **1a**, accordingly their respective rate enhancements are almost entirely attributed to lower enthalpies of activation  $\Delta H^\ddagger$ . However, this is not the case for the cyclopropyl and cyclobutyl compounds **1c** and **1d**. Apparently the decrease in  $\Delta H^\ddagger$  is overcompensated by a firmly negative entropy of activation  $\Delta S^\ddagger$ , resulting in higher Gibbs free energies of activation  $\Delta G^\ddagger$  and therefore lower rate constants. The strained cycloalkyl moiety most likely further restricts the already constrained transition state by additional reduction of degrees of freedom. Similar effects on the activation parameters (lowering of  $\Delta H^\ddagger$  and  $\Delta S^\ddagger$ ) of cycloalkyl-substituted compounds have been reported by Jung and Gervay,<sup>211</sup> although in the examined system a strong decrease in  $\Delta H^\ddagger$  resulted in small rate enhancements. The authors associated this with the presence of the reactive rotamer effect. However, this effect is not applicable in the reaction of our cyclic system, thus the related decrease in  $\Delta H^\ddagger$  is lacking and cannot compensate the firmly negative  $\Delta S^\ddagger$ . As a result, the reaction is slowed down by the leftover angle distortion effect. Various studies discussed the entropic contribution in the accelerated intramolecular anhydride formation of substituted glutarates,<sup>17–9,491</sup> but most of them focus on conformational effects (*via* the NAC approach), which are not applicable in our rigid cyclic system. This is supported by the fact, that we observed only small changes in the entropy of activation  $\Delta S^\ddagger$  for the *gem*-dimethyl and the *gem*-diphenyl derivatives (**1b** and **1e** respectively) in comparison to the unsubstituted compound **1a**. In addition, the determined Gibbs free energies of activation  $\Delta G^\ddagger$  show a linear correlation with the internal  $\beta$  angle (see Figure S27), just as the aforementioned relative rate constants  $k_{rel}$  (Figure 2). Generally, our investigations support the presence of a classic Thorpe-Ingold effect separated from conformational effects, such as the reactive rotamer effect, in the examined solvolysis reaction of *gem*-disubstituted 3-chloropiperidines.

## Conclusion

In conclusion, we investigated the original, angle dependant Thorpe-Ingold effect, excluding the otherwise competing reactive rotamer effect, by <sup>1</sup>H-NMR kinetic and structural analysis of the substituted 3-chloropiperidine derivatives **1a–e**. We could show a rate enhancement by introduction of bulky *gem*-

disubstituents in 5-position compared to the unsubstituted compound **1a** as well as a first-time deceleration of the examined reaction for the novel *spiro* derivatives **1c** and **1d**, containing cyclopropyl and cyclobutyl rings respectively. The introduction of these strained cyclic substituents resulted in an enlargement of the internal  $\beta$  angle, confirmed by single crystal XRD and DFT calculations. In contrast, the internal angle decreases with increasing steric demand of 5-substituents, demonstrated by the *gem*-dimethyl compound **1b** and the *gem*-diphenyl derivative **1e**. As a bicyclic system is obtained in the rate determining aziridinium ion formation, a *gem*-disubstituent effect can be assumed for the investigated solvolysis reaction (MeOH) of our 3-chloropiperidines. Yet, the observed acceleration and deceleration of rate constants cannot be explained by the reactive rotamer effect, since the orientation of the reactive centres is already locked in the cyclic piperidine system. Furthermore, the obtained relative rate constants  $k_{rel}$  as well as the experimentally determined Gibbs free energies of activation  $\Delta G^\ddagger$  show good linear correlations with the internal  $\beta$  angle. Taken all of these results together, there is strong evidence for the presence of a classic, angle dependent Thorpe-Ingold effect separated from the reactive rotamer effect in the formation of bicyclic aziridinium ions. Although these angular distortion effects might be overcompensated by conformational effects in open-chain substrates, cyclic compounds seem to be essentially affected by the internal angle between the reactive centres. Consequently, this effect can be used as another useful approach to tune the reactivity of 3-chloropiperidines as DNA alkylating agents.

## Experimental Section

All solvents were purified by distillation prior to use, in case of anhydrous solvents AcroSeal™ bottles from ACROS Organics™ were used. Commercially available reagents were used as supplied if not stated different. Synthesis using anhydrous solvents were carried out under Schlenk conditions. For purification by flash column chromatography silica gel 60 (Merck) was used.  $^1\text{H}$  and  $^{13}\text{C}$  NMR spectra were recorded at the Bruker Avance II 400, the Avance III 400 and the Bruker Avance II 200 "Microbay" spectrometer ( $^1\text{H}$  at 400 MHz and 200 MHz;  $^{13}\text{C}$  at 101 MHz) in deuterated solvents.  $^1\text{H}$ -NMR kinetic experiments were carried out at the Bruker Avance II 200 "Microbay" spectrometer ( $^1\text{H}$  at 200 MHz) and the Bruker Avance III 600 spectrometer ( $^1\text{H}$  at 600 MHz).  $^1\text{H}$  and  $^{13}\text{C}$  chemical shifts were determined by reference to the residual solvent signals. High-resolution ESI mass spectra were recorded in methanol using a ESI-microTOF spectrometer (Bruker Daltonics) in positive ion mode. All GC/MS spectra were recorded at the Agilent 5977B GC/MSD instrument equipped with a 7820 A GC System. All elemental analysis (CHN) were performed on a Thermo FlashEA-1112 series instrument. NMR spectra of the synthesized compounds **1c-e**, **4c-e** and **5c-e** as well as the synthetic procedures for the known primary amines **4c-e**<sup>[37,38]</sup> and their corresponding nitrile precursors are included in the Supporting Information. The synthesis of compounds **1a** and **1b** has been described elsewhere.<sup>[39,40]</sup>

### General procedure for synthesis of secondary amines (5c–e)

To a solution of the corresponding primary amine **4c–e** in DCM (0.5 mL/mmol) freshly distilled *n*-butylaldehyde (1.1–1.4 eq.) as well

as  $\text{MgSO}_4$  (approx. 5–10 g) were added. The mixture was stirred at room temperature for 2 h, filtered afterwards and the solvent was removed under reduced pressure. The residue was dissolved in MeOH (0.5 mL/mmol) and  $\text{NaBH}_4$  (1.5–2 eq.) was added at 0°C. The mixture was stirred at room temperature for 16–18 h. The reaction was then quenched by the addition of 20%  $\text{NaOH}_{(aq)}$  and DCM was added. The phases were separated and the aqueous phase was extracted with DCM (3x). The combined organic extracts were washed with brine, distilled water as well as brine and dried over  $\text{MgSO}_4$ . The solvent was removed under reduced pressure and the crude product was obtained, which was used in the next step without further purification.

### N-[(propenyl)cyclopropyl]methylbutanamine (5c)

Was prepared according to the general procedure from [(Propenyl)cyclopropyl]methanamine **4c** (0.47 g, 4.25 mmol) yielding the title compound **5c** as a colorless oil (0.45 g) which was used in the next step without further purification.  $^1\text{H}$  NMR ( $\text{CDCl}_3$ , 400 MHz):  $\delta = 5.85\text{--}5.77$  (m, 1H,  $\text{CH}_2 = \text{CH-CH}_2$ ), 5.09–5.00 (m, 2H,  $\text{CH}_2 = \text{CH-CH}_2$ ), 2.62–2.57 (m, 2H,  $\text{NH-CH}_2\text{-CH}_2\text{-CH}_2\text{-CH}_3$ ), 2.48 (s, 2H,  $\text{CH}_2\text{-NH}$ ), 2.13 (dt,  $J = 7.1$ , 1.3 Hz, 2H,  $\text{CH}_2 = \text{CH-CH}_2$ ), 1.51–1.44 (m, 2H,  $\text{CH}_2\text{-CH}_2\text{-CH}_2\text{-CH}_2\text{-NH}$ ), 1.37–1.28 (m, 3H,  $\text{NH}$  and  $\text{CH}_2\text{-CH}_3$ ), 0.92 (m, 3H,  $\text{CH}_3$ ), 0.44–0.34 (m, 4H,  $(\text{CH}_2)_2$ ) ppm;  $^{13}\text{C}$  NMR ( $\text{CDCl}_3$ , 101 MHz):  $\delta = 136.50$  ( $\text{CH}_2 = \text{CH-CH}_2$ ), 116.37 ( $\text{CH}_2 = \text{CH-CH}_2$ ), 56.14 ( $\text{CH}_2\text{-CH}_2\text{-NH}$ ), 49.77 ( $\text{CH}_2\text{-NH}$ ), 39.26 ( $\text{CH}_2 = \text{CH-CH}_2$ ), 32.09 ( $\text{CH}_2\text{-CH}_2\text{-CH}_2\text{-NH}$ ), 20.63 ( $\text{CH}_2\text{-CH}_3$ ), 19.58 ( $\text{C}_\alpha$ ), 14.03 ( $\text{CH}_3$ ), 10.10 ( $(\text{CH}_2)_2$ ) ppm; HRMS (ESI):  $m/z$  calcd for  $\text{C}_{11}\text{H}_{21}\text{N}^+$ : 168.1747, found: 168.1750 [ $\text{M} + \text{H}$ ] $^+$ .

### N-[(propenyl)cyclobutyl]methylbutanamine (5d)

Was prepared according to the general procedure from crude [(Propenyl)cyclobutyl]methanamine **4d** (1.02 g) yielding the title compound **5d** as a colorless oil (1.60 g) which was used in the next step without further purification.  $^1\text{H}$  NMR (400 MHz,  $\text{CDCl}_3$ )  $\delta = 5.77\text{--}5.68$  (m, 1H,  $\text{CH}_2 = \text{CH-CH}_2$ ), 5.03–4.96 (m, 2H,  $\text{CH}_2 = \text{CH-CH}_2$ ), 2.59–2.52 (m, 2H,  $\text{NH-CH}_2\text{-CH}_2\text{-CH}_2\text{-CH}_3$ ), 2.51 (s, 2H,  $\text{CH}_2\text{-NH}$ ), 2.18 (d,  $J = 7.3$  Hz, 2H,  $\text{CH}_2 = \text{CH-CH}_2$ ), 1.78–1.69 (m, 6H,  $(\text{CH}_2)_3$ ), 1.46–1.36 (m, 2H,  $\text{CH}_2\text{-CH}_2\text{-CH}_2\text{-CH}_2\text{-NH}$ ), 1.33–1.19 (m, 3H,  $\text{NH}$  and  $\text{CH}_2\text{-CH}_3$ ), 0.87–0.83 (m, 3H,  $\text{CH}_3$ ) ppm;  $^{13}\text{C}$  NMR (101 MHz,  $\text{CDCl}_3$ )  $\delta = 135.47$  ( $\text{CH}_2 = \text{CH-CH}_2$ ), 116.77 ( $\text{CH}_2 = \text{CH-CH}_2$ ), 57.53 ( $\text{CH}_2\text{-CH}_2\text{-NH}$ ), 50.52 ( $\text{CH}_2\text{-NH}$ ), 42.11 ( $\text{CH}_2 = \text{CH-CH}_2$ ), 41.77 ( $\text{C}_\alpha$ ), 32.15 ( $\text{CH}_2\text{-CH}_2\text{-CH}_2\text{-CH}_2\text{-NH}$ ), 29.70 ( $(\text{CH}_2)_3$ ), 20.61 ( $\text{CH}_2\text{-CH}_3$ ), 15.43 ( $(\text{CH}_2)_3$ ), 14.16 ( $\text{CH}_3$ ) ppm; HRMS (ESI):  $m/z$  calcd for  $\text{C}_{12}\text{H}_{24}\text{N}^+$ : 182.1903, found: 182.1903 [ $\text{M} + \text{H}$ ] $^+$ .

### N-butyl-2,2-diphenylpent-4-en-1-amine (5e)

Was prepared according to the general procedure from 2,2-Diphenyl-4-penten-1-amine **4e** (2.90 g, 9.95 mmol) yielding the title compound **5e** as a colorless oil (2.79 g) which was used in the next step without further purification.  $^1\text{H}$  NMR ( $\text{CDCl}_3$ , 400 MHz):  $\delta = 7.29\text{--}7.25$  (m, 4H,  $\text{Ar-H}$ ), 7.20–7.17 (m, 6H,  $\text{Ar-H}$ ), 5.43–5.34 (m, 1H,  $\text{CH}_2 = \text{CH-CH}_2$ ), 5.04–4.93 (m, 2H,  $\text{CH}_2 = \text{CH-CH}_2$ ), 3.19 (s, 2H,  $\text{CH}_2\text{-NH}$ ), 3.01 (d,  $J = 7.1$  Hz, 2H,  $\text{CH}_2 = \text{CH-CH}_2$ ), 2.52 (m, 2H,  $\text{NH-CH}_2\text{-CH}_2\text{-CH}_2\text{-CH}_3$ ), 1.37–1.31 (m, 2H,  $\text{NH-CH}_2\text{-CH}_2\text{-CH}_2\text{-CH}_3$ ), 1.27–1.19 (m, 3H,  $\text{NH}$  and  $\text{CH}_2\text{-CH}_3$ ), 0.84 (t,  $J = 7.3$  Hz, 3H,  $\text{CH}_3$ ) ppm;  $^{13}\text{C}$  NMR ( $\text{CDCl}_3$ , 101 MHz):  $\delta = 147.10$  (arom.  $\text{C}_\alpha$ ), 135.18 ( $\text{CH}_2 = \text{CH-CH}_2$ ), 128.23 (arom. CH), 128.06 (arom. CH), 126.04 (arom. CH), 117.65 ( $\text{CH}_2 = \text{CH-CH}_2$ ), 56.16 ( $\text{CH}_2\text{-NH}$ ), 50.25 ( $\text{CH}_2\text{-CH}_2\text{-CH}_2\text{-CH}_2\text{-NH}$ ), 50.24 ( $\text{CH}_2 = \text{CH-CH}_2$ ), 41.86 ( $\text{C}_\alpha$ ), 32.15 ( $\text{CH}_2\text{-CH}_2\text{-CH}_2\text{-CH}_2\text{-NH}$ ), 20.50 ( $\text{CH}_2\text{-CH}_3$ ), 14.11 ( $\text{CH}_3$ ) ppm; HRMS (ESI):  $m/z$  calcd for  $\text{C}_{21}\text{H}_{28}\text{N}^+$ : 294.2216, found: 294.2216 [ $\text{M} + \text{H}$ ] $^+$ . These data are consistent with published data.<sup>[50]</sup>

**General procedure for synthesis of 3-chloropiperidines (1 c-d)**

To a solution of the corresponding secondary amine **5c-d** in THF (2 mL/mmol) copper(II)chloride dihydrate (1.2–1.6 eq.) was added. The mixture was stirred at room temperature for 16–18 h and a second portion of copper(II)chloride dihydrate (1.2–1.6 eq.) was added and the mixture was stirred at room temperature for another 18–48 h. Afterwards, the reaction was quenched by the addition of conc.  $\text{NH}_3(\text{aq})$  and DCM was added. The phases were separated and the aqueous phase was extracted with DCM (3x). The combined organic extracts were washed with distilled water as well as brine and dried over  $\text{MgSO}_4$ . The solvent was removed under reduced pressure and the crude product was obtained, which was purified by flash column chromatography.

**N-butyl-5-cyclopropyl-3-chloropiperidine (1 c)**

Was prepared according to the general procedure from crude *N*-[(propenyl)cyclopropyl]methylbutanamine **5c** (53 mg) and purified by flash column chromatography ( $R_f=0.12$  (pentane/TBME 20:1)) yielding the title compound **1c** as a colorless oil (38 mg, 0.19 mmol; 50% from **4c**).  $^1\text{H}$  NMR ( $\text{CDCl}_3$ , 200 MHz):  $\delta=4.13$  (ddd,  $J=14.6$ , 10.7, 4.2 Hz, 1H, CH Cl), 3.22 (dd,  $J=12.0$ , 3.0 Hz, 1H,  $\text{CH}_2$ ), 2.51–2.25 (m, 3H,  $\text{CH}_2$ ), 2.17 (t,  $J=10.7$  Hz, 1H,  $\text{CH}_2$ ), 2.07–1.84 (m, 2H,  $\text{CH}_2\text{-CH}_2\text{-CH}_2\text{-CH}_3$ ), 1.53–1.23 (m, 5H,  $\text{CH}_2$  and  $\text{CH}_2\text{-CH}_2\text{-CH}_2\text{-CH}_3$ ), 0.90 (t,  $J=7.1$  Hz, 3H,  $\text{CH}_3$ ), 0.56–0.31 (m, 4H,  $(\text{CH}_2)_2$ ) ppm;  $^{13}\text{C}$  NMR ( $\text{CDCl}_3$ , 101 MHz):  $\delta=61.67$  ( $\text{CH}_2$ ), 61.13 ( $\text{CH}_2$ ), 57.88 ( $\text{CH}_2$ ), 54.87 (CH–Cl), 44.30 ( $\text{CH}_2$ ), 34.27 ( $\text{CH}_2$ ), 29.01 ( $\text{CH}_2$ ), 22.48 ( $\text{CH}_2$ ), 20.82 ( $\text{CH}_2$ ), 18.10 ( $\text{CH}_2$ ), 14.20 ( $\text{CH}_2$ ), 14.12 ( $\text{CH}_3$ ), 13.09 ( $(\text{CH}_2)_2$ ), 9.64 ( $(\text{CH}_2)_2$ ) ppm; HRMS (ESI):  $m/z$  calcd for  $\text{C}_{11}\text{H}_{21}\text{ClN}$ : 202.1357, found: 202.1357 [M + H] $^+$ ; elemental analysis calcd (%) for  $\text{C}_{11}\text{H}_{21}\text{Cl}_2\text{N}$ : C 55.47, H 8.89, N 7.64; found: C 55.78, H 8.83, N 7.64.

**N-butyl-5-cyclobutyl-3-chloropiperidine (1 d)**

Was prepared according to the general procedure from crude *N*-[(propenyl)cyclobutyl]methylbutanamine **5d** (226 mg) and purified by flash column chromatography ( $R_f=0.29$  (DCM/acetone 50:1)) yielding the title compound **1d** as a colorless oil (82 mg, 0.38 mmol; 33% from **4d**).  $^1\text{H}$  NMR (400 MHz,  $\text{CDCl}_3$ )  $\delta=3.90$  (td,  $J=10.9$ , 5.7 Hz, 1H, CH–Cl), 3.08 (d,  $J=7.9$  Hz, 1H,  $\text{CH}_2$ ), 2.79 (d,  $J=11.5$  Hz, 1H,  $\text{CH}_2$ ), 2.42–2.25 (m, 3H,  $\text{CH}_2$ ), 1.99 (t,  $J=10.9$  Hz, 1H,  $\text{CH}_2$ ), 1.95–1.67 (m, 8H,  $(\text{CH}_2)_3$  and  $\text{CH}_2\text{-CH}_2\text{-CH}_2\text{-CH}_3$ ), 1.50–1.38 (m, 3H,  $\text{CH}_2$  and  $\text{CH}_2\text{-CH}_2\text{-CH}_3$ ), 1.32 (h,  $J=7.5$  Hz, 2H,  $\text{CH}_2\text{-CH}_3$ ), 0.91 (t,  $J=7.3$  Hz, 3H,  $\text{CH}_3$ ) ppm;  $^{13}\text{C}$  NMR (101 MHz,  $\text{CDCl}_3$ )  $\delta=62.87$  ( $\text{CH}_2$ ), 61.90 ( $\text{CH}_2$ ), 57.91 ( $\text{CH}_2$ ), 53.95 (CH–Cl), 47.20 ( $\text{CH}_2$ ), 39.98 ( $\text{CH}_2$ ), 31.54 ( $(\text{CH}_2)_3$ ), 31.17 ( $\text{CH}_2$ ), 29.11 ( $\text{CH}_2$ ), 20.71 ( $\text{CH}_2$ ), 15.94 ( $\text{C}_q$ ), 14.14 ( $\text{CH}_3$ ) ppm; HRMS (ESI):  $m/z$  calcd for  $\text{C}_{12}\text{H}_{24}\text{ClN}$ : 216.1514, found: 216.1514 [M + H] $^+$ ; elemental analysis calcd (%) for  $\text{C}_{12}\text{H}_{24}\text{Cl}_2\text{N}$ : C 57.14, H 9.19, N 5.55; found: C 57.17, H 9.11, N 5.78.

**N-butyl-5,5-diphenyl-3-chloropiperidine (1 e)**

To a solution of the secondary amine **5e** (440 mg, 1.34 mmol) in THF (25 mL) copper(II)chloride (180 mg, 1.34 mmol, 1.0 eq.) was added. The mixture was stirred at room temperature for 3 h and was then heated to reflux for another 22 h. Afterwards, the reaction was quenched by the addition of conc.  $\text{NH}_3(\text{aq})$  and DCM was added. The phases were separated and the aqueous phase was extracted with DCM (3x). The combined organic extracts were washed with distilled water as well as brine and dried over  $\text{MgSO}_4$ . The solvent was removed under reduced pressure and the crude product was obtained, which was purified by flash column chromatography ( $R_f=0.37$  (pentane/TBME 50:1)) yielding the title compound **1e** as a colorless solid (198 mg, 0.60 mmol; 45%).  $^1\text{H}$  NMR (400 MHz,  $\text{CDCl}_3$ )

$\delta=7.43\text{--}7.39$  (m, 2H, Ar–H), 7.31–7.24 (m, 4H, Ar–H), 7.20–7.14 (m, 4H, Ar–H), 3.90–3.78 (m, 1H, CH–Cl), 3.63 (d,  $J=12.1$  Hz, 1H,  $\text{CH}_2$ ), 3.25 (dd,  $J=10.2$ , 3.9 Hz, 1H,  $\text{CH}_2$ ), 2.96 (d,  $J=12.3$  Hz, 1H,  $\text{CH}_2$ ), 2.46 (t,  $J=7.4$  Hz, 2H,  $\text{CH}_2\text{-CH}_2\text{-CH}_2\text{-CH}_3$ ), 2.34 (t,  $J=12.2$  Hz, 1H,  $\text{CH}_2$ ), 2.23–2.14 (m, 2H,  $\text{CH}_2$ ), 1.56 (ddt,  $J=20.6$ , 13.1, 6.4 Hz, 2H,  $\text{CH}_2\text{-CH}_2\text{-CH}_2\text{-CH}_3$ ), 1.37 (h,  $J=7.4$  Hz, 2H,  $\text{CH}_2\text{-CH}_3$ ), 0.96 (t,  $J=7.3$  Hz, 3H,  $\text{CH}_3$ ) ppm;  $^{13}\text{C}$  NMR (101 MHz,  $\text{CDCl}_3$ )  $\delta=147.72$  (arom. CH), 145.39 (arom. CH), 128.72 (arom. CH), 128.47 (arom. CH), 128.21 (arom. CH), 126.58 (arom. CH), 126.47 (arom.  $\text{C}_q$ ), 126.05 (arom.  $\text{C}_q$ ), 62.58 ( $\text{CH}_2$ ), 61.80 ( $\text{CH}_2$ ), 58.01 ( $\text{CH}_2$ ), 53.96 (CH–Cl), 48.30 ( $\text{CH}_2$ ), 46.24 ( $\text{CH}_2$ ), 28.87 ( $\text{CH}_2$ ), 20.82 ( $\text{CH}_2$ ), 14.18 ( $\text{CH}_3$ ) ppm; HRMS (ESI):  $m/z$  calcd for  $\text{C}_{21}\text{H}_{27}\text{ClN}$ : 328.1827, found: 328.1826 [M + H] $^+$ ; elemental analysis calcd (%) for  $\text{C}_{21}\text{H}_{27}\text{Cl}_2\text{N}$ : C 69.23, H 7.47, N 3.84; found: C 68.88, H 7.58, N 3.82.

**Crystallographic data:** Deposition Numbers 2153718 (for **1a**), 2153719 (for **6b**), 2153720 (for **6a**), 2153721 (for **1c**), and 2154152 (for **1e**) contain the supplementary crystallographic data for this paper. These data are provided free of charge by the joint Cambridge Crystallographic Data Centre and Fachinformationszentrum Karlsruhe Access Structures service <url>

**Acknowledgements**

We thank Dr. Heike Hausmann for performing the AV600 NMR measurements. Special thanks go to Dr. Urs Gellrich and Jama Ariai for supporting us during DFT computations. Open Access funding enabled and organized by Projekt DEAL.

**Conflict of Interest**

The authors declare no conflict of interest.

**Data Availability Statement**

The data that support the findings of this study are available in the supplementary material of this article.

**Keywords:** Angle distortion · Geminal disubstituent effect · Kinetics · Structure-Activity relationship · Thorpe-Ingold-Effect

- [1] a) A. J. Kirby, *Adv. Phys. Org. Chem.* **1980**, 183–278; b) B. Capon, S. P. McManus in *Neighboring Group Participation* (Eds.: B. Capon, S. P. McManus), Springer US, Boston, MA, **1976**, pp. 19–75; c) M. E. Jung, *Synlett* **1999**, 1999, 843.
- [2] M. E. Jung, G. Piizzi, *Chem. Rev.* **2005**, 105, 1735.
- [3] a) R. M. Beesley, C. K. Ingold, J. F. Thorpe, *J. Chem. Soc. Trans.* **1915**, 107, 1080; b) C. K. Ingold, S. Sako, J. F. Thorpe, *J. Chem. Soc. Trans.* **1922**, 121, 1177; c) C. K. Ingold, *J. Chem. Soc. Trans.* **1921**, 119, 305.
- [4] N. L. Allinger, V. Zalkow, *J. Org. Chem.* **1960**, 25, 701.
- [5] P. von Ragué Schleyer, *J. Am. Chem. Soc.* **1961**, 83, 1368.
- [6] a) T. C. Bruice, U. K. Pandit, *J. Am. Chem. Soc.* **1960**, 82, 5858; b) T. C. Bruice, U. K. Pandit, *Proc. Natl. Acad. Sci. USA* **1960**, 46, 402.
- [7] F. C. Lightstone, T. C. Bruice, *J. Am. Chem. Soc.* **1996**, 118, 2595.
- [8] F. C. Lightstone, T. C. Bruice, *J. Am. Chem. Soc.* **1997**, 119, 9103.
- [9] T. C. Bruice, F. C. Lightstone, *Acc. Chem. Res.* **1999**, 32, 127.
- [10] S. Hur, T. C. Bruice, *Proc. Natl. Acad. Sci. USA* **2003**, 100, 12015.
- [11] L. Kolesniková, I. León, E. R. Alonso, S. Mata, J. L. Alonso, *J. Phys. Chem. Lett.* **2019**, 10, 1325.
- [12] F. M. Menger, *Acc. Chem. Res.* **1985**, 18, 128.

- [13] F. M. Menger, J. F. Chow, H. Kaiserman, P. C. Vasquez, *J. Am. Chem. Soc.* **1983**, *105*, 4996.
- [14] F. M. Menger, *Tetrahedron* **1983**, *39*, 1013.
- [15] F. M. Menger, *Acc. Chem. Res.* **1993**, *26*, 206.
- [16] F. M. Menger, *Pure Appl. Chem.* **2005**, *77*, 1873.
- [17] F. M. Menger, A. L. Galloway, D. G. Musaev, *Chem. Commun.* **2003**, 2370.
- [18] a) F. M. Menger, F. Nome, *ACS Chem. Biol.* **2019**, *14*, 1386; b) D. S. Souza, J. R. Mora, E. H. Wanderlind, R. M. Clementin, J. C. Gesser, H. D. Fiedler, F. Nome, F. M. Menger, *Angew. Chem. Int. Ed.* **2017**, *56*, 5345.
- [19] a) T. C. Bruce, A. Brown, D. O. Harris, *Proc. Natl. Acad. Sci. USA* **1971**, *68*, 658; b) P. A. Kollman, B. Kuhn, O. Donini, M. Perakyla, R. Stanton, D. Bakowies, *Acc. Chem. Res.* **2001**, *34*, 72; c) S. Marti, M. Roca, J. Andrés, V. Moliner, E. Silla, I. Tuñón, J. Bertrán, *Chem. Soc. Rev.* **2004**, *33*, 98; d) A. D. Meseccar, B. L. Stoddard, D. E. Koshland, *Science* **1997**, *277*, 202; e) M. I. Page, W. P. Jencks, *Proc. Natl. Acad. Sci. USA* **1971**, *68*, 1678; f) A. Warshel, *J. Biol. Chem.* **1998**, *273*, 27035; g) R. Wolfenden, M. J. Snider, *Acc. Chem. Res.* **2001**, *34*, 938; h) G. Jindal, A. Warshel, *Proteins* **2017**, *85*, 2157; i) A. Warshel, *Angew. Chem. Int. Ed.* **2014**, *53*, 10020.
- [20] a) A. L. Parrill, D. P. Dolata, *Tetrahedron Lett.* **1994**, *35*, 7319; b) A. L. Parrill, D. P. Dolata, *J. Mol. Struct.: THEOCHEM* **1996**, *370*, 187.
- [21] M. E. Jung, J. Gervay, *J. Am. Chem. Soc.* **1991**, *113*, 224.
- [22] S. Milstien, L. A. Cohen, *Proc. Natl. Acad. Sci. USA* **1970**, *67*, 1143.
- [23] S. Milstien, L. A. Cohen, *J. Am. Chem. Soc.* **1972**, *94*, 9158.
- [24] R. T. Borchardt, L. A. Cohen, *J. Am. Chem. Soc.* **1972**, *94*, 9175.
- [25] R. E. Winans, C. F. Wilcox, *J. Am. Chem. Soc.* **1976**, *98*, 4281.
- [26] C. Danforth, A. W. Nicholson, J. C. James, G. M. Loudon, *J. Am. Chem. Soc.* **1976**, *98*, 4275.
- [27] P. G. Sammes, D. J. Weller, *Synthesis* **1995**, 1995, 1205.
- [28] a) J. M. Karle, I. L. Karle, *J. Am. Chem. Soc.* **1972**, *94*, 9182; b) M. Caswell, G. L. Schmir, *J. Am. Chem. Soc.* **1980**, *102*, 4815.
- [29] a) A. L. Ringer, D. H. Magers, *J. Org. Chem.* **2007**, *72*, 2533; b) S. M. Bachrach, *J. Org. Chem.* **2008**, *73*, 2466; c) R. D. Bach, O. Dmitrenko, *J. Org. Chem.* **2002**, *67*, 2588; d) R. D. Bach, O. Dmitrenko, *J. Org. Chem.* **2002**, *67*, 2588.
- [30] E. Brenna, F. Distante, F. G. Gatti, G. Gatti, *Catal. Sci. Technol.* **2017**, *7*, 1497.
- [31] a) H. Chen, L. Wang, F. Wang, L.-P. Zhao, P. Wang, Y. Tang, *Angew. Chem. Int. Ed.* **2017**, *56*, 6942; b) H. Chen, L. Wang, F. Wang, L.-P. Zhao, P. Wang, Y. Tang, *Angew. Chem.* **2017**, *129*, 7046; c) M. J. O'Neill, T. Riesebeck, J. Cornella, *Angew. Chem. Int. Ed.* **2018**, *57*, 9103; d) M. J. O'Neill, T. Riesebeck, J. Cornella, *Angew. Chem.* **2018**, *130*, 9241; e) K. Nishimura, K. Ishihara, *Synlett* **2022**, 33, 585.
- [32] T. Helbing, M. Georg, F. Stöhr, C. Carraro, J. Becker, B. Gatto, R. Göttlich, *Eur. J. Org. Chem.* **2021**, 2021, 5905.
- [33] a) C. Carraro, A. Francke, A. Sosic, F. Kohl, T. Helbing, M. de Franco, D. Fabris, R. Göttlich, B. Gatto, *ACS Med. Chem. Lett.* **2019**, *10*, 552; b) T. Helbing, C. Carraro, A. Francke, A. Sosic, M. de Franco, V. Gandin, R. Göttlich, B. Gatto, *ChemMedChem* **2020**, *15*, 2040.
- [34] a) M. S. Newman, W. J. Broger, J. B. LaPidus, A. Tye, *J. Med. Chem.* **1972**, *15*, 1003; b) C. Toniolo, M. Crisma, F. Formaggio, C. Peggion, *Biopolymers* **2001**, *60*, 396; c) T. T. Talele, *J. Med. Chem.* **2018**, *61*, 2166.
- [35] W. Kohn, L. J. Sham, *Phys. Rev.* **1965**, *140*, A1133-A1138.
- [36] a) X. Qi, C. Chen, C. Hou, L. Fu, P. Chen, G. Liu, *J. Am. Chem. Soc.* **2018**, *140*, 7415; b) C. J. Maddocks, K. Ermanis, P. A. Clarke, *Org. Lett.* **2020**, *22*, 8116; c) Z.-J. Liu, X. Lu, G. Wang, L. Li, W.-T. Jiang, Y.-D. Wang, B. Xiao, Y. Fu, *J. Am. Chem. Soc.* **2016**, *138*, 9714; d) F. Liu, K. M. Worthy, L. Bindu, A. Giubellino, D. P. Bottaro, R. J. Fisher, T. R. Burke, *Org. Biomol. Chem.* **2007**, *5*, 367.
- [37] G.-Q. Liu, W. Li, Y.-M. Li, *Adv. Synth. Catal.* **2013**, *355*, 395-402.
- [38] R.-L. Li, G.-Q. Liu, W. Li, Y.-M. Wang, L. Li, L. Duan, Y.-M. Li, *Tetrahedron* **2013**, *69*, 5867.
- [39] R. Göttlich, *Synthesis* **2000**, 2000, 1561.
- [40] M. Noack, R. Göttlich, *Eur. J. Org. Chem.* **2002**, 2002, 3171.
- [41] a) N. de Kimpe, M. Boelens, J. Contreras, *Tetrahedron Lett.* **1996**, *37*, 3171; b) A. Cochi, D. G. Pardo, J. Cossy, *Eur. J. Org. Chem.* **2012**, 2012, 2023; c) D. Gomez Pardo, J. Cossy, *Chem. Eur. J.* **2014**, *20*, 4516; d) E. B. Boydas, G. Tanriver, M. D'hooghe, H.-J. Ha, V. van Speybroeck, S. Catak, *Org. Biomol. Chem.* **2018**, *16*, 796.
- [42] A. J. Kirby, G. J. Lloyd, *J. Chem. Soc. Perkin Trans. 2* **1976**, 1753.
- [43] C. K. Ingold, J. F. Thorpe, *J. Chem. Soc.* **1928**, 0, 1318.
- [44] F. Neese, F. Wennmohs, U. Becker, C. Riplinger, *J. Chem. Phys.* **2020**, *152*, 224108.
- [45] S. Miertuš, E. Scrocco, J. Tomasi, *Chem. Phys.* **1981**, *55*, 117.
- [46] S. Grimme, J. G. Brandenburg, C. Bannwarth, A. Hansen, *J. Chem. Phys.* **2015**, *143*, 54107.
- [47] F. Weigend, R. Ahlrichs, *Phys. Chem. Chem. Phys.* **2005**, *7*, 3297.
- [48] a) S. Grimme, *J. Chem. Theory Comput.* **2019**, *15*, 2847; b) P. Pracht, F. Böhle, S. Grimme, *Phys. Chem. Chem. Phys.* **2020**, *22*, 7169.
- [49] a) T. C. Bruce, W. C. Bradbury, *J. Am. Chem. Soc.* **1968**, *90*, 3808; b) A. A. Armstrong, L. M. Amzel, *J. Am. Chem. Soc.* **2003**, *125*, 14596.
- [50] Y.-M. Wang, T.-T. Li, G.-Q. Liu, I. Zhang, I. Duan, I. Li, Y.-M. Li, *RSC Adv.* **2014**, *4*, 9517.

Manuscript received: May 23, 2022  
 Revised manuscript received: July 22, 2022  
 Accepted manuscript online: July 26, 2022

#### 4.4. Further Co-Authored Publications

Decoding mechanism of action and sensitivity to drug candidates from integrated transcriptome and chromatin state. C. Carraro, L. Bonaguro, J. Schulte-Schrepping, A. Horne, M. Oestreich, S. Warnat-Herresthal, T. Helbing, M. De Franco, K. Haendler, S. Mukherjee, T. Ulas, V. Gandin, R. Goettlich, A. C. Aschenbrenner, J. L. Schultze, B. Gatto, *eLife***11**:e78012. (doi: 10.7554/eLife.78012)

Appended Aromatic Moieties in Flexible *Bis*-3-chloropiperidines Confer Tropism against Pancreatic Cancer Cells. C. Carraro, T. Helbing, A. Francke, I. Zuravka, A. Susic, M. De Franco, V. Gandin, B. Gatto, R. Göttlich, *ChemMedChem* **2021**, *16*, 860. (doi: 10.1002/cmdc.202000814)

Behind the Mirror: Chirality Tunes the Reactivity and Cytotoxicity of Chloropiperidines as Potential Anticancer Agents. C. Carraro, A. Francke, A. Susic, F. Kohl, T. Helbing, , M. De Franco, D. Fabris, R. Göttlich, B. Gatto, *ACS Medical Chemistry Letters* **2019**, *10* (4), 552–557. (doi: 10.1021/acsmchemlett.8b00580)

## 5. Acknowledgment

This work would not have been possible without the help of many different people, especially during the challenging crisis times ("JLU offline" and Corona). First and foremost, I would like to thank my supervisor Prof. Dr. Richard Göttlich for the opportunity to work in his research group and on this specific topic since I started my groundwork with the bachelor thesis. Moreover, I would like to thank Richard for his constant support during my doctoral studies and the ability to do basically all the research I wanted to do. In addition, I want to thank Prof. Dr. Barbara Gatto and Dr. Caterina Carraro as well as their students and co-workers for providing the pharmaceutical evaluation of the synthesized compounds, the beneficial cooperation and their hospitality during my trips to Italy. I also thank Prof. Dr. Siegfried Schindler for co-examination of this work.

I would like to show my gratefulness to the current and former members of the AG Göttlich, who shared their time in the group with me, for the pleasant working environment and many entertaining evenings. Specific credits go to Dr. Alexander Francke, who supervised my bachelor thesis and also supported me during my master thesis and the first months of my doctoral studies. Furthermore, I want to thank my former apprentice Lena Lipovsek for her assistance as well as her everlasting energy and enthusiasm. I would like to as well acknowledge all the students I was allowed to supervise during this time, especially Michael Kirchner whose work resulted in the third publication of this dissertation. Although not included in this work, I would also like to thank Prof. Dr. Joachim Geyer and Dr. Michael Marner for their contribution to my other research projects.

I also want to express my gratitude to Mats Georg and Max Hasenbeck who have been fantastic friends and colleagues, supporting me scientifically as well as emotionally during my doctoral studies and providing an enjoyable time also apart from the lab. In addition, I want to thank my friend and former fellow student Felix Pfanschilling for his encouragement all along the undergraduate semesters and the humorous evenings. The three of you made my academic time much more worthwhile.

Special thanks go to the members of the analytical department, without whom this work would not have been possible. I want to specifically name Steffen Wagner, Stefan Bernhardt, Dr. Raffael Wende, Dr. Dennis Gerbig and Dr. Heike Hausmann for their technical and theoretical support concerning the measurements. Moreover, I would like to thank Dr. Jörg Neudert, Doris Verch, Michaela Richter and Annika Jäger for administrative support, Edgar Reitz for his help with electronic problems and Eike Santowski as well as Mario Dauber for their assistance with the chemical supplies and waste disposal.

By all means, I am grateful for the support that my family granted me during all the time of my academic career, starting with my sudden relocation to Gießen. Michael, Petra and Niko Helbing, I will never forget your decisive help and moral support, especially during the more challenging times.

In particular I want to appreciate my wife Jil-Christine Kramer, without your backing I would probably not be able to write these lines. Your patience, constant motivation and love were without any doubt the strongest support I had during this time. Words cannot express how thankful I am for getting to know you during my first semester and for all the cheerful moments we had since then. I hope that we will have plenty of these in the future and that our mutual encouragement is never ceasing.